Assessment of soil erosion hazard around the abandoned Nyala mine in formerly Mutale Municipality, Limpopo Province, South Africa.

ABIDENCE BVINDI

Master of Environmental Sciences

2019

Assessment of soil erosion hazard around the abandoned Nyala mine in formerly Mutale Municipality, Limpopo Province, South Africa.

By

ABIDENCE BVINDI

11613004

A research thesis submitted to the Department of Geography and Geo-Information Sciences, School of Environmental Sciences at the University of Venda in fulfillment of the requirements for the degree of

Master of Environmental Sciences

Supervisor: Dr. N. S. Nethengwe

Co-supervisor: Prof. B. D. O. Odhiambo

February 2019

DECLARATION

I **Abidence Bvindi**, hereby declare that this proposal submitted for the Master of Environmental Science in Geography at the University of Venda by me has not been previously submitted for any degree at this or any other university. It is my own work in design and execution and all reference material contained therein has been duly acknowledged.

Signature **Date**

…… ……/……/……..

ABSTRACT

Environmental degradation is a quite familiar factor of the mining industry that has been associated with South African mining industry from the beginning. The decommissioning of abandoned mines before the environment legislation, The National Environmental Management Act 107 of 1998 and the Minerals and Petroleum Resources Development Act 23 of 2002, was introduced is of great concern as the abandonment of mines without appropriate remediation and pollution monitoring was the result.

Soil erosion has been recognised as an environmental hazard that emanates from abandoned mines. This study seeks to assess the soil erosion hazard around Nyala abandoned mine. The modified method of Soil Loss Estimation Model for Southern Africa (SLEMSA), for assessing soil erosion hazard, was used to estimate the spatial variation of erosion to achieve the goal of the study. Parameters that were considered for the model include relief (Slope steepness, *S* & slope length, *L*), soil erodibility (Fb), vegetation cover (C) and rainfall erosivity (E). Soil samples were collected from the field and; sieve and hydrometer analysis was conducted to determine the erodibility factor value of the study area. The model was run in a GIS environment (ArcGIS) and the parameters were multiplied to generate a soil erosion hazard map for the abandoned Nyala mine area.

Results from the study indicated that 74.3 % of the watershed experiences low to moderate erosion hazard, with an estimated annual soil loss of 2.76 tons/ha/yr. The low rates of soil erosion in most parts of the watershed are associated with the low topographic ratio and low rainfall erosivity. The research demonstrated that the modified SLEMSA model used within GIS is a very useful tool as it enhances the capacity to assess and model the spatial variation of soil erosion hazard in a timeously and affordable manner.

Keywords: Abandoned mine, GIS, Reclamation and rehabilitation, SLEMSA, Soil erosion hazard.

ACKNOWLEDGMENTS

My deepest and most sincere gratitude goes to God for the grace and strength that he provided to enable me to finish this study.

First and foremost, I would like to extend my sincere gratitude for the collective support and guidance rendered to me in producing this research work to my supervisors, Dr. N. S. Nethengwe and Prof B. D. O. Odhiambo. I appreciate their expertise, constructive criticism and support which I received which enabled the accomplishment of this research project. They not only provided technical assistance but also motivated and encouraged me during my study.

This study would not have been possible without the emotional and financial support of my family. Their support enabled me to conduct this study in the most efficient of ways. I wish to extend my gratitude to my friends, especially Ms. Lucpah P Nekati, for the pivotal role they played in the accomplishment of this work.

I thank the National Research Foundation (NRF) and the University of Venda Research and Publication Committee for funding the research dissertation. The United States Geological Survey (USGS) and South African National Space Agency (SANSA) are acknowledged for providing quality satellite images.

DEDICATION

To my late father, Raphael Bvindi.

TABLE OF CONTENTS

LIST OF FIGURES

Page

LIST OF TABLES

LIST OF ACRONYMS AND ABBREVIATIONS

A	Mean annual soil loss (ton. ha-1. yr-1) (of USLE)
C	Vegetation Cover
DEM	Digital Elevation Model
E	Rainfall Erosivity
EHU	Erosion Hazard Units
ETM+	Enhanced Thematic Mapper Plus
EUROSEM	European Soil Erosion Model
Fb	Soil Erodibility
GIS	Geographical Information System
GPS	Global Positioning System
K	Erodibility Factor
Ib	Erosion Hazard Index
LULC	Land Use Land Cover
LS	Slope Length and Slope Steepness
MAP	Mean Annual Precipitation
RUSLE	Revised Universal Soil Loss Equation
SLEMSA	Soil Loss Estimator for Southern Africa
USLE	Universal Soil Loss Equation
X	Topographic Ratio
Z	Mean annual soil loss

CHAPTER ONE

INTRODUCTION

1.1 BACKGROUND TO THE STUDY

The mining industry has played a significant role in the national economy of South Africa. However, mining has severe impacts on the environment. According to Allen (2001) and Aragon (2012), the environmental legacy of mining activities conducted with minimal concern for the environment has raised a lot of vigilance. A recent South African survey identified a myriad of environmental impacts associated with mining and abandoned mines (Auditor-General SA, 2009); and soil erosion is considered one of South Africa's most important mine-related environmental problems (Meadows, 2003; Garland *et al,* 2000; Haarhoff *et al,* 1994).

Mining activities impact the environment through inter alia, erosion, and with approximately 6000 abandoned mines (Auditor-General SA, 2009: 17); where definitive rehabilitation and reclamation efforts were not undertaken, where the potential of soil erosion and sediment eroding into and significantly affecting water quality and or agricultural activities is a serious problem (Nordstrom and Alpers, 1999; Pyatt and Grattan, 2001). Soil erosion is a major concern since vast areas of land are disturbed by mining activities as well as the vast amounts of earthen materials showing at mining sites. Accordingly, it is apparent that erosion control is accounted for from the onset of mining operations through completion of rehabilitation and reclamation (Peplow and Edmonds 2005; Panagopoulos *et al.* 2009; Lei *et al.* 2010; Sarmiento *et al.* 2011).

An assessment of soil erosion requires collection and analysis of data that have a spatial component that represents environmental parameters like factors that influence erosion which include volume and velocity of runoff from precipitation events, structure of the soil in relation to rainfall infiltration through the soil, the extent of vegetative cover and, the slope length or the distance covering the origin point of overland flow to the point of deposition (Roder and Hill, 2009). Geospatial information technologies that include

Geographical Information Systems (GIS), Remote Sensing (RS), and Global Positioning Systems (GPS) are particularly significant and useful in this context. This study, therefore, assessed the soil erosion hazard associated with an abandoned mine using the SLEMSA model coupled with geospatial technologies.

In South Africa, Geographical Information Systems (GIS) is a preferred tool for soil erosion studies (Le Roux *et al,* 2007). GIS is a powerful tool which aids in data management, analysis and manipulation, and GIS modeling, allowing the perception of the real world in simplified terms by researchers, by modeling complex and dynamic environmental processes such as soil erosion. In this study, GIS technology was applied to assess soil erosion hazard around an abandoned mine site using a common approach that generates rapid soil erosion assessment results at a low cost: The Soil Loss Estimation Model for Southern Africa (SLEMSA).

The Soil Loss Estimation Model for Southern Africa; SLEMSA (Stocking *et al,* 1988), was initially developed mainly from data from Zimbabwe, to assess the erosion hazard that resulted from diverse farming systems, that could illicit proper recommendations for conservation measures. The SLEMSA model is based on a blend of factorial scoring methods and empirical relations with drivers of erosion. The technique has been adopted in most countries in Southern Africa (Elwell 1978). The SLEMSA model is essentially a model for soil removal (Schulze, 1979). It can be regarded as a useful model for differentiating areas of high and low erosion potential (Schulze, 1979).

SLEMSA was developed in Southern Africa based on the USLE and is an attempt to adapt the USLE model to an African environment. The dawn of Geographical Information System (GIS) technology has made it possible for implementation of the equation in a spatially distributed manner because each cell in a raster image represents a field-level unit (Brady, 2000; Strager *et al,* 2010). Within a raster-based GIS, prediction of soil erosion on a cell-by-cell basis using the SLEMSA model is viable. This is particularly beneficial in the attempted identification of the spatial patterns of soil loss that are within a large region. Consequently,

GIS can be utilised in the isolation and query of these locations to produce information essential to the role of individual variables contributing to the observed erosion potential value (Clarke, 2001).

1.2 PROBLEM STATEMENT

The South African mining sector is instrumental in the economy, yet mining activities have been implicated in environmental contamination, particularly old mine sites which have been abandoned without any implementation of proper mine closure plans. In terms of types of hazards and potential impact on the environment, there is nothing separating abandoned mines from active mines. Nonetheless, their major problem relates to the uncertainty in information and lack of data.

Some of these abandoned mines have become the foundation of extensive environmental damage (Chamber of Mines, 2011; Hakkou *et al,* 2009). Reichardt (2012) has identified soil erosion as a major concern with abandoned mines due to the resulting extended areas of disturbed land from mining operations. Open pit areas, heaps and dump leaches, waste rock, tailings piles, and dams, exploration areas, haulage and access roads, vehicles, and equipment maintenance areas have been identified as the main sources of erosion observed at mining sites (Mhlongo *et al,* 2013).

Further apprehension emanates from the possible contribution to sediments with chemical pollutants, particularly heavy metals from exposed materials from mining operations. Exaggerated agility of the pollutants emanating from the highlighted sources is due to exposure to rainfall with the subsequent release of surface runoff that results from rainfall; thus, soil erosion is one of the mechanisms by which pollutants are released in to nearby soils and water bodies.

This adversely affects nearby communities and as such there are constants debates among policy-maker on where environmental pollution is occurring, its potential sources, the scope, and the principal dispersal mechanisms and pathways of the pollution. However, it is

unfortunate that most of the environmental studies seeking to address these questions are solely founded on conventional methods such as ground surveys. The methods are characterized by the lack of data integration, time-consuming analysis and inadequate address of the spatiotemporal issues associated with abandoned mine sites. The main objective of the study was, therefore, to develop a geospatial methodological approach to enhanced soil hazard assessment to identify priority areas where remedial measures can be implemented using an erosion model coupled with GIS.

1.3 RESEARCH AIM AND SPECIFIC OBJECTIVES

1.3.1 Research Aim

The main aim of the study was to assess soil erosion hazard associated with the abandoned Nyala mine using the SLEMSA model and Geographic Information Systems to support abandoned mine reclamation and rehabilitation planning.

1.3.2 Specific Objectives

1. To determine the erosion hazard index around the abandoned mine based on soil erodibility factor and rainfall erosivity factor;
2. To determine the land-use and land-cover around the abandoned Nyala mine;
3. To determine the soil loss ratio dependent on slope length and slope steepness factors; and
4. To model the erosion hazard in ArcGIS model builder.

1.4 RESEARCH QUESTIONS

The following questions were formulated for this study;

1. What is the susceptibility of the soil to detachment and transport in relation to rainfall intensity?
2. What is the extent of land-use/cover around the abandoned mine?
3. To what extent does the topography of the area influence soil erosion?
4. Where is the soil erosion hazard around the abandoned mine and how significant is it?

1.5 JUSTIFICATION OF THE STUDY

There is increased cognizance of the environmental legacy of mining activities practiced with very minimal concern for the environment across the world (Makgae, 2012). Mining, by its nature, consumes, diverts and can seriously pollute water resources (Miller, 1999). The long mining history of South Africa has led to significant mine-water related challenges. Particularly, mine water pollution has been identified as one of the many pressures affecting freshwater systems and resources in South Africa (Younger, 2001); and water yield in a semi-arid environment is greatly influenced by the interconnection between erosion and sediment movement, which in turn holds a lot of relevance to downstream water supply (Renard, 1970: cited in Johnston, 2008). This study, therefore, assessed the spatial variation of the soil erosion hazard around an abandoned mine to provide data useful for defining sources of pollutants and identify potential areas for remediation.

Smith *et al.* (1994) acknowledged extreme erosion and elevated sediment transfer rates as possible tenacious sources of contamination. Some of the problems identified in areas susceptible to erosion and with potential contribution to sediment and other pollutants downstream include steep slopes, acidity, and absence of topsoil (USDA 1973). In a study conducted by Mhlongo (2012), soil erosion and sediment deposition were found to be still prevalent in the abandoned Nyala mine as many tailings and mine roads are not rehabilitated and continue to contribute sediment to the channel system. The focus of this research was on conscientious surface erosion control necessary for reclamation of tailings and waste piles.

The principal contamination pathway that has been identified in mining areas is surface drainage. This is due to its tendency to accumulate contaminated runoff from washed-out soils in abandoned mining areas (Coetzee *et al,* 2006). Determination of the position of an upstream source or possible sources of any contamination at any point in the event of identification of contamination flow and the subsequent determination of paths upon which contaminated run-off downstream from a contamination source facilitated by the mapping of surface pollution dissemination pathways in an abandoned mining area is vital. Using GIS, coupled with the

SLEMSA soil erosion model, possible sources of contamination can be identified, and surface potential contamination pathways mapped. This is an important visualization tool for observing the transport of contamination to areas of possible human contact thus signifying the tremendous importance of this study in a risk-mitigation perspective.

According to Milisav (2014), the purpose of environmental models attempts realistic emulations of spatially distributed and time-dependent environmental processes. GIS can describe the spatial environment through its ability to capture, manipulate, process and display geo-referenced data. Thus, GIS and environmental modeling are synergistic, with a clear overlap and relationship between the two technologies (Mishra *et al,* 2012). However, there is a variation in data structures, functions and methods of spatial information input and output which have attributed to the individual and independent evolution of GIS and environmental modeling. The importance of the study is seen as its integrated GIS with the SLEMSA model, to provide a valuable methodology for modeling the erosion hazard associated with abandoned mine areas and prioritizing surface water resources in reclamation and rehabilitation planning.

Mine reclamation is an integral part of the mineral development process. Unfortunately, most of the environmental studies conducted for reclamation and rehabilitation planning are based only on conventional methods such as ground surveys. These methods are known to be expensive, time-consuming and are characterized by a lack of data integration (Antwi *et al,* 2008; Eweg and van Lammeren, 1996). However, continued improvements in GIS present better opportunities for the analysis of environmental data (Fengxia and Wenbao, 2010; Wang *et al,* 2008). The significance of the study, therefore, lies in the application of GIS and its integration with physical models, complimented with an obligation to develop new technologies that monitor surface water contamination in geographic space, and the chance for discovery of potential influence on the natural and human environment. In addition, the aptitude for timeously gathering of reliable information may be implemented in the

development of measures for the management and enhancement of environmental quality in abandoned mining lands.

1.6 DESCRIPTION OF THE STUDY AREA

1.6.1 Geographical location

The focus of this study was on the abandoned Nyala mine, located within the Mutale Municipality of the Limpopo province, South Africa. The Nyala mine is situated approximately 50 km north-east of Thohoyandou and about 60 km from the Pafuri Gate of the Kruger National Park.

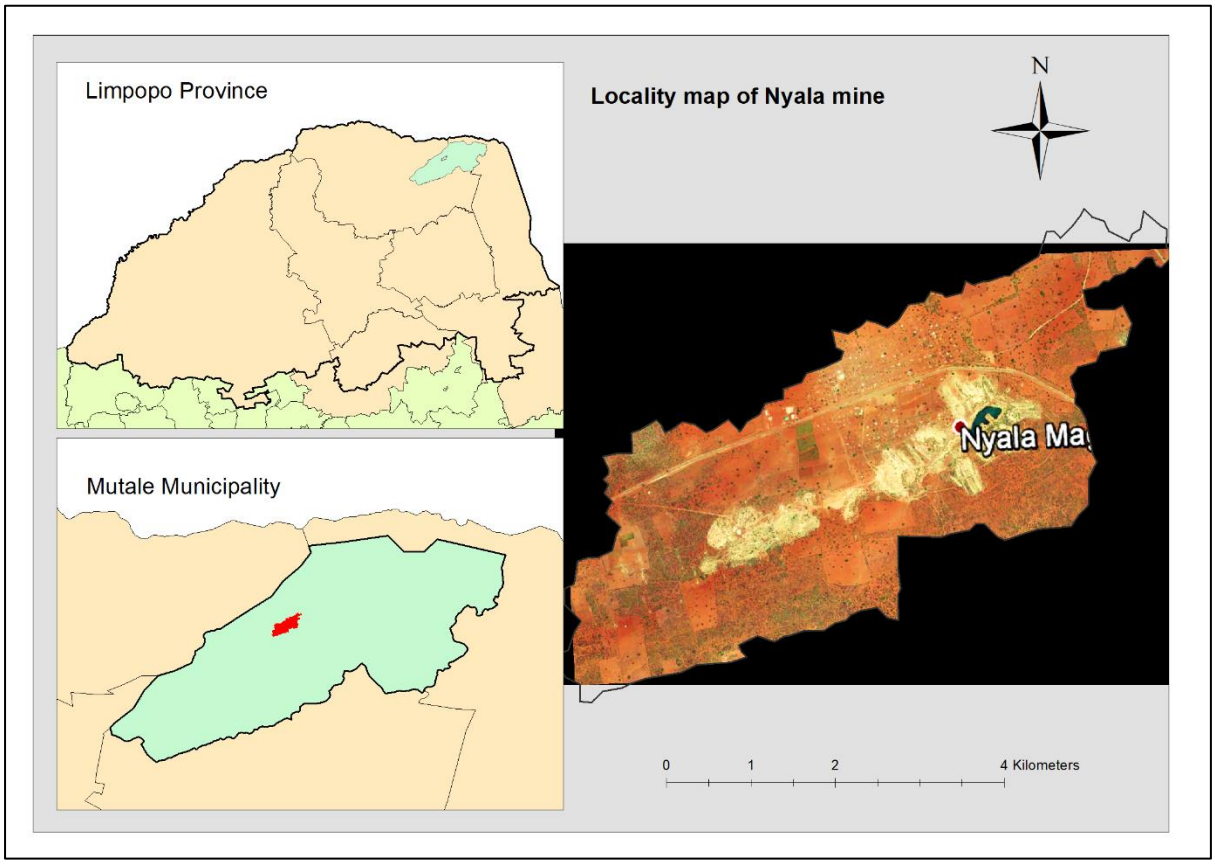

Figure 1.1: Geographical location of the abandoned Nyala mine. Source; developed by the researcher using ArcGIS 10.3.

It is located between the geographic coordinates; 30° 36' E and 30° 39' E. and 22° 45' S to 22° 33' S. The mine site as well as the village area are characterized by relatively gentle topographic relief which is because of the underlying geology, hence there are no significantly

conspicuous high rising lands or hills. The vegetation is characterised by sparse trees, few shrubs, and patches of grass. Various activities ranging from agricultural, residential and recreational activities, and small-scale magnesite mining operations are characteristic of the region. Figure 1.1 shows the geographical location of the abandoned Nyala mine.

Climate

The Nyala mine climate is typical of the north-eastern part of Limpopo province, characterized by extremely hot summers that receive minimal rainfall and mild winters. The monthly average of maximum temperatures for the area ranges from 25 ^{o}C in winter (July) to 33 ^{o}C in summer (February). The region is coldest in July, when temperatures drop to an average of 9°C at night (Figure 1.2). There are no perennial rivers and permanent water bodies, such that the community around the mine relies on groundwater sources for domestic use.

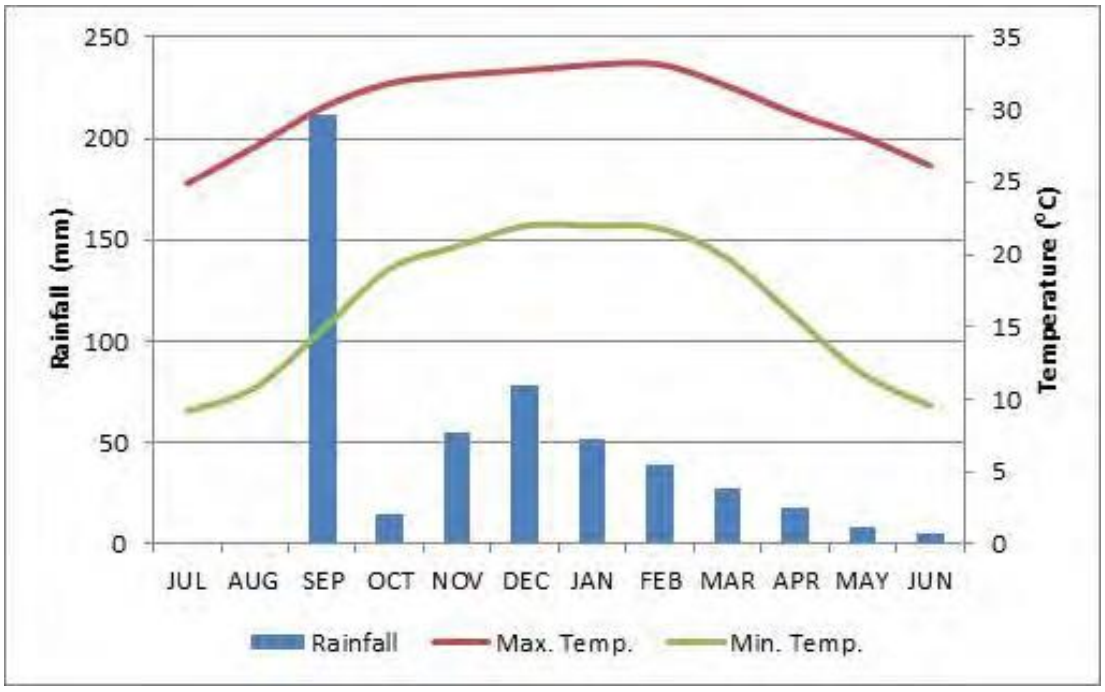

Figure 1.2: Mean minimum and maximum temperature and average annual rainfall for the study area.

The region receives summer rainfall. Frost rarely occurs during the dry winter months, as the temperature seldom drops below 10 °C. The Nyala mine area receives an average annual rainfall of approximately 520 mm per year, with most of it being received during the summer

months. The area receives the least amount of rainfall in August (with an average monthly rainfall of 0.06 mm per month) and the most in September (with an average monthly rainfall of 212 mm per month) as shown in Figure 1.2.

Geology

The geology of the study area comprises various rock formations, some of which are structurally very complex. These include the Archaean Beit Bridge Complex, gneisses and metasediments with sediments and basalt of the Karoo Subgroup; reddish and/or brown sandstone and quartzite, conglomerate, tuff, shale and siltstone of the Soutpansberg Group; as well as Karoo sandstones and basalts (Figure 1.3).

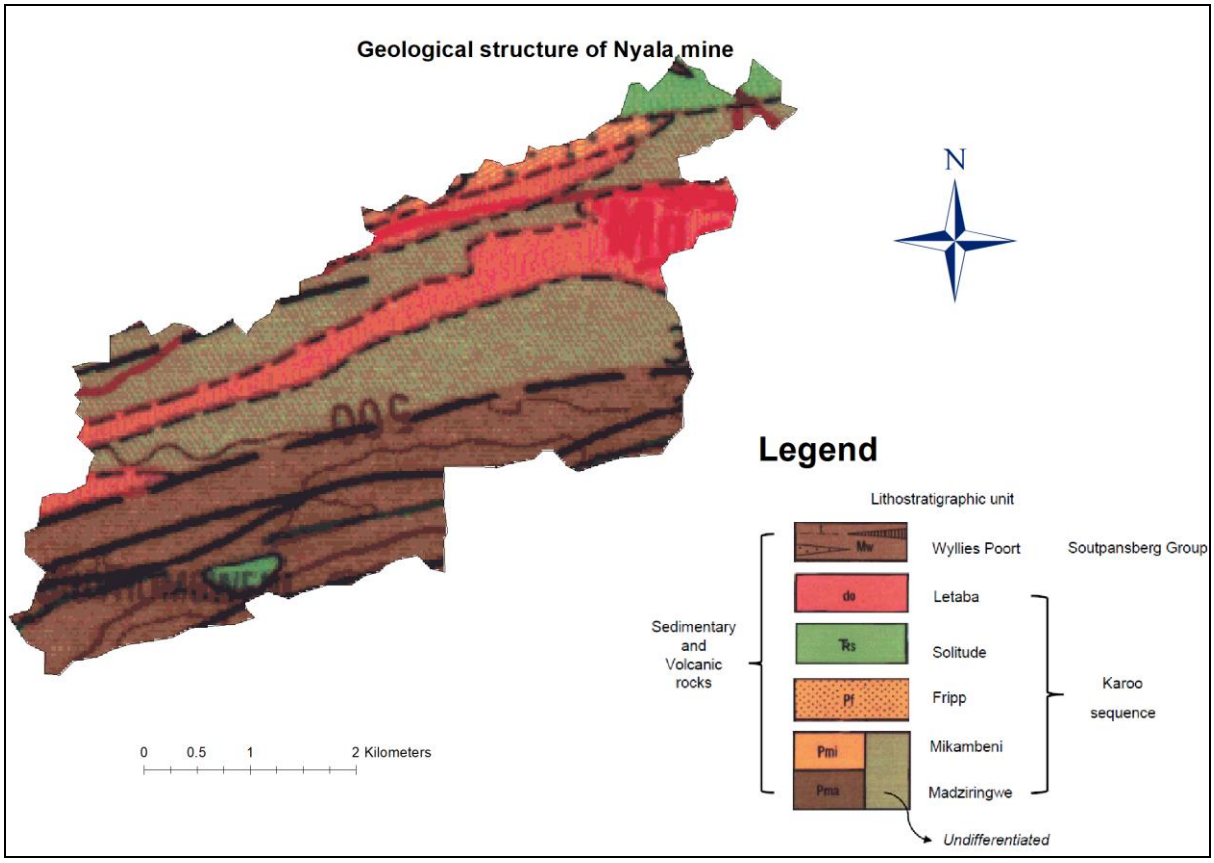

Figure 1.3: The geological structure of the abandoned Nyala mine

Large deposits of amorphous magnesite are encountered in the limburgite of the Drakensberg in the area extending east-northwards from Tshipise over some kilometres. The magnesium is presently found as irregular masses and is derived from the olivine-rich rocks through

weathering. The formation primarily consists of sandstones, siltstones, mudstones, and shale (Nemalili, 2008: 9).

Soils

Soil in Nyala Mine is in three major groups, namely (a) moderately deep, red coloured sandy clay loam soils on the upper parts of the hill slopes and heaving terrain in the topmost reaches of the sub-catchments; (b) shallow to moderately deep, reddish to tan coloured sandy soils facing the valley bottoms around the central reaches of the sub-catchments; and (c) small areas of clay-rich, blackish or mottled soils containing high organic content that covers flood terraces close to the lower reaches of the Limpopo river (DWAF, 1996: 73).

Soils associated with Limpopo Ridge Bushveld range from shallow gravel and sand to calcareous clayey soil. Musina Mopane Bushveld is found on variable soils: From deep red/brown clays, and moderately deep, dark, heavy clays, to deep, freely drained sandy soils and shallower types including skeletal Glenrosaand Mispah soil forms. Soutpansberg Mountain Bushveld is found mainly in rocky areas with miscellaneous soils including acidic dystrophic to mesotrophic sandy to loamy soil. Glenrosa and Mispah soil forms are also common.

Vegetation

The vegetation falls within the savanna biome which has three vegetation types. The vegetation in the area is predominantly open tree savanna with *Acacia caffra* dominating the area and scattered Baobab trees (Adansonia *digitate*) and Mopane trees (Colophospermum *mopane*).

1.6.2 Historical background

The abandoned Nyala Magnesite Mine is situated 5 km west of Klain Tsipise in the village of Zwigodini. According to Strydom (1998), the main magnesite body at Nyala Mine occupies an area of 212 ha and it occurs up to the depth of about 200 m. Mining of magnesite in the area was carried out by surface mining method in which the orebody was quarried by means of

heavy equipment and hand sorted into a product that contains up to 98% $MgCO_3$ (Strydom, 1998). The mine operated for approximately 36 years and was abandoned in 1975 without any rehabilitation of the mined-out land. Historic mining of magnesite affected an area of about 212 ha. Such an extensive area of the mine landscape hosts several large mine waste deposits (i.e. both tailings and spoil dumps) and open excavations

Magnesite mining at Nyala Mine left two large volume unrehabilitated tailing dumps; spoil materials and hazardous excavations (Mhlongo, 2012). The recent growth and expansion of the village towards the mined-out areas justify the need for rehabilitation of the derelict Nyala mine site. In the process of making decisions on the appropriate options of cleaning up the abandoned mine site, there is a need for assessment of the abandoned mine hazards to the environment and society.

The historic Nyala Mine site has two large volume tailing dumps (denoted as Tailing-A and Tailing-B) and several spoil dumps (Figure 1.3). The estimated volumes of Tailing-A and Tailing-B were 385 699 m^3 and 568 163 m^3 respectively. The total area covered by magnesite tailings dumps at Nyala Mine was found to be 102 713 m^2. The slope angles of the tailing dumps were measured and found to be ranging between from 30° to 35°. The average estimated height of Tailing-A and B were found to be 27 m (above 495 m level surface) of and 28 m (above MSL the level surface of 490 m), respectively.

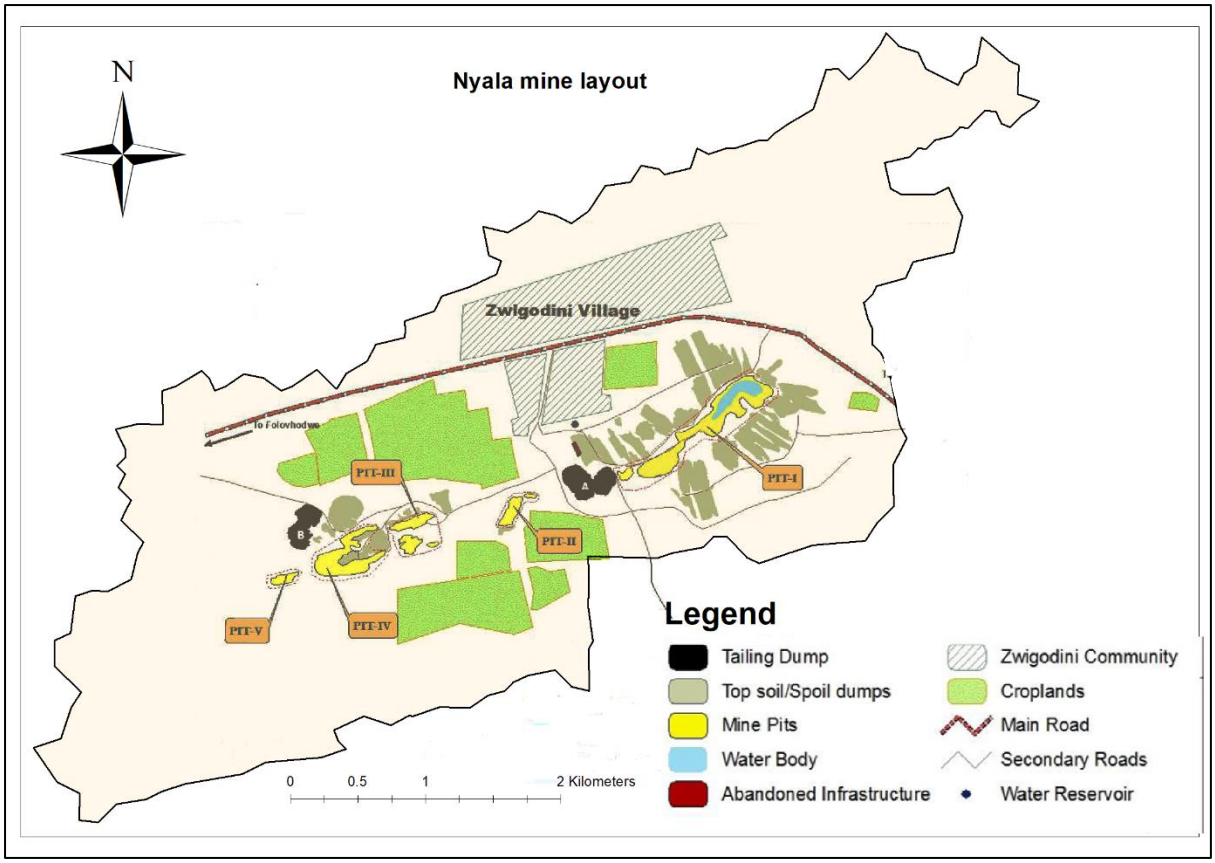

Figure 1.4: Layout of existing features of the abandoned Nyala Mine.

1.6.3 Mining operations

The magnesite deposits of South Africa are generally mined by open pit mining method at a relatively high stripping ratio (Cardavelli, 2008). According to Wicken (1990), open pit mining method is highly adopted where the ratio of waste and overburden to ore is moderate. The country has only two operating magnesite mines, namely; Strathmore Mine and Syferfontein Mine in the vicinity of Malelane and Folovhodwe village, respectively. In both mines, magnesite extraction is by surface mining methods (Ratlabala, 2003).

Magnesite deposits around Folovhodwe area are suitable for artisanal mining since they occur as soft clay-like matrix above the water table (Paul *et al,*1997). The geological setup of these deposits and their host rock make their extraction possible without blasting; consequently, excavators were used at Nyala Mine to remove the top soil and to expose the magnesite seams to the collectors who gathered the materials in piles. The derelict Nyala Mine site is generally characterized by extremely rugged terrain due to the presence of extensive

excavations (denoted as Pit-I to V), two large volume tailings (Tailing-A and B) as well as spoil materials scattered all over the mine site (see Figure 1.3). These features are the major sources of both physical and environmental impact in the area (Mhlongo, 2012; Mhlongo *et al,* 2013).

1.6.4 Soil erosion at the abandoned Nyala mine

Mining operations are responsible for the degradation of large areas of sometimes potentially cultivable land, replacing the existing ecosystem with massive volumes of waste materials such as spoils and tailings dumps which are easily erodible (Singh *et al.,* 2007). According to Smith (2009), the type of mining method used in the extraction of mineral resources as well as the geographical location of the mine are among the major factors that determine the extent to which mining degrades the environment. The environmental effect of mining is localised and only affects the mine lease area, but pollution because of the waste rock, tailings and spoil dumps that is generated can have severe impact that extends to nearby properties (Sahu and Dash, 2011; Allen *et al.,* 2001). Mining of magnesite by surface mining at Nyala Mine has affected the natural landscape (Mhlongo *et al.,* 2013a).

Nyala Mine is characterised by four shallow and less extensive pits. In addition to these pits, the mine has one extensive pit which contains water throughout the year. This pit was rated by Mhlongo *et al.* (2013b); the most hazardous mine feature to both the environment and the members of the public. According to Mhlongo *et al.* (2013b), the pit contains large volume of water, thick sticky mud at the pit floor, and has unstable pit walls and therefore presents a serious physical hazard (Figure 1.4).

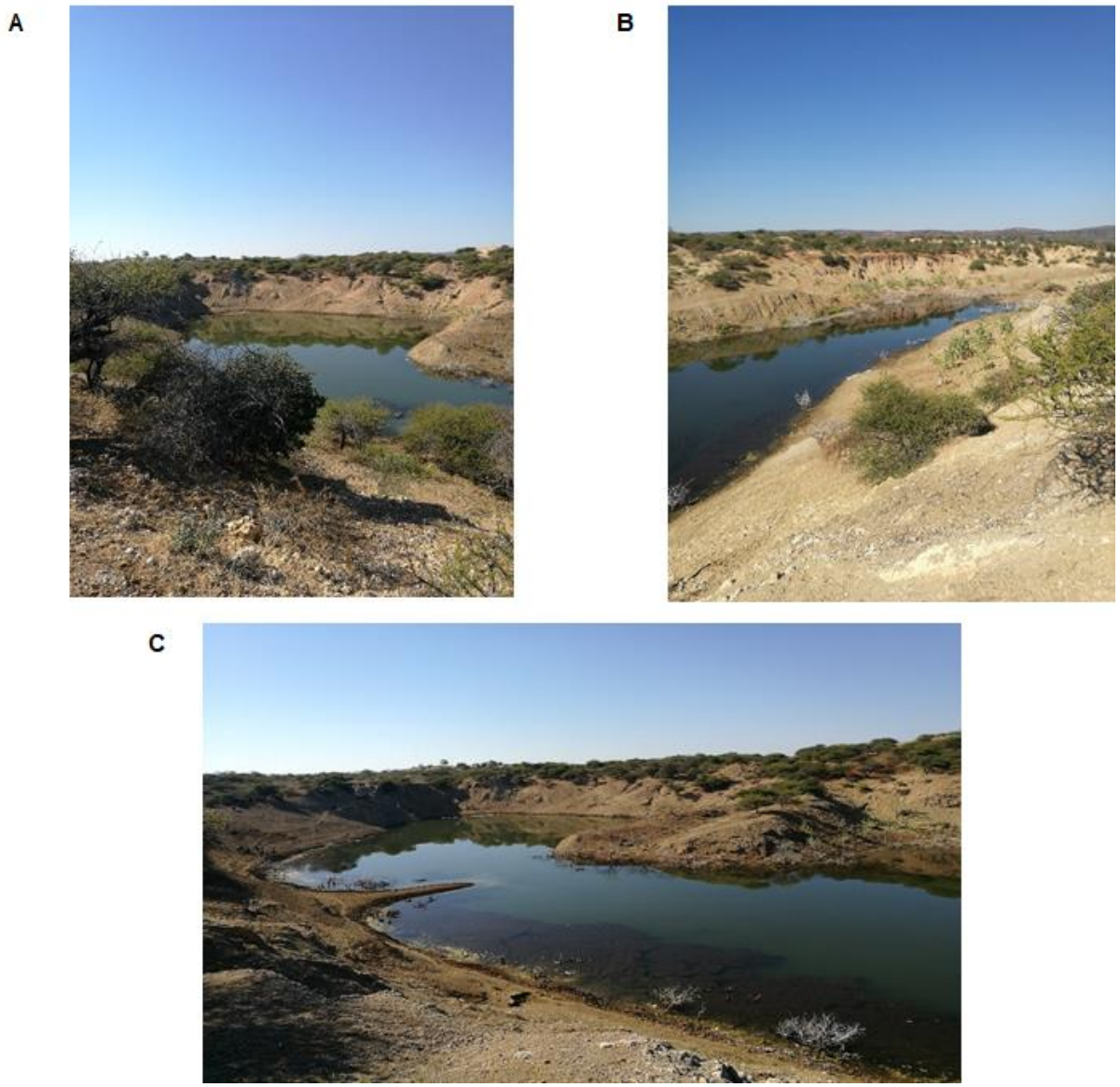

Figure 1.5: A shows the pit lake at Nyala Mine and the surrounding vegetation, in Figure B there are visible signs of erosion and in Figure C there are animals drinking from the pit lake.

Much of surface run-off from the areas are highly disturbed by mining and occupied by highly erodible magnesite tailing material. According to Sibanda *et al.* (2013), the mine tailings at Nyala Mine comprise of 43% gravel, 53% fine sand and 5% fines (i.e. silt and clay). In generally, soils that are dominated by fine sands and silt and lack organic matter are the most erodible soils (O'Geen *et al.,* 2006). The erosive property of fine materials coupled with the high slope angles directly influence surface runoff from the slopes of the tailings dump to the lowest part of the pit lake. It needs to be noted also that other factors such as slope length and unprotected nature of the slopes of the tailing dumps have influence on the soil erosion

problem. Both tailing dumps at Nyala Mine had deep erosion gullies which are evidence of effect of excessive water erosion. The deposition of these alkaline and sandy magnesite tailings in the surrounding farmlands, orchards and woodlands by erosive forces of water and wind is likely to have serious effect on the soil structure and quality in these areas (Sibanda *et al.,* 2013). This is because they are characterized by high pH value (mean = 9. 2) that has potential to affect the availability of plant nutrients such as phosphorus, iron and zinc thus reducing the productivity of the agricultural fields around the mine (Mhlongo, 2012; Quibing *et al.,* 2006).

The different types of water erosion were discussed in the literature (section 2.5). However, the various erosion types were observed within the study area include;

1. Sheet erosion: although not easily observed over a short period, sheet erosion is observed on most undeveloped open lands and areas under development. This is particularly clear from sediment depositions on the planar surfaces.

2. Rill sand inter-rill erosion: On areas with longer overland lengths, rill erosion is observed. This is especially the case on the derelict tailings storage site where gully formation is also observed.

3. Gully erosion: Gully formation was observed on the derelict tailings storage site land use has changed extensively from agricultural to residential and grazing.

1.7 SCOPE OF THE STUDY

The study was focused on assessing the soil erosion hazard associated with abandoned mines using geospatial information technologies. Geospatial technologies are wide and varied, hence this research was limited to the use of Geographic Information Systems, coupled with the SLEMSA soil erosion model as the main methodological approach. Though there are many abandoned mines in South Africa, the scope of this research was based on a case study approach, and in this instance Nyala abandoned mine. Though the results of the study were expected to be restricted to this case study, the whole methodological approach is intended to be applicable to other abandoned mine sites.

The study focused on how abandoned mines affect the susceptibility of soils through assessing the spatial variation patterns in erosion using the SLEMSA erosion model within a GIS environment. The study attempted to provide information useful for effective abandoned mine reclamation and rehabilitation planning. Though it is important to assess the fate of the eroded soil, this study was, however, limited to estimating the potential source areas of contaminated water and ascertain the transport pathways of the mine water. As such no attempt was done to characterize the contaminants in the water and the eroded soils.

1.8 OPERATIONAL DEFINITIONS

Abandoned Mine

An abandoned mine is defined as a non-producing mine whose operation has permanently stopped (Makgae, 2012). Government agencies generally define "abandoned" as mines whose operations halted prior to the introduction of state laws that require reclamation, hence no private party has the mandate for reclamation and no private resources are available to pay for reclamation (Reichardt, 2012).

Erosivity

Rainfall erosivity is the ability of rainfall and runoff to cause soil detachment and transport. Raindrop impact and often runoff from rainfall are the driving forces behind rain or the rainfall energy ability to cause detachment and transport (Lal & Elliot, 1994).

Erodibility

Soil erodibility can be regarded as a measure of the susceptibility of the given soil to particle detachment and its subsequent transportation (Wischmeier & Smith, 1978). Soil erodibility accounts for the influence or response of soil properties on soil loss during rainfall events.

Erosion

Soil erosion is the anticipated rate of soil loss resulting from rain erosion, reliant on the collective and interactive effects of all erosion hazard factors: cultivation system, relief, vegetation, climate, present erosion, land use and soil profile (Bergsma *et al.* (1996: 117).

Geographic Information System (GIS)

A computer-aided system whose purpose is to analyse and display spatial data or a map linked to a database. GIS is an essential instrument for determining nonpoint source pollution control as nonpoint problems are often known to encompass large geographic areas and because the analysis of complex data in various disciplines is instrumental in treatment. Data interpretation and enhanced understanding of causes and solutions are both facilitated by GIS (Clarke, 2001).

Reclamation

It is a process encompassing the rehabilitation of disturbed lands, like mine sites, to their productive purposes and the restoration of disturbed lands to a pre-disturbed state (Mhlongo, 2012).

1.8 STRUCTURE OF THE DISSERTATION

The research thesis comprises six chapters which are as follows:

Chapter one: The first chapter seeks to provide an orientation of the study providing a layout of soil erosion hazard and an introduction to geospatial technologies and the SLEMSA model. It further outlines the motivation and aims of the study and describes the geographical location of the Nyala mine.

Chapter two: A comprehensive review of the literature on soil erosion hazard and modeling is provided in this chapter. The literature articulates the SLEMSA model, its applications, and relevance to the current study.

Chapter three: The chapter looks at the study area by providing the geographical setting, location and contextual background of the abandoned Nyala mine. Furthermore, the chapter looks at the historical background of the mine, mining operations as well as the forms and processes of erosion occurring at the abandoned mine site.

Chapter four: The chapter presents the methodology that was adopted in acquiring, processing and analyzing the relevant data sets used in the research. Thus, it outlines the approach used for the study including the research design, data collection methods, data processing and analyzing techniques.

Chapter five: The chapter details the presentation and analysis of the results obtained from the preceding chapter. The visual presentation is offered in the form of maps and graphs as well as tables where necessary. A detailed interpretation of the results is offered in this chapter accompanied by a discussion of the findings in relation to other similar studies.

Chapter six: The chapter presents the summary and conclusions drawn from the study. The conclusions revolve around the research objectives and questions presented in the first chapter. This identifies gaps in knowledge thus paving way for recommendations and for further studies.

CHAPTER TWO

LITERATURE REVIEW

2.1 INTRODUCTION

Studies on erosion and soil erosion have been ongoing for a long time in the scientific history and the underlying basics of erosion processes have been a subject of study for many decades (Le Roux, 2010; Kim, 2006; Igwe *et al.,* 1997; Lal, 1994). Although the research is a continuous process, more focus is being directed towards the very detailed topic of erosion and soil erosion processes as well as its modeling (Bobe, 2004). Contrary to the comprehensive modeling of physical processes that encompass the splash effect or the influence of clay content on erodibility, there is evidence of intense efforts on the development of universally applicable erosion and soil erosion models. There is considerable diversity behind the concepts of these models extremely; but there is no evidence of any attempts on consistent modeling (Alewell *et al.,* 2015; Alam, 2014).

Various researchers and policymakers across South Africa have recognized erosion as a severe environmental problem. This is supported by references in the National Environmental Action Plan, the State of the Environment Report, and numerous World Bank and other donor-sponsored studies (Garland *et al,* 2000). The link between erosion and environmental pollution is particularly significant. Erosion, however, is one environmental problem with complexities associated with its measure in absolute terms and with its monitoring at different scales (Haarhoff *et al,* 1994). Most current estimates are relied on the results of plot-based empirical modeling, particularly the various derivations of the Soil Loss Estimation Model for Southern Africa (SLEMSA), developed initially by Elwell (1978) in Zimbabwe.

Igwe *et al.* (1997) defined erosion hazard assessment basically as an attempt to evaluate erosion over specified areas under existing land use. The erosion hazard analysis technique is designed to express the physical danger of soil erosion over certain areas. It takes a range of factors of erosion such as rainfall erosivity, soil erodibility and vegetation cover; and

considers which variable best describes each factor's influence on soil erosion, plots individual geographical distributions of each variable and then combines them to estimate overall hazard (Mutowo and Chikodzi, 2013; Nigel and Rughooputh, 2010). A similar degree of hazard can occur on the well-vegetated steep slope as on a bare gentle slope, and the technique is intended to accommodate this as well as discriminate those variables contributing most to erosion. Erosion hazard is basically a way of describing the normal tendency of an environment to permit erosion to occur, and not a survey of the actual erosion (Rydgren, 1996).

The following literature review focuses on the relevant topics in terms of soil erosion assessment using the SLEMSA model and the application of Geographic Information Systems to erosion studies. Moreover, the literature review primarily focuses on the scientific literature of the last several years.

2.2 OVERVIEW OF SOIL EROSION

Soil erosion is a process involving soil particle and material detachment, and their subsequent dispersion by water or wind, which counters the productivity of the land, while promoting land degradation (Mills and Fey, 2003; Morgan, 1995). As such, soil erosion is an issue of great concern in South Africa and throughout Southern Africa (DWAF, 2014; Elwell, 1978). However, because wind erosion appears to be less of a problem in the study area, water erosion will thus be the focus of this study.

2.2.1 Soil erosion dynamics

Soil detachment facilitated by water is a consequence of two processes namely, raindrop impact and surface runoff (Symeonakis *et al,* 2009). In the former, raindrop impact (rain splash) is a result of either the direct through-fall action whereby the soil surface is directly stricken by rainfall or an indirect consequence of leaf drainage whereby the rainfall intercepted by vegetation drips from the vegetation canopy to the soil (Morgan, 1995). It is noteworthy that indirect rain splash impacts less energy on reaching the ground surface than direct rain splash.

From the ground, water may either travel downslope on the land surface where it may either be stored in depressions, or may collect into shallow levels through infiltration, thus contributing to soil moisture, or to deeper levels to increase groundwater storage (Morgan, 1995). The water in the soil tends to occupy or fill the pore spaces between soil particles. Upon maximum infiltration capacity, surface runoff also known as overland flow or sheet is observed (Eltaif *et al,* 2010). Infiltration rate, the rate of soil subsurface penetration by rainfall, is influenced by various factors that include soil texture, compaction levels, and antecedent soil moisture. Soil texture and porosity also influence the rate of rainfall absorption by soil, infiltration capacity (Morgan, 1995).

Infiltration rate is a key determinant of rainfall excess and it can be achieved in two general ways. It can either be by saturation from above, a consequence of short-lived intense rainfall that can quickly exceed infiltration capacity of the soil or saturation from below, a consequence of low-intensity long-duration rain that can slowly saturate the soil (Boardman, 2006). Micro-depressions are the first to accumulate excess rainfall, and upon the soil in micro-depressions reaching their maximum water storage capacity, the lateral flow of water downslope (overland flow) begins (Bobe, 2004). The overland flow may then collect into rills, gullies, and streams. Rills are transient and as such new storm events, weathering, ploughing and tilling of the fields may eradicate them (Saavedra, 2005). On the other hand, gullies are more likely to be more enduring and thus can hold fleeting water flows, making them important agents of accelerated erosion. Gullies, unlike rills, are steep-sided channels which cannot obliterate naturally nor, can they be repaired by normal tilling methods.

Streams are permanent channels in which overland flow concentrates and allow the transportation of water and sediment to the catchment outlet (Boardman, 2006). It is on the hill slopes that inter-rill and rill processes take place. Raindrop detachment is the principal effector of erosion on inter-rill areas, whilst the contribution of transport by shallow flow is minimal (Nearing *et al,* 1994; Le Roux, 2008). Vegetation cover and slope steepness which influence the runoff rate are some of the factors that affect inter-rill erosion.

The mobility of a detached soil particle is depended on the volume of sediment load that can be accommodated in the flow and the flow's capacity (energy) for sediment transport. On the other hand, overland flow rates and slope gradient are the determinants of speed surface runoff and the aspect of the slope is what guides direction. The presence of loosened soil particles together with the capability of the transporting flow to remove the loosened materials impact erosion severity (Morgan, 1995).

2.2.2 Types of soil erosion

Inter-rill erosion

Nearing *et al.* (1994) and Zhang *et al.* (2015) define inter-rill or sheet erosion as detachment of soil by raindrops to be moved by shallow sheet flows. The first phase of inter-rill erosion is detachment of soil by splash erosion (Williams and Ham, 1978; Somayeh *et al,* 2012). Factors that favour the displacement of soil after detachment are topographic, namely, steepness and length of slope (Zhang *et al,* 2015, Panagos *et al,* 2015), runoff rate, and surface roughness (Nearing *et al,* 1994). Zhang *et al* (2015) reported that as slope angle increases there is increased portion of rainfall resulting as runoff having high velocity because of the steepness and flow depth.

Such erosion occurs where there is high rainfall amount that exceeds infiltration capacity and surface depression storage (Morgan, 1995). Depending on this, a land with no pronounced channels may have runoff with smooth depth of water (Panagos *et al,*2015; Morgan, 1995). Consequently, the depth of the removal of soil from the whole area becomes uniform provided that the other soil properties are the same (Samuel, 2014; Nigel and Rughoputh, 2010).

Mutowo and Chikodzi (2013) reported that inter-rill erosion decreases with continued rainfall. This reduction was attributed to the fact that easily erodible soils are eroded whereas the more resistant ones remain uneroded. According to Morgan (2005), generally, overland flow occurs where the area is rich in finer materials. Yet, it is important to note that the detachment capacity of inter-rill flow is smaller than detachment by raindrops because of lower shear force in the

former case (Morgan *et al,* 1998). Since the water depth is shallow the surface roughness causes the flow to vary drastically within a very short distance resulting in considerable scours (Nearing *et al,* 1994; Morgan, 1995).

Most overland flow is related to semi-arid areas or areas with sparse vegetation cover (Nicolau and Asensio, 2000). Thus, vegetation removal becomes responsible for the increase in overland flow (Morgan, 2005). Nearing *et al* (1994) mentioned the occurrence of such erosion on rangelands and no-till situations or on gentle and short-lengthened slopes. According to Mutowo and Chikodzi (2013) reducing rainfall energy by 89%, without decreasing rainfall amount, inter-rill soil loss decreased by 90% or more.

Rill erosion

Rills, which usually range between 100 to 300 mm wide and 50 to 150 mm deep (Mhangara *et al,* 2012), result from overland flow break up and the subsequent channel formation (Morgan, 1995) and can usually be overcome by conventional cultivations (Meshesha *et al,* 2014; Merritt *et al,* 2003). Regarding its formation, however, Morgan (2005) also reported a case in mid-Bedfordshire where rills developed near the bottom of a slope and extended upslope. Sticking to the first notion of rill formation, subsequent development and convergence of flow paths intensify particle movement that causes scouring and channelling. As the channel depth gets deeper, the flow concentration increases to detach more soil particles (Kefi, 2009). Morgan (1995) again echoed studies that showed stages of riling: unconcentrated overland flow, concentrated overland flow paths, micro-channels without head cuts, and micro-channels with head cuts. Since rills, whose sediment source is mainly from inter-rill areas, have concentrated flows, they can transport large grains minimizing size selectiveness (Lal and Elliot, 1994; Morgan, 1995). Morgan (2005) cites the findings of McPhee and Smithen (1984) that reported that 15% of particles carried in rills of 3.5° slope were larger than 1 mm size and that 3% of the particles were larger than 5 mm.

In general, rills account for the most part of erosion (Morgan, 1995). In the USA, a study on a 4.5 m long plot indicated that 80% of sediment was moved in the rills. Mentel *et al.* (2014)

point that rill erosion is predominant in cases of intense storms occurring on soils of high-runoff-producing characteristics and easily erodible topsoil. The sediments enter rills partly from inter-rill areas by overland flow and rain splash (Morgan, 2005). The same author puts the works of Lal (1994) to show that up to 87% sediment in rills may be derived in this way. Whereas, in Belgium it is estimated that half of the material removed from inter-rill areas enter the nearby rills (Morgan, 1995).

The significance of rills is related to their intensity in each area (Morgan, 1995). In Presov, former Czechoslovakia, rills that were spaced 0.330 m apart accounted for 58% of soil erosion that damaged 91 ha of land. Again, in Banska Bystica, of the same country, rills contributed 70% of the total sediment that affected 60% of a potato field. In contrast, rills spaced 300 to 350 m intervals in mid-Bedfordshire, England accounted for only 20 to 50% of sediment loss.

Gully erosion

Gullies are steep-sided channels subject to intermittent flash floods (Hudson, 1995). Unlike rills, gullies are relatively permanent and difficult to reclaim (Zhang *et al,* 2015; Samuel, 2014; Nigel and Rughoputh, 2010). Formation of gullies is so complex to exactly define its process (Mutowo and Chikodzi, 2013). It usually starts with small depressions that allow water concentrations. Concentrated water then joins several depressions and forms channels. Most erosion, here, occurs at the base of the scarp resulting in deepening of the channels, which, in turn, leads to collapse of the headwalls upslope. Further down, sediment loss continues by the scouring action of running water and its sediment, and by falling banks attributed to water saturation. Gullies also form due to sub-surface actions that create tunnels and pipes (Wild, 1993). Morgan (1995) reported that a study in Hong Kong showed that most water was removed from hillsides by sub-surface flow, and heavy rain that fell afterwards resulted in subsidence of the surface leaving the pipes as gullies. Such pipe or tunnel to be a cause for gullying is also observed in the Sudan, the USA, and Hungary (Morgan, 1995).

Gully formation by sub-surface flow is common on slopes where the subsoil has low permeability as in the case of high clay content in the B horizon (Wild, 1993). Landslides are other causes of gully formations. In this case the resulting landform may serve as a channel for running water. Such gully formation was studied in Italy and in Sweden (Morgan, 1995).

The main driving force in gully formation is excessive water on a given land surface that may be caused either by changing rainfall amount or vegetation clearance (Morgan, 1995). Change in rainfall implies higher or lower rainfall to limit vegetation growth, whereas vegetation clearance is usually related to deforestation, overgrazing, and burning of vegetation (Morgan, 1995). Boardman *et al* (2003) reported that overgrazing during the past in the Sneeuberg uplands of Great Karoo, South Africa, is responsible for major gully formations.

2.2.3 Factors that influence soil erosion

The immediate factors that influence soil erosion are rainfall erosivity, soil erodibility, topography, plant cover, and conservation practice (Morgan, 1995). These factors are examined in the following sub-sections.

Erosivity

Erosivity is the ability of an eroding agent to detach and transport soil (Lal and Elliot, 1994; Morgan, 1995). Rainfall and wind are the two important eroding agents of which water erosion is the dominant one (Hudson, 1995). The contribution of rainfall to soil erosion has two phases: detachment and transportation commenced in their respective order (Lal and Elliot, 1994).

Detachment of soil particles occurs as the raindrop strikes the soil. Hence, this part of erosion depends on the energy of the raindrop that, in turn, is the direct result of the speed and the drop size (Birte, 2010; Lal, 1994a). Elaborating, the action of rainfall erosivity, Troeh *et al (1980)* gave ~three effects. First, a raindrop breaks aggregates into smaller aggregates and/or individual particles. Second, it displaces the detached particles as water splashes back into the air. Third, a raindrop compacts the soil aggregates to create surface crust thereby reducing infiltration capacity.

The second step of erosion due to rainfall is transportation. Once soil particles are detached, they are liable to be displaced. Water excess from infiltration and water holding capacity of the soil results in runoff (Onchev, 1985; Morin, 1996). A steep land with minimum vegetation cover or surface roughness allows the surplus water to flow down the slope carrying with it the detached soil particles.

Nevertheless, it is difficult to specifically tell the important characteristics of rainfall erosivity. Ruangpanit's (1985) work at Doi Pui, Kog-Ma Watershed, northern Thailand recognized the existence of the direct relationship between amount, duration, and intensity of rainfall on the one hand and runoff and erosion on the other. Yet, in most cases, it is the rainfall intensity rather than the amount that is directly linked with soil loss (Goldman *et al,* 1986; Morgan, 1995). According to Goldman *et al* (1986), intense rainfall over a short period of time is more erosive than high rainfall amount over long-duration of time with low intensity. Earlier, based on an experiment in Tien Shuy it is stated in Birte (2010) that with an increase in rainfall intensity, surface runoff grew and led to increased soil erosion.

Morgan (1995) reported that rain falling on an area, which is already saturated with previous moisture, results in runoff regardless of its amount or intensity. The next question is finding the threshold value of rainfall erosivity. Studies in various places showed that 25 mm hfl is the critical value, which is a high value for England and Germany that use la mm hfl and 6 mm hfl, respectively. In developing a universal index of erosivity, Onchev (1985) specifies a rainfall intensity of 10.8 mm hf1 and a storm depth of greater than or equal to 9.5 mm as erosive and should be used to derive the rainfall erosivity factor. This approach was shown to have the highest correlation (r=0.877) of all indices including the Universal Soil Loss Equation's EI30 index.

Erodibility

Erodibility is the resistance of a soil to detachment and transport (Flugel *et al,* 2003). Bobe (2004) and Lal and Elliot (1994) define soil erodibility as the measure of soil susceptibility to detachment and transportation. Although soil erosion depends on various factors, erodibility,

which refers to the inherent properties of the soil, is considered one of the most important one (Bobe, 2004). The properties included in erodibility are texture, structure, shear strength, infiltration capacity, organic matter, and chemical content (Borselli *et al,* 2012; Goldman *et al,* 1986; Lal and Elliot, 1994; Miller and Gardiner, 1998). The same sources define soil texture as the relative size and distribution of sand, silt, and clay. Large particles such as sand are erosion resistant because of the force required to displace them, and fine particles such as clay resist erosion because of the difficulty to detach them due to their cohesiveness (Lal and Elliot, 1994). But, once clays are detached from soil aggregates, they are easily transported in suspension until they reach stagnant water (Goldman *et al,* 1986).

Silts, which are classified in between sands and clays, are the most erodible soil particles (Borselli *et al,* 2012; Lal and Elliot, 1994). Soils with 60 % silt are highly susceptible to erosion (Morgan, 1995). Researchers like Evans (1980, cited in Morgan (1995)) preferred to use clay content for determining soil erodibility and defined that soil with 9-30% of clay is taken as the most erodible. Defining erodibility based on clay content looks acceptable since clays readily combine with organic matter content to form a stable aggregation that is significant to reduce detachment and thereby erodibility (Borselli *et al,* 2012*;* Morgan, 1995).

Another soil property that influences erodibility is shear strength, which is defined as a measure of soil's cohesiveness and resistance to shearing forces (Morgan, 1995). Forces that create shear strength are gravity, moving fluid, and mechanical loads. Whenever an external force is applied on soil, the particles tend to slide over one another or break the interlocking forces that include a frictional force (Morgan, 1995). This frictional force is the strength that varies for different soils and hence determines the overall shear strength. Shear strength is also influenced by plant roots and this was shown by Mamo and Bubenzer (2001) who found out a 20% greater strength for corn and soya bean plots than for fallow plots.

Because of their effects on aggregate stability, organic and chemical contents of the soil are

important in determining infiltration capacity (Morgan, 1995; Bobe, 2004). Siegrist *et al* (1998) conducted an experiment to assess the effect of organic agriculture on soil erodibility and concluded that organic plots had better aggregate stability. The other important factor affecting soil erodibility is the type of exchangeable cations that affect dispersion/flocculation (Bobe, 2004; Norton et al., 1999). These authors report that Al^{3+} and Ca^{2+} are known for their binding effects on soil particles creating well-structured soil aggregates, whereas Na^{+} is a dispersal ion that breaks soil aggregation.

Slope

Topographic factors of an area can be characterized by steepness, slope length, slope aspect, and slope shape (Birte, 2010; Morgan, 2005). There is agreement that soil erosion increases directly with slope length and steepness. A steep slope implies a high runoff velocity, and a long slope results in increased runoff volume (Mutowo and Chikodzi, 2013). Birte (2010) reported that doubling the steepness of the slope increases the kinetic energy of runoff proportionally but the carrying capacity increased 32 times.

In addition, raindrops splash soil particles more downslope than upslope and the extent is directly related to the steepness. Morgan (1995) reports that the top of the slope is usually considered as no erosion belt. At some distance from top slope enough water accumulates on the surface to start flowing, which gets deeper as the length of the slope increases (Morgan, 1995).

Plant cover

The role of vegetation in soil erosion prevention is in interception of the raindrops (Goudie, 1981; Stocking, 1994; Morgan, 1995), obstructing surface runoff (Goudie, 1981; Birte, 2010), increasing infiltration (Morgan *et al,* 1997; Haigh and Sansom, 2000; Aragon and Rud, 2012), and binding the soil particles by the root systems (Goudie, 1981; Stocking, 1994). Aragon and Rud (2012) reported that vegetative cover reduced soil erosion in Australia from 30-35-ton ha-I at 0% vegetative cover to 0.5-ton ha-I at 47% cover. Similarly, Mamo and Bubenzer (2001) compared soil detachment of soya bean plots with fallow soils and found out that the former

had one half detachment of the latter. The interception of raindrops breaks them down and reduces the kinetic energy before the raindrops reach the surface (Troeh *et al,* 1980; Stocking, 1994). To prove this an experiment was conducted at a research station in Zimbabwe, where mean annual soil loss from bare ground was 4.63 kg m^{-2} compared with 0.04 kg m^{-2} from *Digitaria* covered land within the same period (Morgan, 1995). The mosquito gauze experiment of Hudson and Jackson (1959, cited in Morgan (1995)) was tested on two identical bare plots, but over one plot fine wire gauze was suspended.

The results showed that the mean annual soil loss over a ten-year period for the open plot was 126.6 kg m^{-2} and 0.9 kg m^{-2} for the gauze-covered plot. Thus, the wire gauze reduced the impact of raindrops on the ground by absorbing the energy. Vegetation contributes to soil loss prevention depending on its height, canopy cover, and root density (Morgan, 1995). Increasing the canopy alone may worsen erosion unless there is enough litter to intercept the drops (Troeh *et al,* 1980). A canopy as high as 7 m can maintain 90% of terminal velocity of raindrops (Morgan, 1995). In addition, raindrops intercepted by leaves usually form a larger drop that exerts greater force on a bare soil below than the drops that reach the leaves (Foster *et al,* 1985; Stocking, 1994; Morgan, 1995). A 3.1 times of open ground soil detachment was observed under beech canopy (Morgan, 1995). In addition, tall trees usually red lice ground cover by their shading effect on understorey growth and this leads to unobstructed surface runoff and exposure of the soil to raindrops (Stocking, 1994). Zhou *et al* (2002) from a study in southern China noted that *Eucalyptus* increased the kinetic energy of the raindrop that led to increased soil erosion when the rainfall amount was greater than 5 mm and rainfall intensities were less than 20 mm.

Such explanation might lead to preference of plants based on the height and size of canopy. For example, according to Morgan (1995), a study showed that cotton reduced the volume of rain reaching the ground but increased the median drop size. Foster *et al.* (1985) reported that an increase in drop size even with short canopies might not be followed by increased soil erosion since raindrops falling from these canopies have low velocity.

The other effect of vegetation on soil erosion is acting as a barrier against surface runoff (Goudie, 1981; Morgan, 1995). Runoff is slowed down only if the obstruction is on the surface that depends on the surface vegetation cover (Antwi *et al,* 2012). Although runoff is not completely blocked, vegetation creates roughness that reduces runoff velocity significantly (Birte, 2010). Moreover, vegetation due to its improvement of granulation increases infiltration rate that has an effect in reducing runoff (Stocking, 1994; Morgan, 1995). A well granulated soil has a higher porosity that improves moisture-holding capacity (Antwi *et al,* 2012; Birte, 2010). Thus, removing vegetation for any purpose results in increased surface runoff and consequently soil erosion (Aragon and Rud, 2012).

2.2.4 Causes of soil erosion

The main driving forces of soil erosion are wide range of human activities that tend to disturb natural stabilities. The causes range from removal of vegetation cover and its impacts to shaping of surface topography that might induce or accelerate soil displacement and movement. The most important causes are summarized separately in this section.

Agriculture

From all-natural components land is the first asset that a human being acts on. The most important reason behind this is agriculture (Miller and Gardiner, 1998). Cultivation in South Africa, for example, on erodible soils has been one of the main reasons for soil erosion (Scotney and McPhee, 1992; Laker, 2000). Agriculture requires considerable land and every new land must be obtained by clearing a relatively well-established natural forest area. For example, five sixth of South Africa's total land is under agricultural use (Adler, 1985). Agriculture can be linked to soil erosion in different ways some of which are explained as follows. First, removing the natural vegetation cover exposes the soil to any kind of external actions that lead to its removal (Troeh *et al,* 1980). Heat, rainfall, and wind readily make their actions and erode the soil.

The second effect of agriculture on soil erosion is cultivation through disturbance of the top layer of soil, which should be given more attention. Since crops are seasonal or short-lived,

they are removed after the harvest is exploited, every time of which leaving the soil loose and easy for dislocation. So, two effects are registered here, namely, breaking up of the soil particles as compared to the well-stabilized characteristics under natural condition and exposing the ground surface unlike the full canopy and litter cover of the natural vegetation. To study the effect of cultivation on soil loss, Choudhary *et al* (1997) took three soil samples representing mould board ploughed, chisel-ploughed, and no-till soils from a Wooster silt loam of Ohio, which was under corn cultivation for 32 years. After subjecting the samples to a simulated rainfall, soil erosion and runoff were found to be the highest for mouldboard-ploughed and the least for no-till soil.

The third effect can be related to the system of tillage. Tapia-Vargas *et al* (2001) examined the impacts of various combinations of residue cover and tillage levels on runoff and sediment yield in Mexico. The treatments were conventional tillage, no-till with zero residue cover, no-till with 33% residue cover, and no-till with 100% residue cover. The results showed that the first two treatments had higher runoff and sediment yield leading to the recommendation of no-till farming.

Overgrazing

In addition to cultivation, overgrazing is also an important cause of vegetation clearance and the subsequent soil erosion. This is the main cause in South Africa (Laker, 2000). Uncontrolled or poorly managed grazing brings about removal of vegetation that exposes the soil to all types and processes of erosion. Bari *et al* (1995) conducted an experiment in Pakistan by applying various levels of grazing on different plots and found that no-grazing treatment produced the least sediment accumulation. In southern Iceland, Simpson *et al* (2001) conducted a study to examine the effect of grazing on soil erosion and reported that the management aspect of grazing is more responsible than the stock numbers, a view shared by Zobisch (1993) from a study in Kenya. The work of McEldowney *et al* (2002) in Colorado, USA related high amount of sediment deposition with decrease in stem density, due to increased overland flow from grazed field as compared to the non-grazed.

Another major problem usually related to livestock is their trampling effect as assessed by Eldridge (1998). The researcher used a sheep's hoof at different levels to represent stocking rates and found that trampling increases soil erosion significantly. The results of this study indicated that trampling accounted for 33% of the total soil erosion. In assessing grazing effects on soil physical properties in eastern Nigeria, Asadu *et al* (1999) revealed that trampling compacted the soil surface under study and reduced the macro porosity and total porosity resulting in reduced hydraulic conductivity. Compared to non-grazed arable fields the reduction in total porosity and hydraulic conductivity amounted to 15 and 60%, respectively.

Fire

Johansen *et al* (2001) conducted a study in New Mexico, USA to examine the effects of fire on runoff and soil erosion. The findings revealed that 45% of the applied 120 mm precipitation resulted in runoff from the burned plot as compared to 23% of the same precipitation amount from the unburned plots. Soil loss from post-burned was 25 times greater. This study formulated a correlation of r=0.84 between sediment yield and percentage of bare soil.

A similar finding is reported by O' Dea and Guertin (2003) in an area of southern Arizona grassland. The authors also recorded increased bulk density, runoff, and soil erosion on the one hand and lower plant cover, aggregate stability, and water intake on the other after burning grassland plots. A comparable conclusion of higher erosion and sediment yield was obtained by Wilson *et al* (2001) in New Mexico who compared pre-fire with post-fire scenarios by employing a GIS aided profile-based model called hillslope erosion model (HEM-GIS). However, prescribed and controlled burning well before the rainy season might have a positive effect on sustaining or improving the vegetative cover of an area and thereby reducing sediment production as observed in the montane grasslands of Natal (Everson *et al,* 1989).

Construction and roads

Construction sites pose very high risk of soil erosion (Hudson, 1995). Goldman *et al* (1986) reported that construction results in the most concentrated soil erosion that could reach from

2 to 40 000 times the undisturbed rate. Li *et al* (2011) examined the effect of wheels on infiltration under simulated rainfall. Their results concluded that traffic wheels reduced infiltration rate and time to ponding. The decrease in the rate of infiltration rate was found to be 4-5 times as compared to non-wheeled surface. Another study undertaken in Sam Mun, Thailand by Ziegler and Giambelluca (1997) to assess the impact of rural roads on runoff generation also recognized that the infiltration rate and hydraulic conductivity of unpaved roads were low leading to overland flow.

Nyssen *et al* (2002) recorded the effect of roads on gully formations in north Ethiopia. On a road segment of 6.5 km, 9 new immediate segments were created with additional seven further downslope. The researchers explained the reasons for the gullying as the road introduced concentrated runoff, increased catchment size, and diverted concentrated runoff to other catchments.

2.3 SOIL EROSION ASSESSMENT

Parallel to the awareness of the soil erosion problem people have long been trying to sustain agricultural productivity while fighting soil loss (Hakkou, 2014). In modern days, fighting soil loss has based itself on the result of an appraisal of the problem (Hakkou, 2014). Clearly, this approach helps where and how to act depending on the nature and extent of the problem. Assessment of soil loss has grown from the simplest and qualitative methods to more comprehensive and quantitative methods. Recently, the vision in soil erosion assessment has turned towards accounting for much more complex parameters, which, no doubt, provide a more reliable estimation, with the need for large input data (Lorentz and Schulze, 1994).

Of all the approaches, the USLE and its successor the RUSLE, are the most widely applied in the world (Lorentz and Schulze, 1994; Lorentz and Howe, 1995; Smith, 1999; Ritchie, 2000) despite their development from the database of the USA. These models were developed to help guide conservationists in the design to fight soil loss (Wischmeier and Smith, 1978; Renard *et al.,* 1997). Though the USLE was earlier considered unsuitable for Southern Africa

by Elwell (1978), Smith (1999), in his revision of empirical models, concluded the RUSLE model to be potentially robust if applied in South Africa.

While soil erosion assessment is yet a difficult task (Higgitt, 1991) because of the complexity of the factors governing the problem, it is becoming an interesting field of study credited to its integration with remote sensing and Geographic Information Systems (GIS) technologies (Rooseboom *et al, 1992).*

The use of GIS appears to be a necessity in soil erosion assessments (De Roo *et al,* 1989; Flacke *et al,* 1990) as the latter involve spatial variation due to nature's complexity and management impact. In most recent times nearly, all soil erosion assessment methods are integrated well with GIS because of the simplicity of spatial analyses.

Remote sensing has been used in land degradation studies by using ground based and aerial photos (Ritchie, 2000). The technique makes use of sensed spectral difference of ground features to interpret and classify an area based on its erosion status. Ritchie (2000:276-277) summarized the application of the technology in soil erosion assessment to be in the form of "photointerpretation / photogrammetry, model/GIS inputs, spectral properties, and topographic measurements." With time, this technology increased its involvement by providing more reliable information that can be quantified with better confidence. The technology is enjoying its wide acceptance for many reasons including its coverage of large and inaccessible areas, collection of data within short periods of time that helps take repeated information from a given area within a year, collection of data in a continuous form which leaves no space for non-measurement-points, and provision of data that can readily be read and analysed in a GIS environment (Engman, 1995).

2.4 SOIL EROSION MODELS

A soil loss model is a way of bringing together the various factors and process of erosion in a way that they accurately reflect what occurs and soil loss is predicated accurately (Anache *et*

al, 2015; Bartsch *et al,* 2002). However, because soil erosion is the result of complex factors and interrelationships, a perfect model with universal applicability and extension to any combination of circumstances is unattainable. As such, most soil erosion models are of parametric 'grey-box' type which picks what are the assumed important variables and establish statistically significant relationships between these and the output of the model i.e. soil loss (Bizuwerk *et al,* 2008).

Modelling is vital for the mathematical description of soil (Gregory, 2004; Nearing *et al,* 1994). From Gregory's (2004) point of view erosion models can;

1) Be used as tools for predicting soil conservation and land conversion planning, and for the assessment of soil erosion and productivity;
2) Aid erosion reduction activities by predicting the time and place for the probable occurrence of erosion;
3) Be used as tool whose priority is data collection and research emphasis through the enhanced understanding of erosion processes.

Erosion assessment techniques founded on uncomplicated erosion models with limited input data are essential for defining high-risk areas of erosion (Mallick *et al,* 2014). In addition, they serve a purpose in assisting with the design of appropriate conservation strategies that offer guidance in regional planning, environmental monitoring, and land utilization programs. Kamarange *et al.* (2016) indicated that various changes in model parameters and sub-parameters, the relative sensitivity of land to erosion hazard can be assessed with the aid of erosion assessment techniques. According to Stocking (1984), it is vital for erosion models to possess inputs, outputs with some connection to preservation actions and economic action plans for better soil management, connections to physical or observed expressions that link erosion to productivity losses, and suitable structure to govern planning of proper or essential field research.

The three types of soil erosion models are either empirically based, conceptually based or physically based (Mantel, 2014; Bobe, 2004).

2.4.1 Empirical Models

Empirical models are a basic representation of natural processes founded on empirical observations. Due to their basis of observations of the environment, empirical models are often of statistical relevance (Nearing *et al,* 1994). Some of the uses of empirical models include modeling complex processes and, with regards to erosion and soil erosion, the identification of the sources of sediments (Merritt *et al,* 2003). Table 2.1 highlights some of the common empirical models and their sources.

Table 2.1: Empirical models

Model	**Reference**
Equation (MUSLE) Sediment	Renfro (1975)
Universal Soil Loss Equation (USLE)	Wischmeier and Smith (1978)
Soil Loss Estimation Model for Southern Africa (SLEMSA)	Elwell (1978)

2.4.2 Physically-Based Models

Physically-Based models represent natural processes through the description of each individual physical process of the system and the subsequent merging of these systems into a complex model. Thus, physical equations describe such natural processes as streamflow and/or sediment transport (Merritt *et al,* 2003). High resolution spatial and temporal data are necessary for this complex approach. Specificity is a significant quality of physically-based models that result from the complex approach incorporated in their design (Merritt *et al,* 2003). In Table 2.2 are physically-based models that are vital in aiding the explaining of the spatial variability of the crucial features of land surface, that include topography, slope, aspect, vegetation, soil, as well as climate parameters that encompass precipitation, temperature, and evaporation (Legesse *et al,* 2003).

Table 2.2: Physically-based models

Model	**Reference**
Areal Non-Point Source Watershed Environment Response Simulation (ANSWERS)	Beasley *et al.* (1980)
Chemical Runoff and Erosion from Agricultural Management Systems (CREAMS)	Knisel (1980)
Water Erosion Prediction Project (WEPP)	Laflen *et al.* (1991)

2.4.3 Conceptual Models

Being a mixture of empirical and physically-based models (Table 2.3), conceptual models are efficient in answering general questions (Bartsch *et al,* 2002). Conceptual models are simple as they usually incorporate general descriptions of catchment processes which require inexhaustive catchment information (Merritt *et al,* 2003). It is thus apparent to take note of the importance these models as indicators of quantitative and qualitative processes within a catchment.

Table 2.3: Conceptual models

Model	**Reference**
Renard-Laursen Model	Renard and Laursen (1975)
Sediment Routing Model	Williams and Ham (1978)
Agricultural Catchment Research Unit (ACRU)	Schulze (1995)

2.4.4 Soil Erosion Modelling Parameters

According to Elwell (1978b) and Elwell & Stocking (1976); climate, soil, vegetation, and topography are the physical factors that are involved in controlling erosion. The modeling of soil erosion is governed by the following measurable and estimable factors; rainfall erosivity, soil erodibility, vegetation cover and topography (Smith, 1999; Dee Roo, 1996). It is noteworthy that these parameters are more interconnected than they are independent. Erosion pattern and magnitude are governed by the extent of association amongst these

parameters is what controls the pattern and magnitude of erosion (Morgan, 1995). On the other hand, rainfall erosivity, which is the ability of rain splash to detach soil particles by the dispersive capability of rain (Smithen and Schulze, 1982) and soil erodibility, which is the dispersive ability of the rain to disengage soil particles through rain splash (Smithen and Schulze, 1982) are what best describe climatic factor. Soil erodibility is the resistance to dispersion and the subsequent removal of soil by raindrop impact and running water.

Rainfall Erosivity

The climatic factor in the estimation of soil loss, rainfall erosivity, is the capability of rainfall to remove soil particles by the power exerted by raindrops smashing the soil surface (Stocking and Elwell, 1976a; 1976b). Physical conditions that are influenced by the amount and distribution of precipitation include soil moisture, the extent of soil erosion and vegetation cover (Elwell, 1996). Precipitation is instrumental in soil erosion by facilitating the detachment of soil particles through the impact exerted by rainfall and their subsequent entrainment by overland flow (Choi, 2012).

Apart from rainfall intensity and duration of rainstorms, some features of raindrop like mass, diameter, and velocity are important factors that impact rainfall erosivity (Morgan, 1995). The kinetic energy of rainfall is the major factor in the erosivity index of all models discussed in this study. A research by Lal (1994) in the eastern part of the United States showed a positive linear relationship between the size of drop and the intensities of rainfall. In addition, Eltaif (2010) observed a positive linear relationship rainfall erosivity and rainfall intensity.

This observation agrees with the relationship that exists between the average soil loss increase and increasing rainfall intensity in temperate climates observed in a study by Nearing *et al.* (2014). Research in Zimbabwe by Mutowo and Chikodzi (2013), however, indicated that at rainfall intensities greater than 100 mm/hr, this observation did not hold true despite the increase in raindrop size associated with increasing rainstorm intensities. On the contrary, it was observed that the median drop size decreased with increasing rainfall intensity at higher levels (Mutowo and Chikodzi, 2013).

Soil Erodibility

Soil erodibility, which is also responsible for soil loss, refers to the resistance the soil exhibits to the detachment and the subsequent transportation by erosive agents (Yang *et al,* 2005). In a study by Antwi *et al.* (2012); topography, the amount of bioturbation and; the level, intensity, and type of human and animal activity were identified as factors that influence the soil's ability to resist erosion. In addition to the above-mentioned factors, are soil characteristics namely; texture, cohesiveness, antecedent soil moisture content, infiltration capacity, organic matter content, and chemical composition that influence soil erodibility (Mills and Fey, 2003; Morgan, 1995).

It has been observed that the greater amount of energy that is required to transport large-sized soil particles allows them to exhibit some level of resistance transportation, whilst the cohesive nature of the finer particles equips them with the resistance to detachment (Mills and Fey, 2003). The cohesiveness of soil relies on the chemical bond that exists between the clay minerals and on the surface tension forces within the moisture that covers unsaturated soils (Lal and Elliot, 1994). Soil and cover properties are two important resistance factors that equip the soil's resistance to the forces of water flow (Amsalu and Mengaw, 2014). Erodibility is greatly determined by the chemical composition of soil, which in turn regulates the proportion of easily dispersible clays.

Soil resistance and cohesiveness wielded by running water, gravity and mechanical bonds are both influenced by soil moisture content (Morgan, 1995). Any upsurges in soil moisture content may cause changes in soil behaviour, for instance, wet soils are less erodible than dry soils. However, beyond a certain threshold, further wetting of the soil may cause loss of soil cohesion, leading to the soil reacting like a liquid. Yang *et al.* (2005) noted that organic matter and clay are important soil components that aid soil particles to stick together into clumps that can resist being washed or blown away, thus soils that contain both materials tend to be more resistant to erosion. Organic matter, whose buildup is promoted by both cooler climates and long rainy seasons, tends to add to good absorption properties of soils, hence soils with plenty

of organic matter behave like sponges which absorb a lot of rainfall. Due to the long dry season characteristic of Southern Africa, most Southern African soils have little amounts of clay and organic matter (Flugel *et al,* 2003).

Vegetation Cover

There are three known ways in which soil erosion is affected by plant cover. Firstly, there is a direct relationship between the detachment facilitated by raindrop impact and the amount of protection that plant cover provides. Therefore, the canopy aids in minimising the erosive energy of raindrop impact as most of the energy is absorbed by the leaves, branches, stems, and trunks prior to rainfall hitting the soil surface (Elwell, and Stocking, 1976).

Secondly, the surface roughness of the soil brought up by plant roots and litter slows the overland flow, which also reduces erosion. The surface roughness that is characterized by both vegetation cover and soil surface characteristics, influences both the amount and the rate of runoff. Also, the amount of plant litter, often composed of dead biomass or crop residue enhances surface roughness, therefore reducing overland flow.

Finally, the root mass of the vegetation which enhances soil structure and makes up organic matter upon decomposition plays a vital role under the soil surface. Organic matter is a rich nutrient reservoir that provides the nutrients essential for increased plant productivity. Increased plant productivity increases canopy cover, which in turn leads to reduced rainfall erosivity as it minimizes the impact rainfall has on the soil. Furthermore, soil types with certain types of organic matter are thought to exhibit increased resistance to erosion by promoting the stability of soil aggregates.

2.4.5 Model Selection

According to Gobin *et al.* (2003), the availability of input data may be an essential influencing factor in the selection of an erosion model on the regional or national scale. This is because of the impracticality associated with the usage of a sophisticated model in the presence of insufficient data. On the regional scale, making certain variables and model parameters

constant may be the best and only option for running a complex model (Nearing, 1998). Prosser *et al.* (2001) identified this as the dominant reason for selecting the empirical relationships as a model of choice for predicting soil erosion on a regional scale. The Universal Soil Loss Equation (USLE) which is one of the 1970s developments of the United States Department of Agriculture (USDA), together with its upgraded version, the Revised USLE (RUSLE) is the extensively used empirical model for soil loss estimation at the regional scale (Wischmeier and Smith, 1978; Renard *et al,* 1994).

The target for the development of USLE were for hill slopes and fields and not larger drainage basins. Although the database of USLE is restricted to the Eastern United States, over 10,000 years of records are represented by USLE and it is extensively recognized as reliable (Morgan, 1995; Renard, 1997). Further restrictions limit its application to slopes where cultivation is permissible at 0-18 degrees under normal conditions (Morgan, 1995; Renard, 1997). The most commonly used empirical model to estimate and predict soil erosion in the US and the rest of the world is USLE. USLE takes the following form:

$$E = R \times K \times L \times S \times C \times P \qquad (2.1)$$

where;

- E, the average yearly soil loss,
- R, the rainfall erosivity factor,
- K, the soil erodibility factor,
- L, the slope length factor,
- S, the slope steepness factor,
- C, the crop management factor, and
- P, the erosion control factor.

The fundamentals of USLE lie within the statistical relationships that exist between input and output of the hydrologic system. On the other hand, RUSLE (Revised USLE) is a computer-based modification of USLE, which uses new ways for the estimation of the six factors in the

model (Ganasri and Ramesh, 2016). With the application of computers in both models, it has been possible to conduct increasingly complex quantitative analyses.

Many regional scale erosion studies from all over the world have incorporated the (R)USLE and its derivatives (NRI, 2001; Gobin *et al,* 2003; Lu *et al,* 2003). The commonly used empirical models in South Africa include USLE (Crosby *et al,* 1983; McPhee and Smithen, 1984; Smith *et al,* 1995; Smith *et al,* 2000), RUSLE (Haarhoff *et al,* 1994; Pretorius and Smith, 1998) and the Soil Loss Estimation Model of Southern Africa (SLEMSA), which was developed by Elwell (1976) (Schulze, 1979; Hudson, 1987).

For this study, several factors were taken into consideration in choosing a specific empirical model. These factors include;

1) the physical authenticity of empirical equations resulting from independent experimental research;
2) simplicity, which refers to the relative availability of the input data; and
3) applicability, as proven by the capability of being used by other Southern African nations with similar climatic conditions and physiographic regions.

The study adopted the Soil Loss Estimation Model of Southern Africa (SLEMSA) because it is better at predicting spatial patterns of differences (Stocking *et al,* 1988). Most Southern African countries have adopted the model (Elwell, 1978) and Schulze (1979) further argues that the model may be considered useful in differentiating areas of high and low erosion potential. The model is versatile and is easily adaptable to available data, or to a specific case study. It can also allow the combination of reasonable accuracy without requiring extremely elaborate and costly field experiments. In addition, flexibility is maintained using rational and easily-measurable parameters such as rainfall interception, while refinement and updating of incorporated information can be done depending on the availability and the time of availability of new data.

2.5 THE SLEMSA MODEL

As highlighted in section 2.1, Soil Loss Estimation Model for Southern Africa (SLEMSA) was initially developed principally from data from Zimbabwe for evaluating the erosion emanating from diverse farming systems, to ensure recommendation of proper conservation measures could be recommended. Southern African have adopted the technique (Elwell 1978). The SLEMSA model is essentially a model for soil removal (Paris, 1990), which is regarded useful in differentiating areas of high and low erosion potential (Igwe, 1997).

According to Stocking et al (1988), the foundation of SLEMSA lies within is built on a mixture of factorial scoring methods and empirical relations with drivers of erosion. Through the SLEMSA model, soil erosion environment has been categorized into the following four physical systems; land cover, climate, soil and topography (Elwell, 1978). The design of the model is like that of USLE, but there is a difference in the method for combining the inputs. The USLE assigns the same weight to all inputs, whilst SLEMSA assigns more weight to the crop factor. Estimation of the erosion risk with SLEMSA requires that an initial erosion hazard index (Ib), which incorporates rainfall energy (R) and the soil erodibility class (K) be calculated first. The definition of Ib is the erosion hazard for bare soil at a 4.5 % slope of 30m long with potential exponential increase related to increasing rainfall energy and increasing soil erodibility. Calculation of the final erosion hazard index is conducted through the multiplication of *Ib* by a cover factor (C) and a slope factor (X).

2.5.1 Calculation of the SLEMSA Model

Data from the Zimbabwe Highveld is the largest contributor to the data used to develop SLEMSA. According to Elwell (1996), the creator of the model, the SLEMSA framework is a methodical approach for developing models with the main function of estimating sheet erosion that arises from arable lands in southern Africa. A body of experimental data complemented with extrapolated data (date in which relationships are presumed) are the significant components of the model (Stocking, 1980). Its design allows the integration of practical advantages of empirical methods which can accommodate new variables with no prior

individual monitoring (Stocking, 1980). Elwell (1978) acknowledged that this compromise would lead to a lot of inaccuracy, however, there it was pertinent that developing countries like Zimbabwe and South Africa find the urgent answers of the right order of magnitude to allowing planning for conservation.

As highlighted in Figure 2.1, the SLEMSA model allows the division of the soil erosion environment into the following four physical systems: crop, climate, soil, and topography.

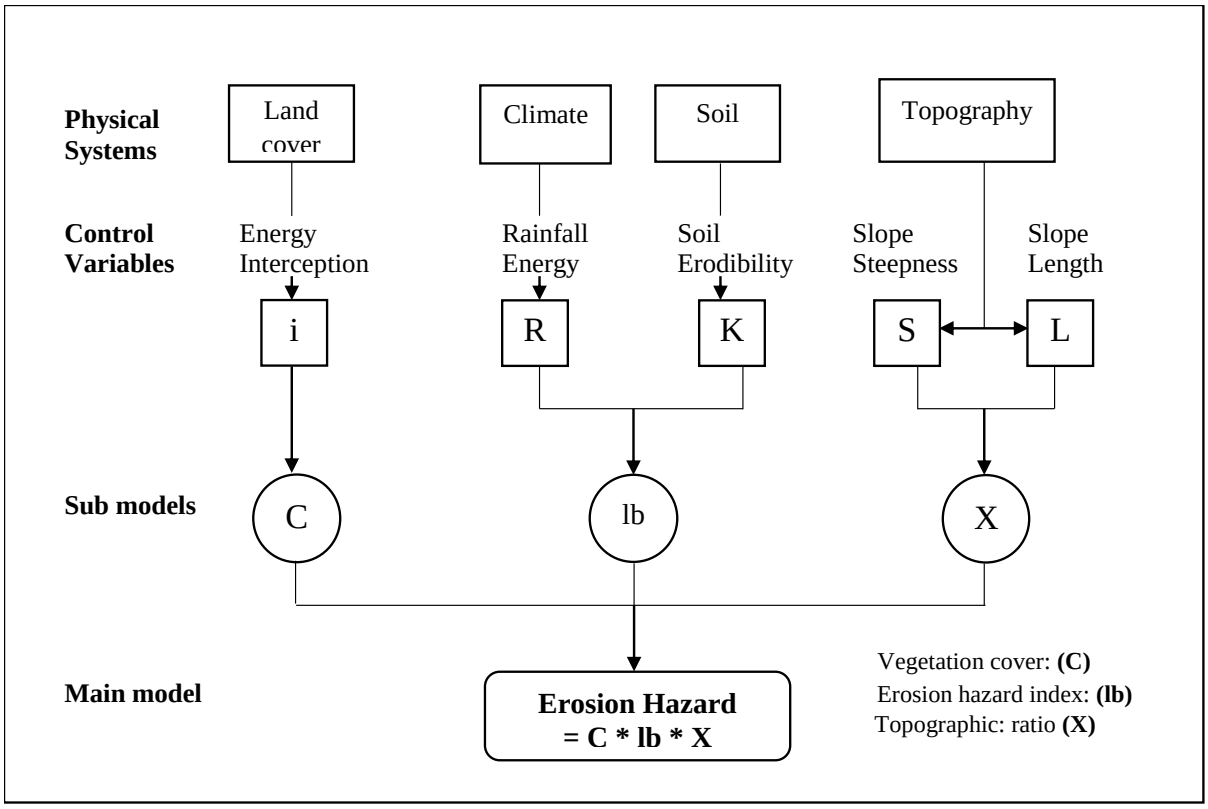

Figure 2.1: The SLEMSA model (Adapted from Elwell and Stocking, 1988)

Subsequently, the selection of the main control variables for each system based on their measurability is done, and they are the dominant factor in each system (Stocking, 1980). Thereafter, the control variables are pooled into the following three sub-models: the bare soil sub-model, the topographical sub-model, and the crop sub-model. The main model is thus represented by these three sub-models multiplied together. The SLEMSA equation is as follows:

$$\boldsymbol{Erosion\ Hazard = lb * C * X} \quad (2.2)$$

Where:

lb = Erosion Hazard Index

C = Land cover factor

X = Topographic Ratio

2.5.2 SLEMSA Model Parameters

Accumulated and individual rainstorm are empirical regression equations of the seasonal rainfall energy of mean annual rainfall (Ali and Hagos, 2016; Angima *et al,* 2003; Jain *et al,* 2001). Soil type (F-factor): Respective combination of soil type-texture is classified into a soil erodibility class that ranges from 1 to 10. Land use and management are factors that determine the erodibility of most soils (Elwell, 1988). Incorporation of a range of factors including soil management, internal drainage, lithic contact, abrupt soil textural exchange and/or the sensitivity to capping can allow for the modification of the F-factor. SLEMSA is very sensitive to these modifiers. Vegetation: Estimation of the proportion of rainfall intercepted by vegetation is done with the aid a crop-specific cover percentage. Its calculation is based on a non-linear function of rainfall interception and is associated with a cover factor that articulates soil loss ratio relative to bare ground (C). The mean % slope and slope length. This is recalculated into a slope factor (X).

Erosion is a complex process and can certainly not be quantified exactly in any simple formula where conditions vary. The Erosion Hazard Index (EHI) is expressed as a dimensionless number in Erosion Hazard Units (EHU) on a scale of 0-100. According to Stocking *et al.* (1988), these should not be interpreted as soil loss in tons per ha, but it is more the relative variation in the number than the actual values that are important when comparing erosion hazards over an area.

2.5.3 Erosion Hazard Index

The erodibility factor (*K*) is expressed as the yearly soil loss (tons. ha-1. yr-1) from an ordinary traditionally cultivated field plot 30m by 10m on a 4.5 % slope for a soil with known erodibility, *F*, under a weed-free fallow (Stocking, 1980). The determination of the erodibility factor is based on the rainfall energy and soil erodibility control variables.

The soil loss sub-model (lb) is an expression of soil erodibility (Fb) and rainfall energy (E) in the general form;

$$\ln(K) - b \ln(E) + a \quad (2.3)$$

Where:

$$a = 2.88 - 8.121(Fb) \quad (2.4)$$

$$b = 0.468 + 0.766(Fb) \quad (2.5)$$

and thus

$$K = \exp(2.88 - 8.121(Fb) + \ln(E)(0.468 + 0.766(Fb)) \quad (2.6)$$

Where:

E = rainfall energy and

Fb = soil erodibility.

E - Rainfall energy

Due to the complexity associated with the derivation of rainfall erosivity, which is simply the dispersive ability of the rainfall that detaches soil particles, Elwell (1978b) thus used the annual rainfall data for a forty-four-year period regressed with rainfall energy to formulate the relationships used in SLEMSA. And since the calculation of rainfall energy is dependent on data from a recording rain gauge, Elwell then went on to develop a regression relationship between rainfall depth (P) and rainfall energy (E) for the available stations.

Rainfall energy is the average seasonal rainfall energy for the growing season. Thus, the calculation of SLEMSA has relied on recording rain gauge data from seven locations in Zimbabwe for over a 20-year period. Data from 22 other sites with about 10 years of recordings and intensity data for sic different intensity classes were used as supplement to the data (Elwell, 1978b; Stocking and Elwell, 1976).

Several methods are used to calculate rainfall energy (Eltaif *et al,* 2010; Symeonakis *et al,* 2009). The relationships between rainfall kinetic energy in Joules/m^2 (KE) and average rainfall intensity in mm/hr form the foundations for the energy calculations for SLEMSA (i):

$$KE = 29.82 – 127.51/i \quad (2.7)$$

The relationships highlighted above were formulated for the Zimbabwean areas prone to receiving high rainfall intensities. Rainfall energy for each event in Joules/m^2 is then calculated by multiplying the rainfall depth for the storm (in mm) with the above-mentioned value. Annual rainfall energy is a measure of all combined events for the year. With E from linear regression analyses between seasonal rainfall energy and mean annual rainfall, Elwell (1978b; 1988) managed to develop the following SLEMA relationships;

For "*non-guti*" areas:

$$E = (18.84)\ (PPT) \quad (2.8)$$

For *"guti"* areas:

$$E = (17.36)\ (PPT) \quad (2.9)$$

Where:

PPT is the long-term mean annual rainfall.

Figure 2.2 represents the correlation of the K sub-model and rainfall energy for mean annual precipitation between 800mm and 2000mm. The variations in the importance of rainfall energy in calculating K above and below the point of increase in the slope of the line at about 22,000 J/m^2 are indicated. According to Equation 2.8, there is a relationship between a rainfall energy of 22,000 J/m^2 with approximately 1400 mm of mean annual precipitation.

Fb - Soil erodibility

Lal and Elliot (1994) defined erodibility as the soil's resistance to dispersion and removal and the initial soil erodibility designations were based on soil texture, using a scale of 1 to 10, with 1 representing most erodible and 10 representing least erodible. Adjustments were made for the soil profile characteristics and for tillage and crop management practices for this basic soil

erodibility (Lal and Elliot, 1994). There is an inverse proportion between the sub-parameter Fb as defined by Elwell (1978b) and soil loss. Consequently, higher resistance to erosion is represented by corresponding high value of F, and, on the other hand, the relationship between other sub-parameters and soil loss is directly proportional.

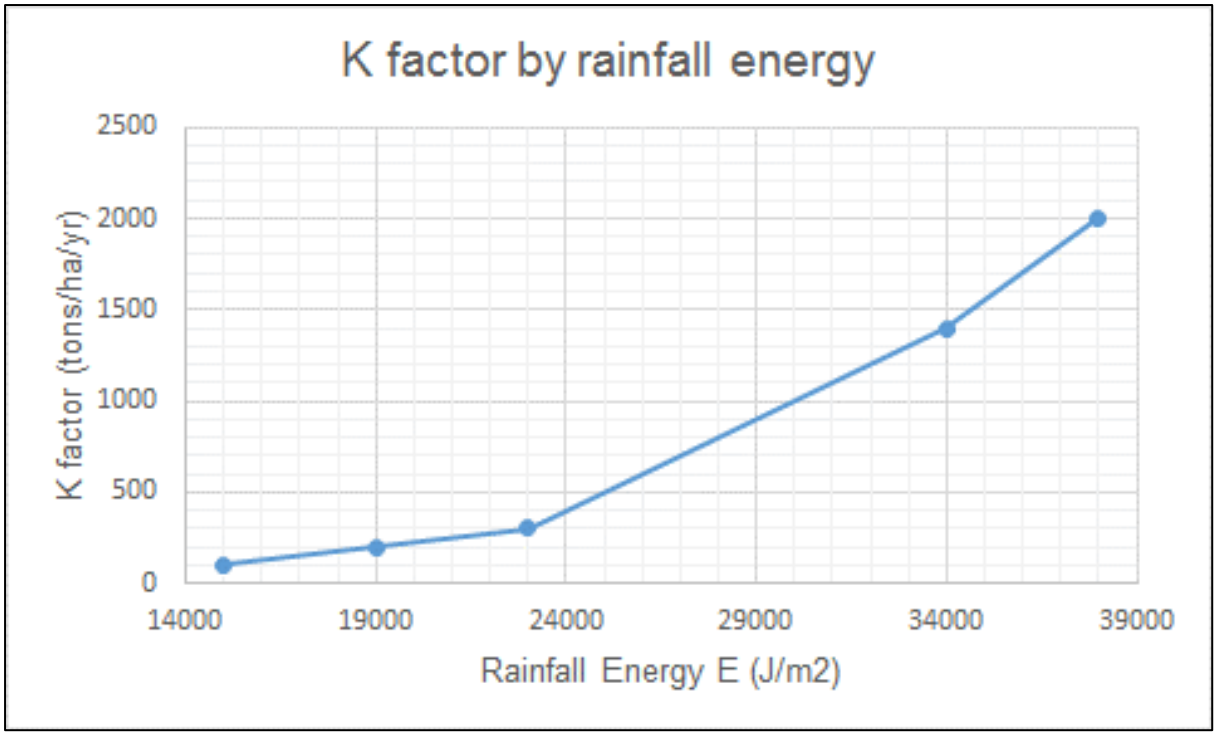

Figure 2.2: Relationship between K sub-model and rainfall energy (E) using a constant soil erodibility (Fb) in the SLEMSA model (Elwell, 1978b).

The absence of a direct way for measuring soil erodibility prompted the use of a simple indexing method based on soil texture (light, medium or heavy) and soil type to produce soil erodibility values (Antwi *et al,* 2014). Soil treatment from previous and current management practices with the ability to reduce infiltration while increasing runoff or alter the soil's resistance to detachment was used as template for modifying the basic index. Figure 2.3 shows that when the slope of the line increased, the influence of the Fb values less than 4.5 on the K sub-model was also increased (Lal and Elliot, 1994).

Determination of the basic soil erodibility index, Fb, is governed rating soil characteristics of soil groups like textures and others. The modification of Fb values can be done through the

subtraction and addition of an incremental value called Fm, which represents farm management practices. The sum of Fb and Fm gives us soil erodibility (Elwell, 1978b):

$$F = Fb + Fm \quad (2.10)$$

Where;

Fb is the base soil index modified by texture and other characteristics and

Fm represents farm management practices.

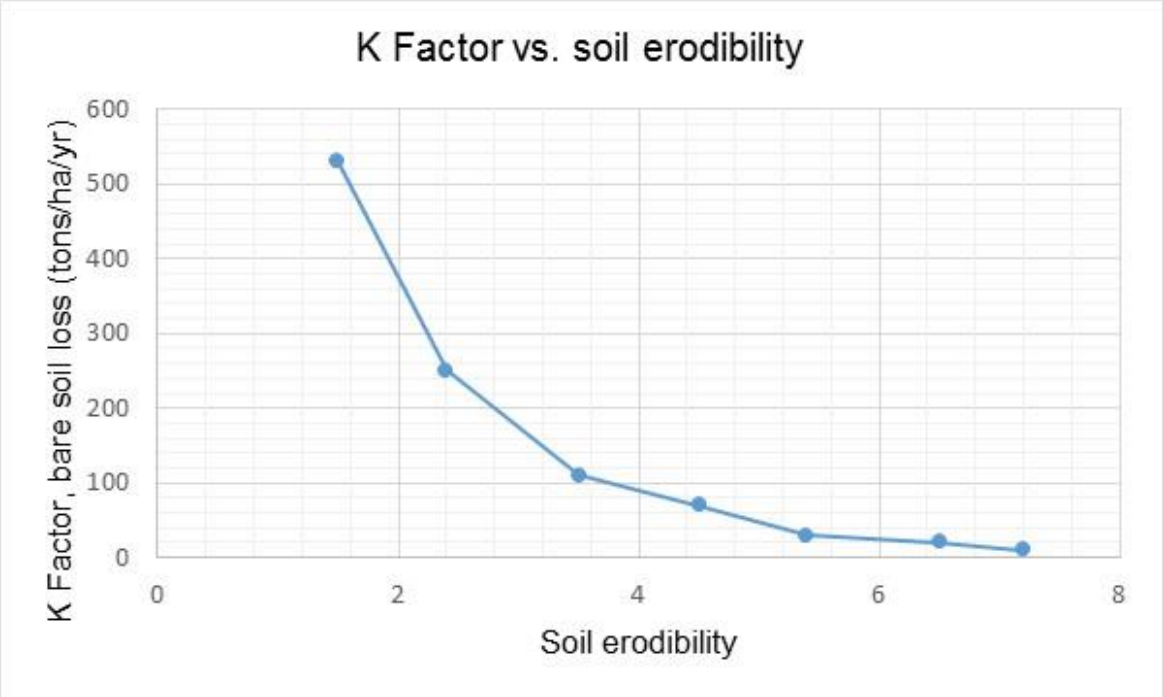

Figure 2.3: Relationship between K factor and the sub-parameter soil erodibility (Fb) in the SLEMSA model while rainfall energy is held constant (Elwell, 1978b).

2.5.4 Land Cover Factor

The land cover factor (*C*) is the ratio of soil loss from a vegetated land to the lost from bare fallow land (Alphan *et al,* 2009). The energy interception factor, *i*, is a derivative of C, and *i is* in turn determined by the vegetation type, yield, and natural grasslands, dense pastures and mulches (Mughogho, 1998).

Elwell (1978) was the developer of the relationship that exists between energy interception and soil loss, and the development was done in Zimbabwe. This relationship forms the basis of the cover sub-model (C), whose variation is exponential and is between 0 and 1 (Stocking,

1987; Garland *et al,* 2000). The interception value, i, which is the percentage rainfall energy that is caught by vegetation offers a reasonable explanation for soil protection from erosive forces due to vegetation by percentage of rainfall energy intercepted by vegetation. The value of i that is calculated as shown below, governs the relationship of i to C:

when the interception value (i) is less than 50%, then

$$C < 50\% = e^{-0.06i} \quad (2.11)$$

when the interception value (i) is greater than 50%, then

$$C > 50\% = (2.3 - 0.01(i)) / 30 \quad (2.12)$$

In the USLE model, effects of factors that encompass plant canopy cover, surface litter, surface roughness and often previous soil moisture and previous land use, are considered with respect to the C sub-model (Igwe *et al,* 1997). In the original SLEMSA, the i values signify the evaluation of diverse crops, planting densities, planting and emergence dates, and management levels. There are more connections that can be used to file measurements to yield C in USLE than in the empirical SLEMSA. This, however, has not limited the gathering of many crop-cover measurements from Zimbabwe for the accurate access of the average cover of each crop at a given growth stage (Mutowo and Chikodzi, 2013).

The establishment of the comprehensive cover/yield curves for each crop was facilitated by using the relationship between average percent canopy cover and crop yield (Elwell, 1978b). The planning of commencement of the seasonal rains is essential to the process of soil erosion. As a result, the relationship between crop emergence dates and energy interception values for various crop yields and a variety of crops in the Highveld of Zimbabwe was established (Mutowo and Chikodzi, 2013). Figure 2.4 clearly shows very minimal SLEMSA cover factor response for areas with cover types having at least 50% energy interception. This suggests that the sensitivity of SLEMSA is higher for i values less than 50%, and the change in slope and the curvilinear character of the relationship shown in Figure 2.4 supports this observation.

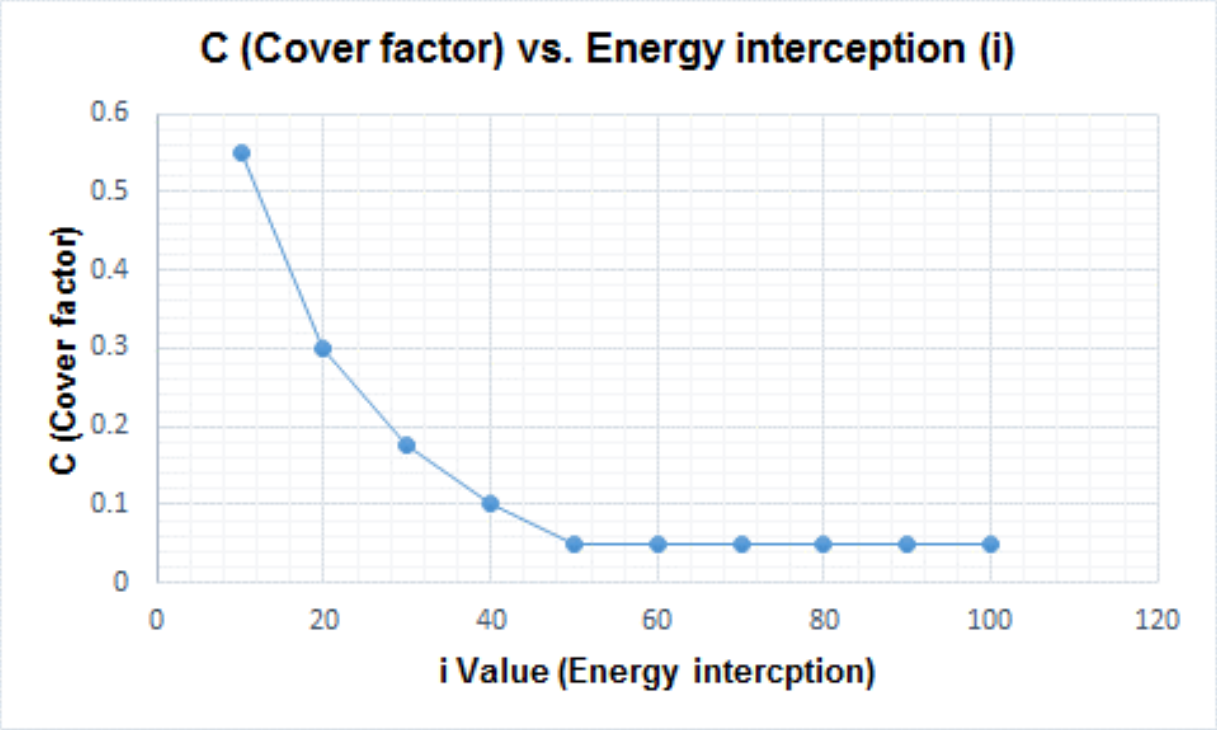

Figure 2.4: Relationship between vegetation cover factor (C) and energy interception (i) showing the bimodal nature of the curve at i value greater than or less than 50 (Elwell, 1978b).

2.5.5 Topographic Ratio

The topographic factor (*X*) represents the ratio of soil loss from a field slope of length, *L*, in meters and slope percent, *S*, to that lost from a standard plot (Kakembo *et al,* 2009). Topography has a complex effect on erosion; for flow velocity is influenced by the slope gradient and, in turn, the flow velocity influences the rate of erosion (Wischmeier and Smith, 1978; Renard *et al,* 1994). On the other hand, the distance covering the origin and termination of inter-rill processes is best illustrated by the slope length (Wischmeier and Smith, 1978; Renard *et al,* 1994). Hence a steeper and longer slope corresponds with greater erosion.

The insufficient data from Zimbabwe makes the SLEMSA topographic factor *X* more less the same as the USLE slope length (L) and slope steepness (S) factor. Modifications were thus done to the equation as an indication of metric units and a variation between the standard plot to 4.5% slope gradient and a 30-meter slope length which are close approximations of field designs in Zimbabwe. The quantity and rate of overland sheet erosion are influenced by the

topographic characteristics in the model. Since the scouring action responsible for rills and gullies formation is not captured, it is imperative that independent estimations by other means are done. The SLESMA *X* factor symbolises the consequence of topography on erosion using the following relationships (Elwell, 1996; 1978b):

$$X = \frac{L^{0.5}(0.76+0.53S+0.076S^2)}{25.65} \quad (2.13)$$

where:

• *S* = slope steepness in %

• *L* = slope length (m)

From Figure 2.5, there is no variation observed in X topographic sub-model and changes in percent slope for values of 0 - 20%. The graph clearly shows a positive relationship for slopes greater than 20%.

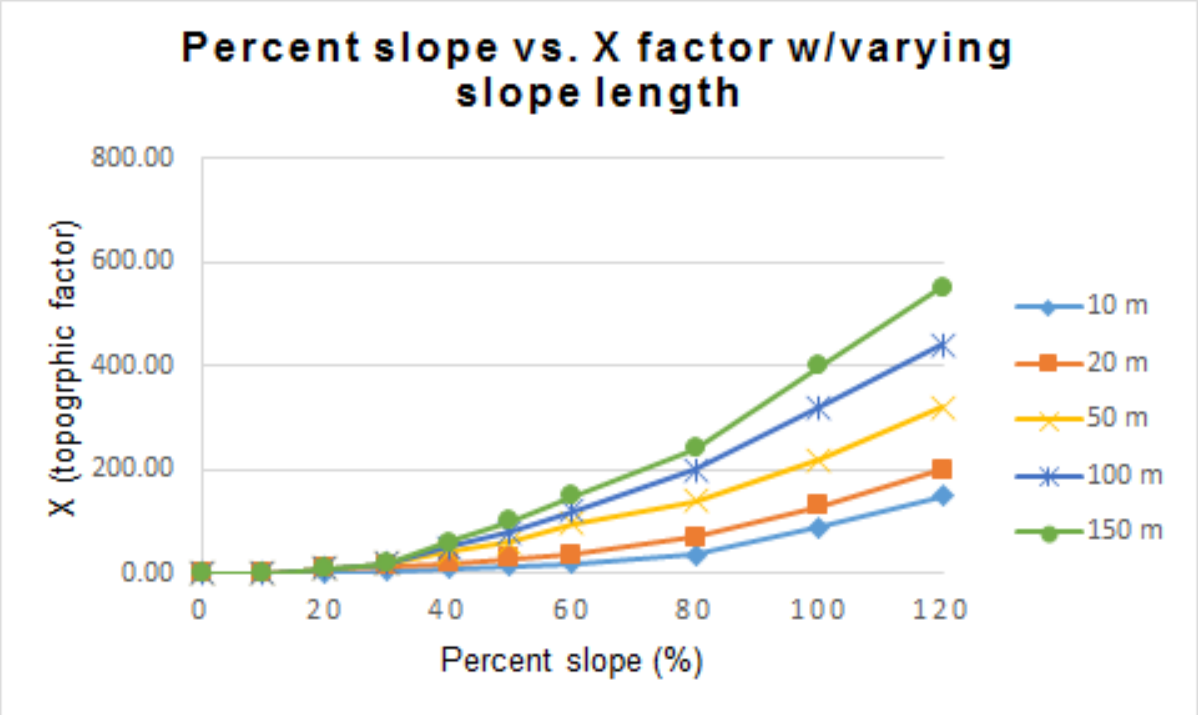

Figure 2.5: Relationship between the topographic sub-model and percent slope steepness at varying slope lengths using the SLEMSA model (After Elwell, 1978b).

2.6 SLEMSA and USLE

USLE was the foundation for the SLEMSA model, adapted to circumstances in Zimbabwe by Paris (1990), as he indicated the short coming of USLE in recognising the greater significance of slope steepness in areas of intense rainfall typical of the tropics. Mutowo and Chikodzi (2013) discovered that the slope has greater influence tropical conditions where rainfall is heavier.

SLEMSA functions like USLE in that the former is a model that has simple multiplicative relationships as the interactions between sub-parameters are often misunderstood due to the minimal availability of measured input data, which often is the case in Southern Africa (Igwe *et al,* 1997). Developing countries often have missing or incomplete information on long-term rainfall records, rainfall intensity, soil erodibility values, and detailed information regarding land use practices. Relative soil loss estimates are often used in SLEMA estimations of soil loss instead of absolute soil estimates, and these can also be used for many planning purposes (Mutowo and Chikodzi, 2013).

Comparable to USLE, SLEMSA is unable to justify the interaction and interdependence among variables. Each parameter for both SLEMSA and USLE is treated as an independent variable, however, per Wischmeier and Smith (1978: 72), "the relation of a particular parameter to soil loss is often appreciably influenced by the levels at which other parameters are present.". Working on the assumption that each variable is independent, empirical models like USLE, RUSLE, and SLEMSA give the limited perception to variable interaction (Bartsch *et al,* 2002; Smith, 1999). Thus, the hydrologic system is simplified, and even though there is independence in the processes, the system does not completely mirror what occurs in nature.

The major variation between SLEMSA and USLE is in the exclusion of the management factor (P) of USLE by SLEMSA after the realisation that consideration can be extended to the results of local conservation practices in the slope factors (L or S) within the topography system, or in erodibility (F) in the soil system (Mutowo and Chikodzi, 2013). Quantification of other factors is facilitated by methods that requires less data and require simplicity in their calculations. A

measure of the total kinetic energy of rainfall that simplifies calculations from rainfall records substitutes the rain erosivity factor (R) in USLE (Igwe *et al,* 1997; Stocking *et al,* 1988).

The proportion of soil lost from a vegetated plot to soil lost on an identical plot under clean-tilled, continuous fallow represents the cover factor (C) in the USLE (Morgan, 1995). There is variation in the mean annual values diverse crop and management. The definition of cover factor in SLEMSA is the percentage of rainfall intercepted, and it is exponentially related to the cover percentage (i). Additionally, the soil erodibility index (F) in SLESMA base on soil type and texture substitutes for the soil erodibility factor, based on texture and organic carbon content (K in USLE). The calculation of relief factors (LS in USLE and X in SLEMSA) is the same (Mutowo and Chikodzi, 2013).

2.6.1 Strength of the SLEMSA model

The SLEMSA model ensures that curvilinear relationships such as erosion and vegetation cover are accommodated, and it provides a more realistic way of combining factors, other than by simple addition. It also gives adequate relative weighting to the factors and thus addressing the more important interactions (Stocking *et al,* 1988; Leenaers, 1990).

SLEMSA has various advantages for developing countries like South Africa and these include its ability to combine reasonable accuracy without the need for excessively elaborate and expensive field experiments; flexibility is maintained using rational and easily-measurable parameters such as rainfall interception; and refinement and up-dating of information can be incorporated as and when new data become available.

To assess the spatial variation of erosion hazard in using an improved method for erosion hazard mapping based on the empirical model SLEMSA. For this study the SLEMSA Model was used because it ensures that curvilinear relationships such as erosion and vegetation cover are accommodated, and it provides a more realistic way of combining factors, other than by simple addition. It also gives adequate relative weighting to the factors and thus addressing

the more important interactions (Stocking *et al,* 1988; Leenaers, 1990). There have not been any quantitative measures that have been implemented, especially at the sub-catchment level.

2.6.2 Limitations of the SLEMSA model

However, the main limitation of the SLEMSA model is that it assumes that each factor in erosion has equal weight and importance, which is not true because for instances, under tropical conditions erosion rates are far more sensitive to changes in vegetation than to changes in soil type (Stocking *et al,* 1988). Secondly, the technique uses the ordinal or ranking scale of measurement where erosion is implicitly linearly related to the rank of the variable. This ignores, for example, the important exponential relationship between vegetation cover and erosion (Elwell and Stocking, 1976 in Stocking *et al,* 1988), meaning that a change in cover from 10 to 20% is proportionately far more effective in reducing erosion than a change from 70 to 80%. Thirdly, it assumes that erosion hazard is the sum effect of each variable, ignoring known complex interactions.

2.7 GIS, REMOTE SENSING AND EROSION HAZARD MODELING

2.7.1 Application of remote sensing

Remote sensing refers to the acquisition of data about an object by a sensor without direct physical contact with it (De *long,* 1994a; Lillesand and Kiefer, 1994). Application of remote sensing to natural resources inventory has become fundamental for management that is friendly to the environment (Lillesand and Kiefer, 1994). It gives information about the physical characteristics and variation of features on the ground that can be converted into image for interpretation and analysis. This variation of land features, which reflects the inherent differences of their build-ups, is sensed and recorded by the remote sensor that receives the electromagnetic response of the features (Lillesand and Kiefer, 1994; Nizeyimana and Petersen, 1998). Such capability to differentiate features is being well applied in soil survey. Remote sensing classifies soils according to their chemical and physical differences that are readily sensed by remote sensors (Nizeyimana and Petersen, 1998; Ritchie, 2000).

Such variations are most likely due to soil moisture, organic matter, mineral content, and others (Lillesand and Kiefer, 1994). Weismiller *et al* (1985) summarized studies that showed the relationship of reflectance with soil erosion. Most of these studies have indicated that organic matter and iron oxide have strong effect on reflectance characteristics. Collins et al (1998) suggested that indirect relationship could be made between soil reflectance properties and soil structure. This can be explained by the fact that the structure of clay soils improves the moisture holding capacity that has low reflectance. In contrast, sandy soils have low water holding capacity, which has high reflectance. Remote sensing can be applied directly or indirectly to assess soil erosion (Pelletier, 1985; Ritchie, 2000). Photo interpretation and photogrammetry are used to directly identify eroded areas from images or images can be used as inputs in GIS. For example, crop cover or rainfall interception by vegetation can be assessed from remotely sensed images (De Jong et al*., 1999).*

Garland and Broderick (1992) used aerial photos of 1944/5 and from 1976-81 to assess soil erosion change in the Tugela catchment of KwaZulu-Natal in which they found a decline in the problem. Randall (1993) delineated gully and sheet erosion areas using Landsat TM images in Olifants River catchment, South Africa to find that gullies could be mapped more accurately. Similarly, Liggit (1988) used remotely sensed data to assess soil erosion in Mfolozi. Liggit (1988) interpreted orthophotos and aerial photographs taken at different times and scales to estimate the spatial extent of gullies and sheet erosion. Delineation of gullies using aerial photos was also undertaken in Spain by Garg and Harrison (1992) by using their differences in tone and texture from the surrounding land surfaces.

Hochschild *et al* (2003) used aerial photographs of 1990 at 1:30 000 scale and Landsat 5 TM image of 1996 in their assessment of soil erosion in Mbuluzi river catchment (Kingdom of Swaziland). The study mapped existing erosion types and extents by creating negative correlation between the erosion levels and the percentage of vegetation cover. The satellite image was used to derive the vegetation cover density and the R(USLE) C-factor using the vegetation indices and leaf area index. A similar technique was applied in the upper Mkomazi

river catchment of KwaZulu-Natal, South Africa by Flugel et al (2003). In Nsikazi, Mpumalanga Province of South Africa, Wentzel (2002) used satellite imagery to derive bare soil index for likely soil erosion mapping.

Daba *et al.* (2003) employed remote sensing technique to directly assess gully erosion by measuring gully erosion change in eastern Ethiopia using aerial photographs taken in 1966 and 1996, both at 1:45 000 scales. The technique used the break lines and constructed straight lines to create closed polygons from which volumes were calculated using cut and fill system. The result showed soil loss of 1.7-ton m-2 over the 30 years' time period. The break line measurement agreed with the field measurements of the gully depth and width. Similarly, Khan and Islam (2003) identified a great deal of riverside retreat by using time series analysis of satellite images in Brahmaputra-Jamuna River, Bangladesh.

Researchers such as Sayago (1986) applied remote sensing in conjunction with field measurement of erosion using the USLE to map erosion hazard in the northwest of Argentina, where multi-temporal Landsat images and conventional aerial photos were used to delineate mapping units. This study, which, in general, produced a map of high erosion risk in the area, has concluded that remote sensing is efficient in detecting erosion hazard areas economically and within a short period of time. Earlier, Morgan et al (1978) examined the advantage of remotely sensed data in soil erosion assessment in Wisconsin, USA. They estimated soil loss using the USLE by entering data obtained from aerial photographs. The predicted soil loss figures were found closely comparable with the results derived from field-gathered data.

The advantage of remote sensing in extracting information from a larger area and much quicker than the conventional survey systems is acknowledged by several researchers including Morgan *et al.* (1978) and Engman (1996). Time scale is an important consideration that helps gather repetitive data from the same space. In addition to its wide area coverage, remote sensing also provides areal data as opposed to point data made by sampling in conventional surveys (Baumgartner and Apel, 1996; Engman, 1996).

2.7.2 Application of Geographic Information Systems (GIS)

A GIS is a system that deals with georeferenced spatial data to perform such processes as capturing, storing, retrieving, manipulating/analyzing, and displaying the output of such spatial data (Burrough, 1986). A widely accepted definition of GIS is that it is a computerized system to process spatially related information (Collet *et al,* 1996). This description includes three portions, namely, the computer hardware integrated with the software component, processing of information, and the spatial nature of the information.

Recent developments of Digital Elevation Models (DEMs), soil databases, remotely sensed data, and the related computers performance to process large data sets have increased the role of GISs in natural resource assessment (Petersen *et al,* 1998). According to Zhu et al (2001) mapping of soil landscape showing detailed spatial and attribute anomalies is possible with more regular updates and less cost compared to the conventional soil survey technique. De Roo (1996) pointed out two advantages of using GIS in soil erosion models. First, it resolves spatially variable runoff and soil erosion process through generation of cells to account for the variations.

Second, GIS is capable of inputting large data automatically, which is difficult to enter manually. Such quality of GIS has also helped develop more detailed distributed erosion and deposition models (Lorentz and Howe, 1995; Jetten *et al,* 2003). Mongkolsawat et al (2002) based on a study in Thailand reported the advantage of GIS in analyzing multi-layer data spatially and quantitatively. GIS is also credited to its capability of assessing soil erosion at large scale (Wijesekera and Samarakoon, 2001; Lufafa *et al,* 2003). It also has become possible to readily estimate soil loss from existing digital data sets of soil map, terrain data, and remotely sensed data (Petersen *et al,* 1998). More important, since the conventional surveys require extensive manpower, time, and cost, GIS has become an excellent tool to perform environmental studies (Marble, 1987).

GIS is also being used with soil erosion assessment models. Brazier et al (2001), for their study in Cambridge, UK, used GIS with MIRSED (minimum requirement version of WEPP) to assess hillslope scale soil erosion rates. Similarly, De Jong et al (1999) applied the Soil Erosion Model for Mediterranean areas (SEMMED) that integrated Landsat TM images, a digital terrain model, a digital soil map, and soil physical field data to assess soil erosion at regional scale in southern France and in Sicily.

Linkage between GIS and a soil erosion model depends on both the GIS and the model itself. GIS and grid cell-based models can easily be combined because of the capacity of GIS to analyse raster data (Petersen *et al,* 1998). It is easy to interface empirical models such as the RUSLE with GIS because of the simplicity of the equation (Ferro *et al,* 2001), whereas process-based models require detailed data input to make multiple layers (Petersen *et al,* 1998).

2.8 CONCEPTUAL FRAMEWORK

The preceding sections set the groundwork for a conceptual framework that will inform this study. The original SLEMSA model adapted from Elwell (1978) was used to construct the framework. The conceptual framework in Figure 2.6 represents natural processes with a description for each individual physical parameter of the system and their subsequent combination into a complex model. The framework is based on the spatial variability of most important land surface characteristics such as topography, slope, soil and vegetation that influence soil erosion hazard.

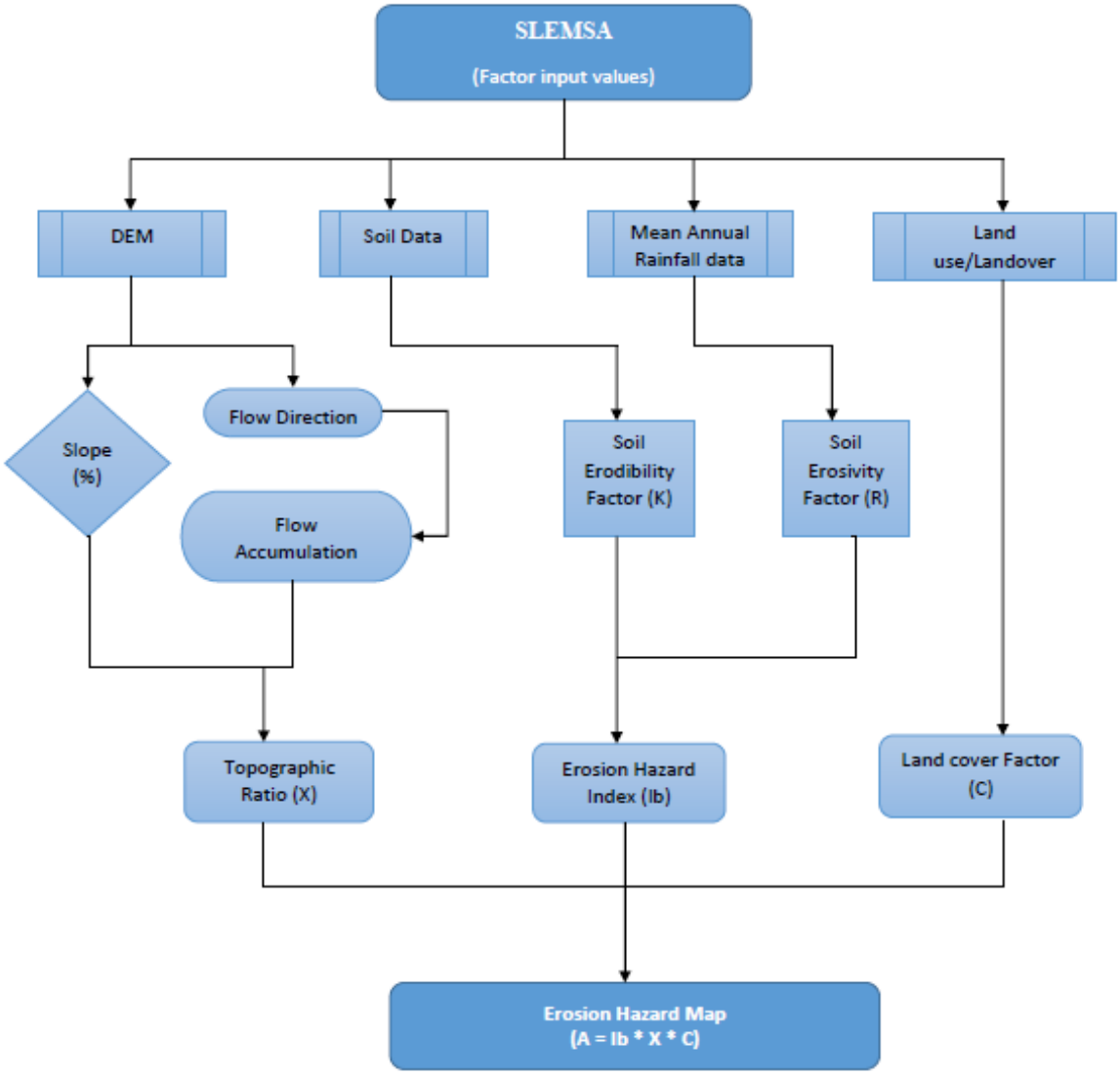

Figure 2.6: Conceptual framework of the research

The spatial distribution of erosion hazard will be assessed based on physical systems that include climate, soil, vegetation, and topography. From the physical systems, the control variables in the study are derived. These variables are soil erodibility factor, erosivity factor, energy interception, and topographic ration respectively. The control variables are used to determine the sub-models. As indicated in Figure 2.6, the erodibility factor and erosivity factor will determine the erosion hazard index, while slope steepness and slope determine the topographic ratio. The vegetation sub-model will be combined interactively with the other submodels within ArcGIS for the main model to assess the erosion hazard.

2.9 CHAPTER SUMMARY

Though there have been numerous studies on aspects of soil erosion hazard modelling by scholars, the use of the SLEMSA model has received little attention. Little is known about its extent of applicability within anthropogenic disturbed environments particularly previously mined areas. In addition, the spatial distribution of soil erosion at catchment scale and identification of active sites of erosion and deposition still need to be mapped accurately. This gap can be filled by applying GIS and remote sensing to model the spatiotemporal soil erosion dynamics occurring in the catchment as well as quantifying the spatial extent of soil erosion. The integrated application of remote sensing, GIS and empirical modeling is a powerful means to determine erosion hazard. GIS can integrate the complex variables that affect soil erosion. Soil erosion models integrated within GIS software also provide an effective means to predict soil erosion processes.

CHAPTER THREE

RESEARCH METHODOLOGY

3.1 INTRODUCTION

Soil erosion models, process-based or empirical, require the quantification of the most important factors. The RUSLE model uses five factors, namely: erosivity, erodibility, slope length and slope steepness, cover management, and conservation practice. Because of their spatial nature, the collection and analysis of such variables has always been a difficult task. However, such a problem has been minimized since the development of remote sensing and GIS technologies and their involvement in hydrological models. While part of the data sets such as rainfall is acquired using direct ground measurements and others with the support of remotely sensed data as in the case of soil and land cover mapping, it has become possible to obtain data on others, for example topographic data, completely using GIS. Once the available and required data is gathered, storing and manipulating them, and producing an output for the easiest interpretation is performed in a GIS environment. This chapter discusses how the overall methodology was executed in this work. The first section deals with the data sets that were used in the study while the second section describes the procedures undertaken to achieve the outlined objectives of the study.

3.2 RESEARCH DESIGN

The research methodology is based on geospatial information technologies particularly Geographical Information Systems and Remote Sensing. The GIS methodology approach permits complex spatial analysis that makes use of using extensive range of data, that is mainly represented by spatialized geographic elements (vector and raster layers), each one quantified with the help of specific attributes.

This research is composed of three main stages namely: pre-fieldwork, fieldwork, and post-fieldwork phases. In the first phase was the preparation phase consisting of development of a research proposal that was inclusive of definition of the problem, formulation of research

objectives and related research questions, literature review, defining methods, identification of the obligatory data types as well as the corresponding methods of collection and preparation of fieldwork plans.

In the second phase is fieldwork, which involved information and data collection. This phase included data collection, and the primary and secondary data necessary for the research was collected during field visits. This involved collection of soil samples around the abandoned mine site, field surveys, as well as visiting important places of the study site such as waste dump sites, closed shafts, abandoned infrastructure and so on, to gain a general impression and to familiarise the researcher with the study area.

3.2.1 Ethical Considerations

Ethical issues that were considered in this study included obtaining a written permission from the relevant authorities where the research was undertaken. To gain access to the location in which the data was collected, permission was obtained from the Mutale Local Municipality. This ensured that the researcher avoided the invasion of privacy, dissemination of sensitive information and trespassing into private property. The access permit thus ascertained that the researcher is confined to data relevant for academic purposes only. Further access was sorted and granted by the local chief who acts as the custodian of the abandoned mine and its environs.

3.3 DATA SOURCES AND TYPES

The main aim of data collection was to gather any available data concerning the abandoned mine land which was then used to form a base for further analysis. For the estimation of the spatial variation of erosion hazard of mine wastes at the abandoned mine, the following data were collected for use with the SLEMSA model. A Mutale Municipality boundary map, as well as the Aster Digital Elevation Model (DEM) with a resolution of 30 metres, was obtained from the Global ASTER Gdem website. The soil map of Mutale Municipality was obtained from the Food and Agriculture Organization (FAO) World Reference Base (WRB). To generate erosivity

values, mean annual and monthly rainfall data for a period of 30 years (1984 - 2014) was utilized. Satellite imagery from Landsat ETM+ was obtained for the purposes of land cover classification.

3.3.1 Data Collection

Both primary and secondary data were applied in this study to ensure that the objectives of the study were met. Governmental and non-governmental organizations were both consulted for collection of secondary data, which included satellite imagery, aerial photographs, topographic maps, meteorological data, etc. In addition, literature review and open source websites were also an important source of secondary data, whereas important primary data and information were obtained through fieldwork.

3.3.2 Reference Data

One of the most significant primary data required from fieldwork for this research was ground truth data. There were frequent field observations using Global Positioning System (GPS) that were conducted for the generation of primary information concerning the ground truth for image classification and soil type verification. The collection of primary data consisted of usage of field surveys, GPS instruments and digital cameras were used to photograph the land cover material of the study site as well as the evidence of environmental impacts posed by the existence of the abandoned mine.

3.4 DATA ANALYSIS AND DERIVATION OF SLEMSA PARAMETERS

To run the SLEMSA model for erosion hazard mapping, various factors were considered for the model, based on the improved modified method of the model (Stocking *et al,* 1998). The factors that were contemplated for the model are relief (S & L), soil erodibility (Fb), vegetation cover (C), and erosivity of rainfall (E). A GIS geodatabase was created for the abandoned Nyala mine containing attributes and data necessary to run the SLEMSA model. The GIS layers; Mutale boundary map, drainage network, soil, land cover, digital elevation model from

DEM and rainfall, were spatially organized with the same resolution and coordinate system using the GIS software.

Data analysis and processing were prepared via digitization, calculation and classification of the necessary information of each thematic layer using ENVI 5.1 and ArcGIS 10.3 software. Lastly, the MCE and Analytical Hierarchy Principle were used to weigh all parameter influences (Saaty, 1971). Additionally, some simple statistical methods inclusive of percentage, average and graphic tabulation were also utilized for the analysing and interpreting. In Figure 2.7 is the representation of the fundamental methodological approach that was followed in SLEMSA.

3.4.1 Determination of Erosion Hazard Index (EHI)

The Erosion Hazard Index (lb), which is the same as soil loss from bare soil (K) in the SLEMSA model, refers to a standard plot of bare soil, 4.5% slope, and 30 metres. The EHI was determined by relating soil erosivity (E) and soil erodibility (Fb) using the exponential relationship (Morgan, 1995):

$$lb = \exp[(0.468 + 0.766Fb)InE + 2.88 - 8.121Fb] \quad (3.1)$$

3.4.2 Soil Erodibility

Soil erodibility is an expression of its characteristic resistance to particle detachment and its subsequent transportation by rainfall. Its determination is based on the cohesive force between the soil particles and may vary, depending on the particle size and composition, the soil's water content as well as its structural development (Wischmeier and Smith, 1978).

The soil erodibility (fb) of Nyala mine was delimited using the relationship between organic matter content and soil texture class as recommended by Schwab *et al.* (1981). According to Kim *et al.* (2012), mined areas have low organic content hence in this study, organic content is assumed to be 0.5 %. Table 3.1 presents the soil erodibility factor (fb) based on soil texture class.

Table 3.1: Soil erodibility factor values (Schwab *et al,* 1981)

Textural class	**Organic matter content %**	
	0.5	**2.0**
Fine sand	0.16	0.14
Very fine sand	0.42	0.36
Loamy sand	0.12	0.10
Loamy very fine sand	0.44	0.38
Sandy loam	0.27	0.24
Very fine sand loamy	0.47	0.41
Silt loamy	0.48	0.42
Clay loamy	0.28	0.25
Silty clay loamy	0.37	0.32
Silt clay	0.25	0.23

Soil samples were collected from the study area using a stratified composite sampling technique based on the four divided grids of the study area, that is; a field is broken down into areas of similar topography, soil moisture and land cover which were determined using a global positioning system. A total of 32 soil samples weighing approximately 1 kg each were collected from various sites around the Nyala mine (Figure 3.1). Since soil erosion is a surface phenomenon, samples were taken from the top 30 cm of the soil surface as proposed by the SLEMSA guideline (Renard *et al,* 1997). In the sampling, an auger was used for soil collection and each sample point location captured using a portable Garmin GPS 60. The samples were collected into plastic bags, labelled and were transported to the University of Venda Environmental Science laboratory for further analysis.

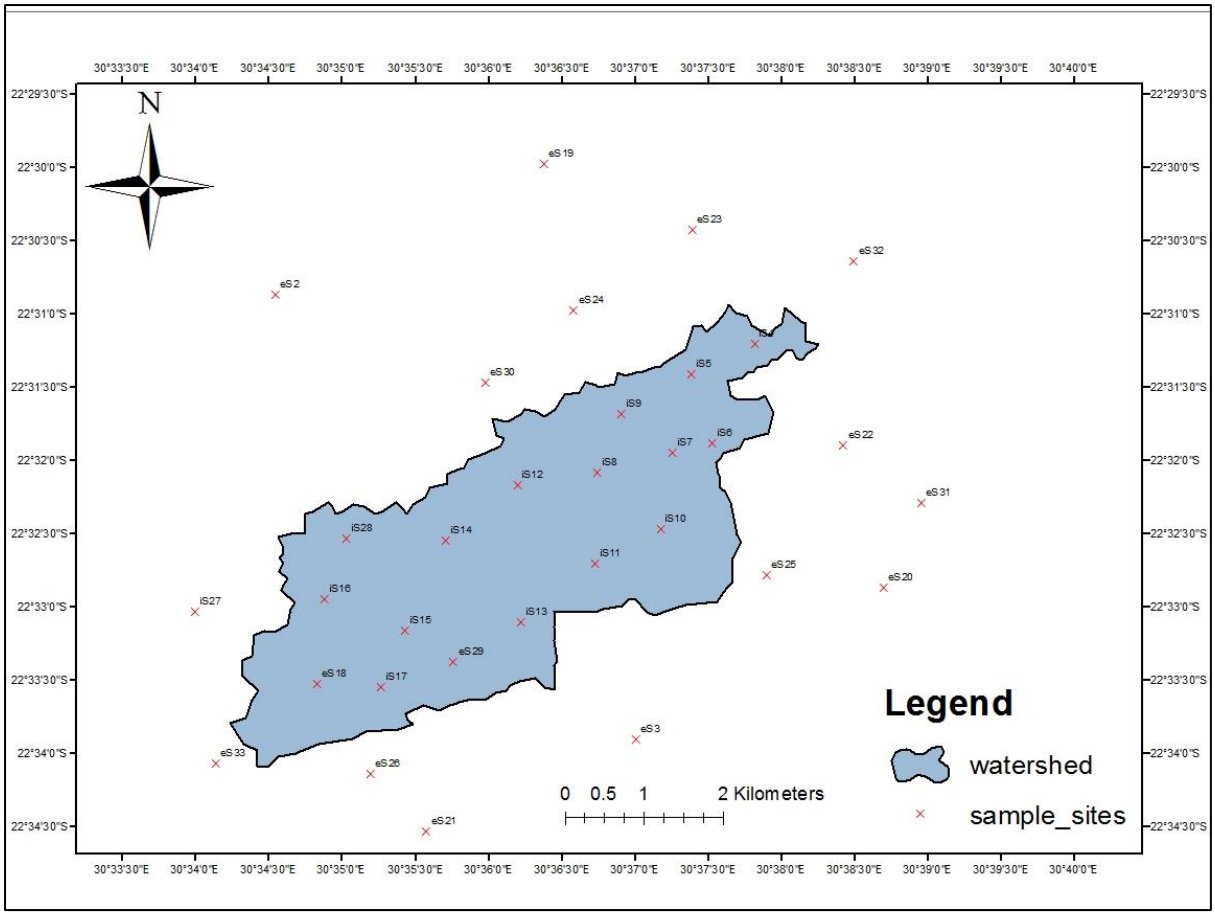

Figure 3.1: Map of the sample points where measurements and soil samples were taken.

Figure 3.2: Soil sample collection in the study area.

Particle size analysis

Particle size analysis was conducted in the laboratory to determine the particle size distribution at each soil sample site. Soil texture of each sample was determined by implementing two dissimilar particle size analyses, which are sieve and hydrometer analyses. The facilitation of particle size distribution for the coarse grain sediments, gravel and sand, was through sieve analysis, facilitation of particle size distribution for the fine grain sediments, silt and sand, was through hydrometer analysis.

Sieve analysis

The sieve or mechanical analysis is comprised of determination of the proportional quantities of particles that can be retained or can pass through each of a set of sieves that are arranged in decreasing sizes. The implementation of the percentages of weights retained in each sieve allows a semilogarithmic graph, called a particle size distribution curve is to be drawn up by plotting the log of the opening size on the x-axis and the percentage of particles, by weight, coarser than or finer than the sieve on the y-axis.

Firstly, the sieve analysis consisted of the light crushing of each oven-dried sample to a size less than 2 mm and capturing of the sample mass. The sequence of sieves that utilised include sieve numbers 4, 10, 20, 40, 60, 100, 200 corresponding to a range of particle sizes 4.75, 2, 0.85, 0.425, 0.25, 0.15 and 0.075 mm, respectively, together with a pan for collecting the fine particles. Cleaning and assembling of the sieves in decreasing pore size starting with the largest pore size on top and the pan on the bottom were the next steps. Subsequently, the sample was introduced to the top sieve, and then the sieve nest was placed on the shaking apparatus for about 10 minutes. Following was the removal of the sieves the shaking apparatus and their separation. Each retained sediment on every sieve was weighed on the mass balance and the weights were recorded to determine the coarse grain particle size distribution.

Hydrometer analysis

Particle size distributions of the fine-grained sediment particles in each sample was determined with the hydrometer method. A soil sample of known weight was spread in water in which the soil particles individually settled. The soil particles are presumed to be spheres and expression of the velocity of the particles can be done using Stokes Law below:

$$v = \frac{2}{9}\frac{G_s - G_f}{\eta}\left(\frac{D}{2}\right)^2 \quad (3.3)$$

Where: v = velocity of fall of the spheres (cm/s)

G_s = specific weight of soil solids (g/cm^3)

G_f= unit weight of water (g/cm^3)

η = absolute/dynamic viscosity of the fluid (g/cm*s)

D = diameter of soil particles

The presence of specific grains with a soil-water mixture can be determined by solving for the diameter. Solving for D using an assumed specific gravity of water, G_s, at 20℃ is 1.0 g/cm^3 can be done using Equation 3.4.

$$D = \sqrt{\frac{18\eta v}{G_s - G_w}} \quad (3.4)$$

A 50g sample of each fine grains sample was measured and mixed with 125mL of the 4% sodium hexametaphosphate solution for 4 hours. Flushing of the solution into a 1000mL glass cylinder followed the 4 hours, after which the mixture was made up to the 1000mL mark with deionized water. Stirring of the mixture was then done for two minutes, after which the hydrometer (ASTM 152H) was inserted into the glass cylinder. This time was recorded as t=0. Readings of the hydrometer (R_{ACT}) were taken at 2, 5, 15, 30, 60, and 240 minutes after the initial mixing of the sample and deflocculating solution. Further readings were taken at 24 hours (1440 minutes). After an observed reading at t=5min, the hydrometer was removed and

kept in the 1000mL graduated cylinder that contained water and deflocculating agent. Reinserting of the hydrometer in the bath soil was done to record the readings at the remaining time intervals to take readings. The hydrometer was removed and placed in a 1000mL graduate for cleaning after each reading.

The hydrometer test employs multiple constants whose determination is necessary for the calibration of the results from the readings. The calculations were conducted in fulfilment of each factor. A corrected hydrometer ready (R_c) must first be calculated before continuing all computations:

$$R_c = R_a - zero\ correction + C_T \tag{3.5}$$

Where: R_c= corrected hydrometer reading (cm)

R_a= actual hydrometer reading (cm)

C_T= temperature correction (Table A1.3)

The percent finer at each time step is then calculated using Equation 3.6. The assumed specific gravity G_s of the soil particles present is 2.65.

$$\%\ Finer = \propto R_c/M_s \tag{3.6}$$

Where: $\propto$ = correction factor for unit weight of solids

R_c = corrected hydrometer reading (cm)

M_s = mass of soil used (g)

To calculate the corrected meniscus hydrometer reading (R), 1 can be added to the value of the actual hydrometer reading. See Equation 3.7.

$$R = R_a + 1 \tag{3.7}$$

The Stokes' formula can be used to calculate diameters of particles related to the values for effective depth that is required for calculating velocity directly related to D. Table A1.1 (Appendix A) illustrates the corresponding L values with respect to the meniscus corrected readings.

The particle velocity (v) is then calculated as,

$$v = L/T\ (cm/mm) \tag{3.8}$$

As highlighted in Table A1.2, K value generation can be done be done using the predicted specific gravity G_s, and the temperature of the soil-water solution that has been recorded. The computation of particle diameter can be done using the K and particle velocity values as shown in Equation 3.9.

$$D\ (mm) = K\sqrt{L/t} \tag{3.9}$$

A soil grain distribution chart for fine particles in the soil samples can be formulated using the following captured data; dates, time elapsed, temperature, actual and corrected readings, percent finer, values for L and K as well as the D.

Table 3.2: Soil classification based on grain size (Khanna & Justo, 2001)

Gravel	Sand			Silt			Clay		
	coarse	medium	fine	coarse	medium	fine	coarse	medium	fine
		0.6mm	0.2mm		0.02mm	0.006mm		0.0006mm	0.0002mm
2.0mm				0.06mm			0.002mm		

The soil erodibility values (Fb) were derived based on soil textural classes and calculated using the following formula developed by (Wischmeier and Smith 1978, Loch *et al,* 1994 and Igwe, 1997):

$$K = 2.8 \times 10^{-7} M^{1.14}(1.2 - a) + 4.3 \times 10^{-3}(b - 2) + 3.3 \times 10^{-3}(c - 3) \tag{3.10}$$

Where *a = % organic content matter*
b = soil structure class code
c = soil permeability class code
M = (% silt + % very fine sand) or (100% - % clay)

Since these values represent only sampling points, the non-sampled areas had to be filled in by interpolating the calculated point values in ArcView GIS. For the interpolation, 32 points representing the spatial locations of the soil samples were taken for the interpolation (Ahmed, 2003). The three interpolation methods, namely, spline, inverse distance weighting (IDW), and ordinary kriging were tested for the best fit.

3.4.3 Rainfall Erosivity

Erosivity factor (R) is a measure of the erosivity of rainfall and it is the average yearly amount of individual storm index values, EI_{30} (Renard, 1997). It is a product of storm kinetic energy and maximum 30-minute rainfall intensity, with E representing the total storm kinetic energy and I_{30} representing the maximum rainfall intensity in 30 minutes. The computation of compute storm EI_{30} requires continuous rainfall intensity data which is not readily available. Therefore, for this study, average yearly and monthly rainfall data were implemented for estimation of the erosivity factor.

The mean annual rainfall was determined using records from randomly selected local weather stations within and around the study area. Rainfall erosivity factor was calculated with monthly amounts of precipitation recorded from the stations over 30 years, from 1984-2014. Determination of the value of each cell based on the values of nearby cells (E) in J/m^2 was carried out with interpolated (IDW) monthly precipitation surface leading to the adaptation of the following regression equation (Wischmeier and Smith, 1978 and Igwe, 1997):

$$E = 18.84 * P \quad (3.11)$$

Where P = Total Annual Rainfall

3.4.4 Determination of Vegetation Cover

The Landsat ETM+ imagery of the area was digitally classified for the purpose of obtaining vegetation cover values. Owing to its popularity and wide acceptance (Brito & Quintanilla, 2012), the supervised Maximum Likelihood classification method was used in a GIS environment to generate the land cover map. Similar classes were grouped together manually,

based on a land cover point map generated from GPS points collected from fieldwork. The interception (I) values for the area were derived from the South African National Landcover map (SANBI, 2013), where the interception values of the land cover were adopted from the study of Orr *et al.* (1998). Thus, the following equations from Morgan (1995) were used to determine the cover values:

when I < = 50; C = exp (-0.06 * I) (3.12)

When I > 50; C = (2.3 – 0.01 * I)/30 (3.13)

Where: I = Interception

C = Vegetation Cover

3.4.5 Determination of Soil Loss Ratio

The slope length factor (L) and the slope steepness factor (S) consider the influence of topography and an ASTER Digital Elevation Model with a resolution of 30 m was used to obtain slope. The DEM was pre-processed to obtain hydrologically correct elevation grid with sinks filled and a suitable cell size to generate meaningful geographical and flow related information from the DEM.

In any hydrological modelling that uses DEM, the primary requirement IS assurance of even elevation surface, which are usually considered as errors (ESRI, 1996; Hickey, 2000). DEMs with depressions/sinks obstruct flow that creates discontinuity of the latter and a grid or a set of grids with lower altitude than the surrounding cells is the cause for this. Removal of depressions, which works based on increasing the altitude of the sink to a level of the lowest neighbouring cell, was applied to the DEM of WGR within ArcView GIS.

The values for Topographic Ratio (X) were calculated from the average slope, where the slope length was at a constant 100 m (Stocking *et al,* 1988). The advantage of this modification is that it works based on flow accumulation. Mitasova et al (1996) further simplified the formula to derive the LS factor at a point and produced the following GIS executable equation. The equation that was used to calculate the Topographic Ratio is as follows:

$$X = \frac{L^m(0.76+0.53S+0.076S^2)}{25.65} \quad (3.14)$$

Where: X = Topographic Ratio

L = Slope Length (m)

S = Slope Steepness (%)

3.4.6 Erosion Hazard Modelling

After determining all the required input parameters for the model, the Erosion Hazard Units were calculated from the resulting erosion hazard index (lb), vegetation cover (C) and the topographic ratio (X). The RUSLE calculates soil erosion by multiplying the factors listed in the previous subsections. Application of this equation in GIS follows the conversion of conformity of all these factors regarding grid cell size. After specifying a side of 30 m grid cells for each factor, all the four factors were multiplied with results to be presented per grid cell. The results were then interpreted based on their severity and comparisons were made with related works done elsewhere.

The Erosion Hazard was then determined through cell by cell analysis of the soil loss surface by multiplying the respective SLEMSA factor values interactively in ArcGIS 10.3 using the equation:

$$Erosion\ Hazard = lb * C * X \quad (3.15)$$

Basing on the work by Stocking (1988), cited in Dube (2011), the erosion hazard was divided into five different classes as indicated below:

Table 3.3: Erosion hazard classes

Class		
1	EHU < = 10: erosion hazard	Low
2	10 < EHU < = 25: erosion hazard	Moderate
3	25 < EHU < = 50: erosion hazard	Moderately high
4	50 < EHU < = 100: erosion hazard	High
5	EHU > 100: erosion hazard	Very high

3.5 SENSITIVITY ANALYSIS

Sensitivity analysis of a model such as SLEMSA is a method to determine the relative and absolute significance of model input parameters in affecting the model output. Conducting a sensitivity analysis of the model input parameters aids in determining data collection and experimental needs and provides further insights into the physical processes. The relative impact of each of the preceding factors in modelling soil loss for as particular area is critical. Conducting a sensitivity analysis of the model input parameters assists in the data collection process, and in determining the experimental needs as well as providing further insights into the physical processes involved (Bonda *et al,* 1999).

A sensitivity analysis was performed for the area. The analysis entailed investigating the effects of increasing and decreasing the factors by an arbitrary percentage. While one parameter is analysed, values for all other parameters are held constant. The sensitivity index was determined for each parameter i.e. rainfall erosivity, soil erodibility, and the topographic factors of slope length and slope steepness. The obtained sensitivity index value represents a relative normalised change in output to a normalised change in input. This makes allowance

for a valid mean of comparing sensitivities for different input parameters that have different orders of magnitude. The Sensitivity Index (SI) is given by the following equation:

$$SI = \frac{\left[\frac{(O_2 - O_1)}{O_{12}}\right]}{\left[\frac{(I_2 - I_2)}{I_{12}}\right]} \qquad 3.16$$

Where:

I_1 and I_2 are the least and greatest input values, I_{12} is the average input.

O_1 and O_2 are the associated outputs for the two input values and O_{12} the average.

Values greater than zero indicate a high rate of sensitivity to changes.

3.6 CHAPTER SUMMARY

The chapter outlined the methods and procedures employed to obtain reliable and valid results and subsequent answers to the research questions. The research design was based on geospatial technology, which the modified SLEMSA model being implemented with a GIS environment. The SLEMSA parameters i.e. erosion hazard index (a function of soil erodibility and rainfall erosivity), vegetation cover and the topographic ratio (a function of slope length and steepness) were derived with ArcGIS to produced thematic maps. The relevant parameters were processed with the ArcGIS raster calculator to produce the soil erosion hazard map. In order to validate the model predicted results, a sensitivity analysis was carried out for each individual model input parameter. The results are explained in the following chapter.

CHAPTER FOUR

RESULTS AND DISCUSSION

4.1 INTRODUCTION

This chapter presents the findings from the study. The results are presented and discussed in relation to the specific objectives of the study. The EHI, a function of soil erodibility and rainfall erosivity was derived in the first section followed by results of the land cover C factor and the topographic ratio (X factor), respectively and lastly with the erosion hazard modeling and summary of the results.

4.2 EROSION HAZARD INDEX

4.2.1 Soil erodibility

According to Robert & Hilborn (2000), erodibility depends on the texture of the soil particularly sand of 100-200µm and silt of 2-100µm and the amount of organic matter in the soil. The soil data used for analyzing the soil erodibility factor (Fb-value) in the research were generated from laboratory experiments i.e. the sieve and hydrometer analysis performed on the soil samples. This allowed the researcher to determine the grain size distribution of each sample which was later interpolated in ArcMap to produce a soil erodibility map.

Grain size distribution

After the completion of the particle size analysis from mechanical sieving and the hydrometer test, the type of soil and different proportions of sizes in each sample have been identified. The cumulative percentage frequency curves of all the soil samples have indicated similarities and differences in particle sizes between soil types. Analysis of the results has shown that all the soil samples from the study area are positively skewed hence indicating significant amounts of the finer material. The coefficient of uniformity (Cu) and Coefficient of curvature (Cc) have also been determined for each sample and based on the results, all the soil samples have Cc value within the range of 1 - 3 which falls within the criteria of well-graded soil in the

Unified Soil Classification system (USCS). Only 25 % of the samples have a Cu value greater than 6.

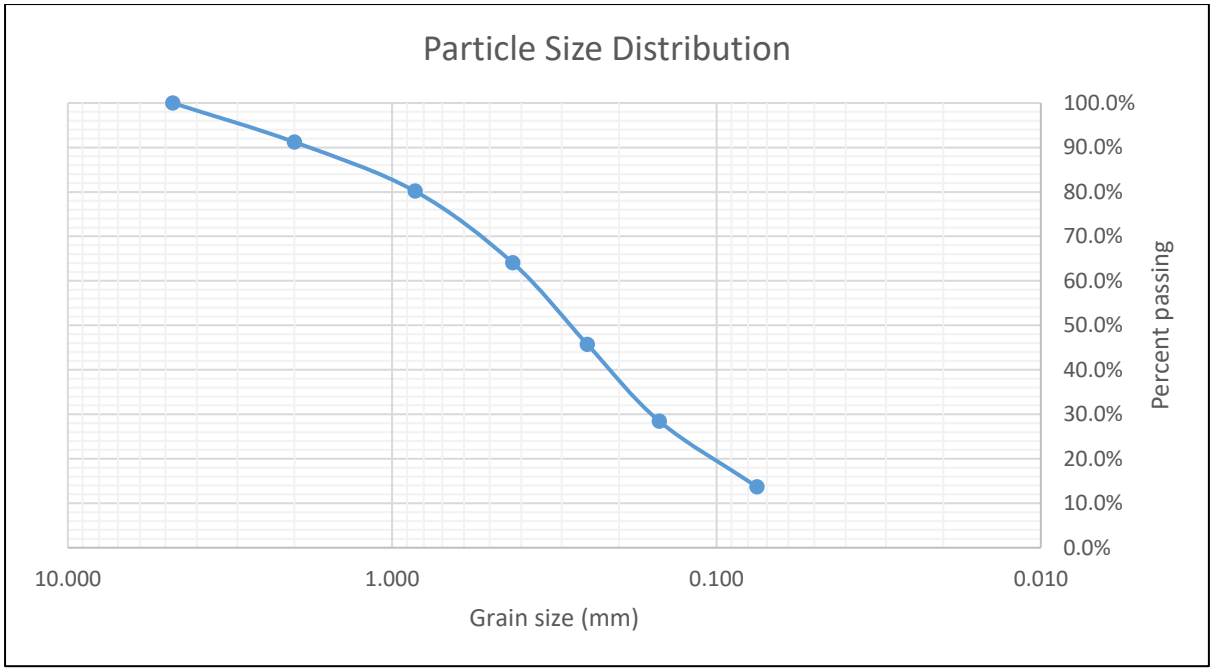

Figure 4.1: Particle size distribution curve of soil sampled for sieve analysis.

However, for the soil to be well graded, the value of Cu should be greater than 6. The current study, therefore, shows that soil samples in the proximity of tailings deposit are composed of a poorly graded material as most of the samples failed to attain one of the criteria of well-graded soil. These findings are consistent with Evans' (2000) findings which showed that disturbed soil from mining activities is predominately more erodible in relation to consolidated soil under natural conditions.

Sample point values

Using the Equation 3.2, the K-factor value in the study area was calculated. The K-factor values varied from 0.14 to 0.28 t ha h ha−1 MJ−1 mm−1, with mean and standard deviation of 0.205 and 0.053, respectively. Results of soil sample analyses that represent the point observations are given in Table 4.1. The textural analysis shows that, 14 soil samples have clayey texture. The permeability classes, assigned based on these textural classes, indicate

that 17 soil samples have a class of 6, i.e. their contribution towards surface runoff is the highest, whereas only one sample has the lowest runoff-contribution potential.

Table 4.1: Results of the grain size analysis

Soil Sample		Fraction %			Texture	Permeability class	Structure code	**Erodibility K value**
		Sand	Silt	Clay				
1	SNE1	36.63	24.24	36.24	SaCl	5	1	0.148
2	SNE2	32.94	28.17	39.36	SaCl	5	1	0.142
3	SNE3	18.75	27.32	53.75	Cl	6	3	0.227
4	SNE4	49.28	40.85	9.65	SaLo	2	2	0.223
5	SNE5	64.83	27.64	8.52	SaLo	2	2	0.164
6	SNE6	51.28	35.74	12.48	SaLo	2	2	0.254
7	SSE1	73.02	24.98	3.48	Sa	1	3	0.190
8	SSE2	36.43	22.47	43.25	SaCl	5	2	0.174
9	SSE3	67.80	23.54	12.35	SaCl	5	1	0.124
10	SSE4	50.34	32.88	17.25	Cl	6	2	0.147
11	SSE5	60.94	22.36	49.96	SaCl	5	2	0.127
12	SSE6	24.87	25.48	24.85	Cl	6	2	0.176
13	SSE7	46.70	29.76	32.22	SaLo	2	2	0.152
14	SSE8	43.41	26.54	50.95	Cl	6	3	0.201
15	SSE9	28.57	21.54	49.85	SaCl	5	2	0.235
16	SSE10	14.51	36.14	42.47	Cl	6	3	0.281
17	SSE11	13.81	45.78	52.62	SaLo	2	1	0.234
18	SNW1	18.72	23.48	60.14	SaLo	2	3	0.156
19	SNW2	12.27	28.19	32.41	Cl	6	2	0.311
20	SNW3	39.98	4.67	41.85	SaClLo	4	3	0.181
21	SNW4	18.91	57.14	41.98	SaClLo	4	1	0.153
22	SNW5	28.18	40.47	65.97	Cl	6	3	0.252
23	SNW6	21.63	44.19	51.57	Cl	6	2	0.254
24	SNW7	11.05	36.97	46.23	Cl	6	2	0.211
25	SNW8	17.45	22.46	55.21	Cl	6	1	0.244
26	SNW9	10.51	30.08	59.47	SaClLo	4	3	0.156
27	SSW1	11.81	25.96	52.13	SaLo	2	1	0.281
28	SSW2	41.89	24.76	31.58	Cl	6	2	0.321
29	SSW3	17.84	39.94	45.78	Cl	6	4	0.237
30	SSW4	16.98	27.80	55.15	SaLo	2	2	0.215
31	SSW5	23.45	23.32	42.31	Cl	6	3	0.230
32	SSW6	22.63	31.01	54.68	Cl	6	1	0.165

Selection of interpolation method

Since the erodibility values were representatives of sampled points, filling non-measured areas was undertaken using spatial interpolation technique. All 32 points K values were then interpolated using the exponential kriging interpolation to create a continuous surface (Figure 4.2).

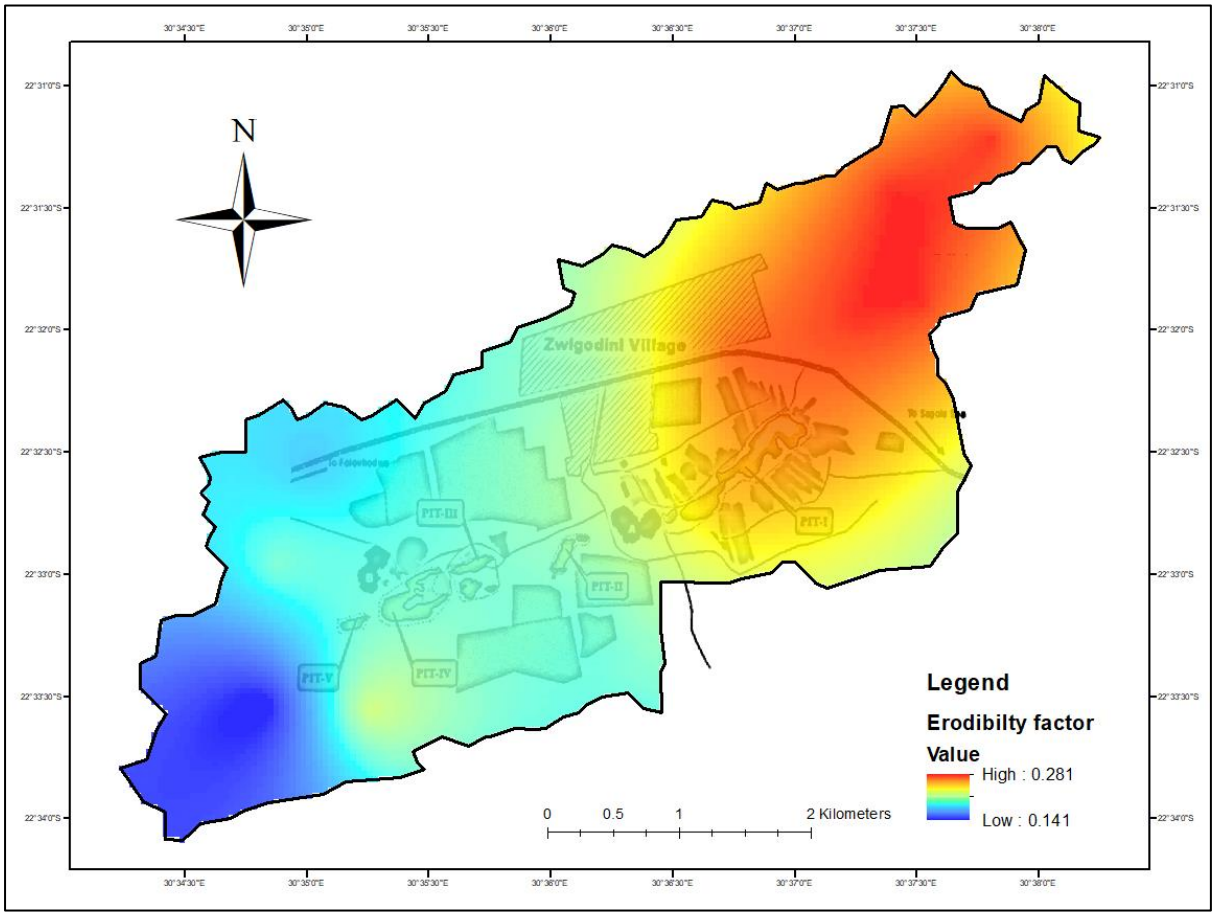

Figure 4.2: Erodibility factor map for the study area.

From the derived map (Figure 4.2), it could be seen that the higher soil erodibility K values were mainly located in the north eastern and south-eastern part of the study area. In this study, soil erodibility factor values were mostly influenced by soil properties. The areas with heavy textured soil and low organic matter content had the lowest values of soil erodibility since detachment decreases as soil particle size either decreases or increases beyond the range of 20–200 µm. Above this range, it is more difficult to detach particles because of the mass, and below this range, cohesive forces counter particle detachment (Carlos & Odette 2012). The

sand and silt fraction values showed the highest correlation with soil erodibility, whereas the clay has the low influence.

4.2.2 Rainfall erosivity

According to Morgan (1995), there is a close relationship between erosion hazard and rainfall; i.e. through the detaching power of raindrops on the soil surface and through the contribution of rain to run-off. Table 4.2 shows the seven randomly distributed rainfall stations within the vicinity of the study area that were applied in the calculation of the rainfall erosivity factor. The calculation of the R-value was conducted with the aid of monthly rainfall records for the period from 1984 - 2014 of the highlighted seven stations.

Table 4.2: Rainfall stations and the mean average precipitation (MAP) of 30 years average. Source: South Africa Weather Bureau (2016)

	SAWB Number	**Station Name**	**Coordinates**		**MAP *(mm)***
			Latitude	**Longitude**	
1	0766277W	Tshipise	-22.48333	30.81667	340
2	0766324W	Siloam	-22.8993	30.19456	562
3	0766779W	Palmaryville	-22.98363	30.43317	811
4	0766842W	Folovhodwe	-22.58915	30.42505	279
5	0812567W	Pafuri	-22.38333	31.16667	306
6	0723070W	Elim	-23.15797	30.05644	855
7	0765607W	Mopane	-22.61702	29.85744	305

The ArcGIS software was used to produce incessant rainfall data for respective grid cell using the average yearly rainfall data using the Inverse Distance Weighted interpolation technique. Figure 4.2 shows the mean annual rainfall distribution maps for R factor which were generated using ArcGIS.

Spatial interpolation of all data points was done using the Ordinary Kriging method from the ArcGIS Spatial Analyst tool to ensure the resolution or grid cell size was like that of the other

maps inserted in the ArcGIS. The parameters used for the Kriging method are shown in Table 4.3.

Kriging is founded on a statistical model inclusive of autocorrelation, that is, the statistical relationships among the measured points. As such, in addition to the ability to produce a prediction surface, geostatistical techniques can also make provisions for some measure of certainty or accuracy of predictions. The R-value of each grid cell was then calculated using equation 3.3. Figure 4.6 shows the rainfall erosivity distribution in the study area with a maximum erosivity value of 176 MJ.ha-1.mm.hr-1 and a minimum of 167 MJ.ha-1.mm.hr-1.

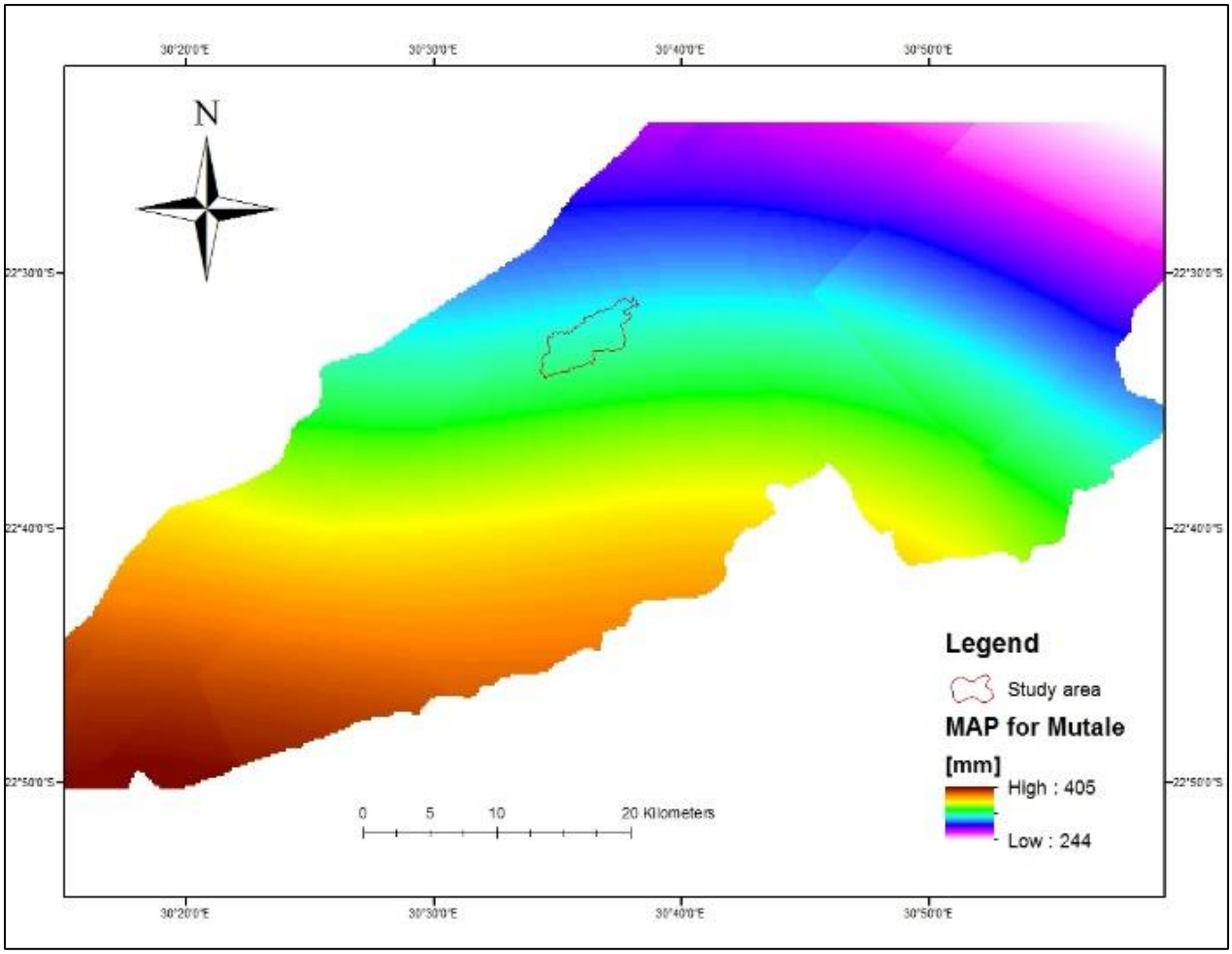

Figure 4.3: Mean annual precipitation map for Mutale municipality showing the study area.

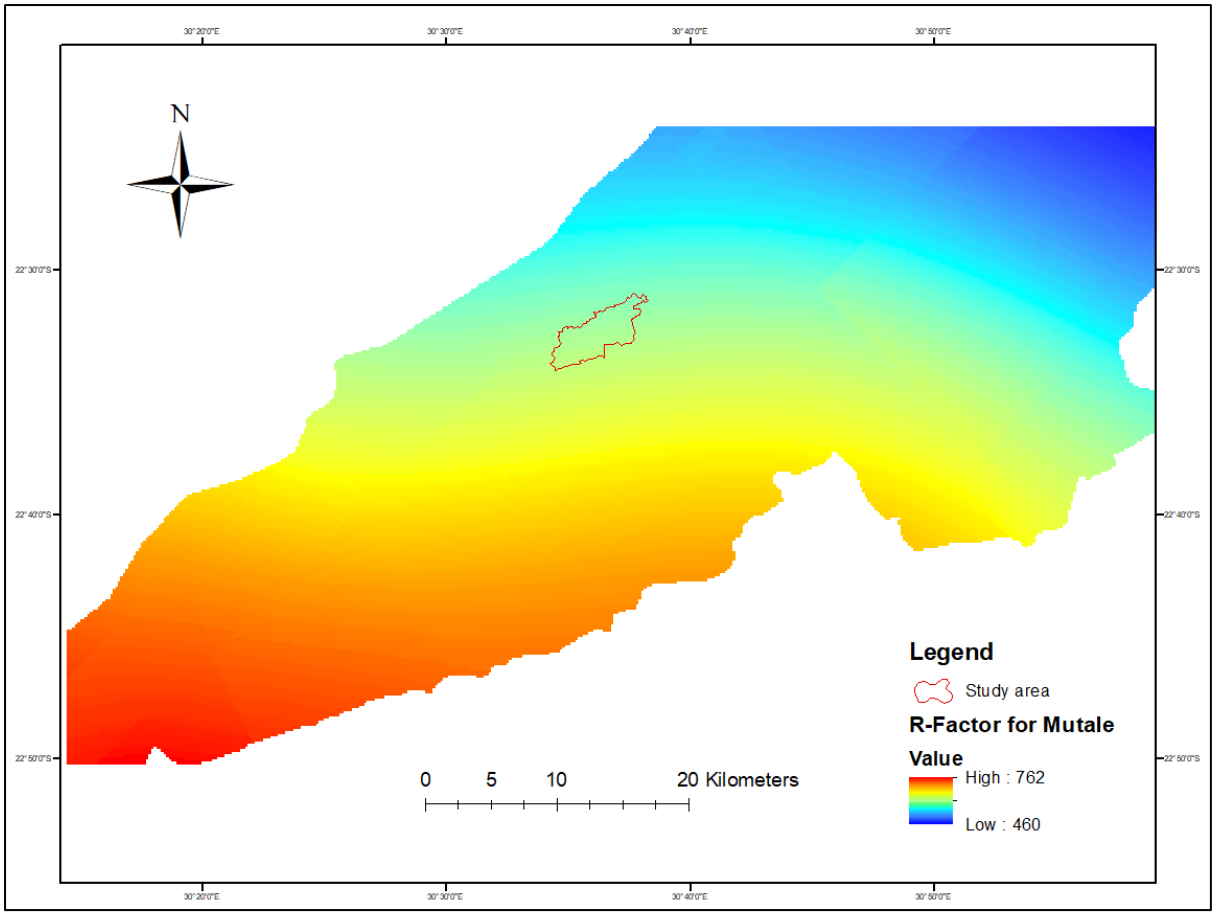

Figure 4.4: The erosivity factor map for Mutale municipality.

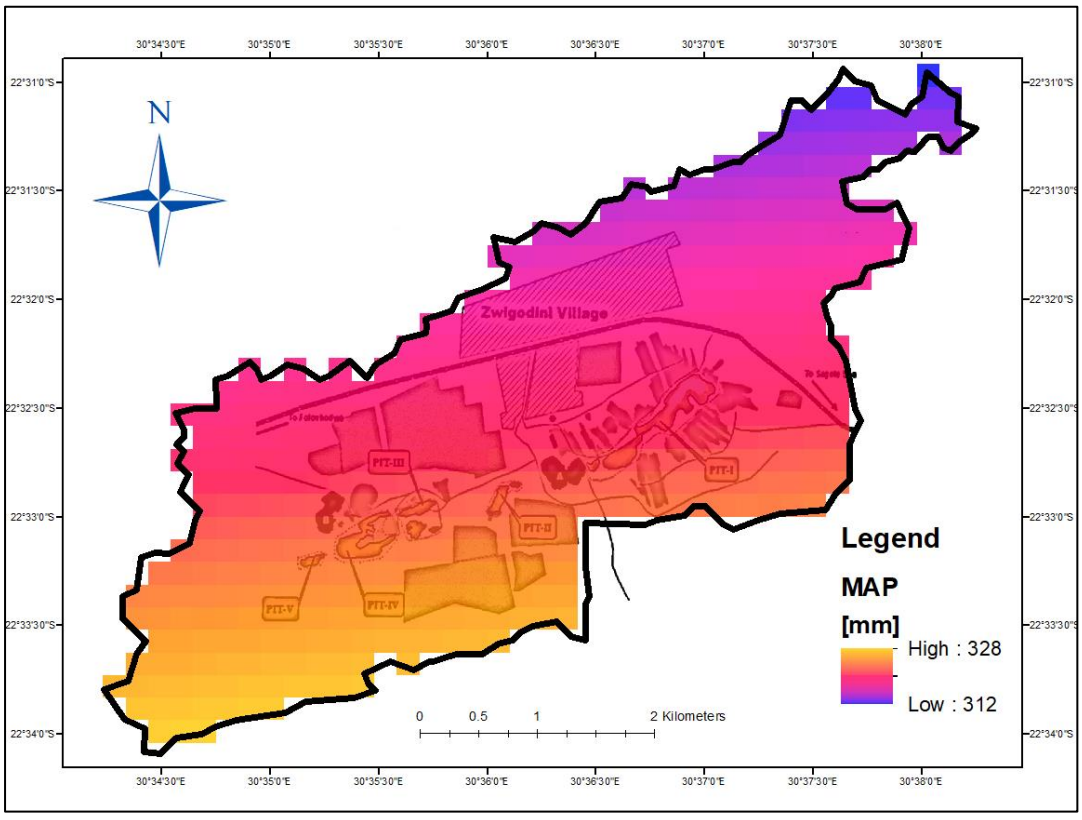

Figure 4.5: Mean annual rainfall within the Nyala mine catchment area

Table 4.3: Summary of interpolation parameters using Ordinary Kriging

Parameter	Values
Values to be interpolated	R-value
Semivariograms Properties A. Kriging method B. Semivariogram model	 Ordinary kriging Spherical
Interpolation size	5 x 5 km
Kriging parameter A. Search type B. Number of points C. Maximum search distance	 Fixed 15 20 km

The small range of the erosivity values can be accounted for by the spatial extent of the study area that receives relatively the same amount of rainfall. The erosivity values are low since the area has a very low mean annual rainfall of 494 mm. This has little effect on the extent of the overall soil erosion hazard in the area which is in line with a study carried out by Mulooka (2008), which concluded that high erosivity values have a strong impact on the detachment of soil particles and transport through runoff.

A study by Rydgren (1996) in Lesotho and South Africa showed that total soil loss could be highly dependent on isolated large single storm events. He indicated that in areas of low rainfall, very intensive isolated storms were responsible for much of annual soil loss. However, the findings of this study are more in line with reports from Mutowo & Chikodzi (2013); Hoyos (2005) and Trustrum *et al.* (1999); that single storms play an insignificant role in comparison to the cumulative of more frequent and lower magnitude events. Li *et al.* (2011) pointed out that the actual erosive power of the rain depends mostly on plant cover which accounts for the low erosion hazard findings of this study.

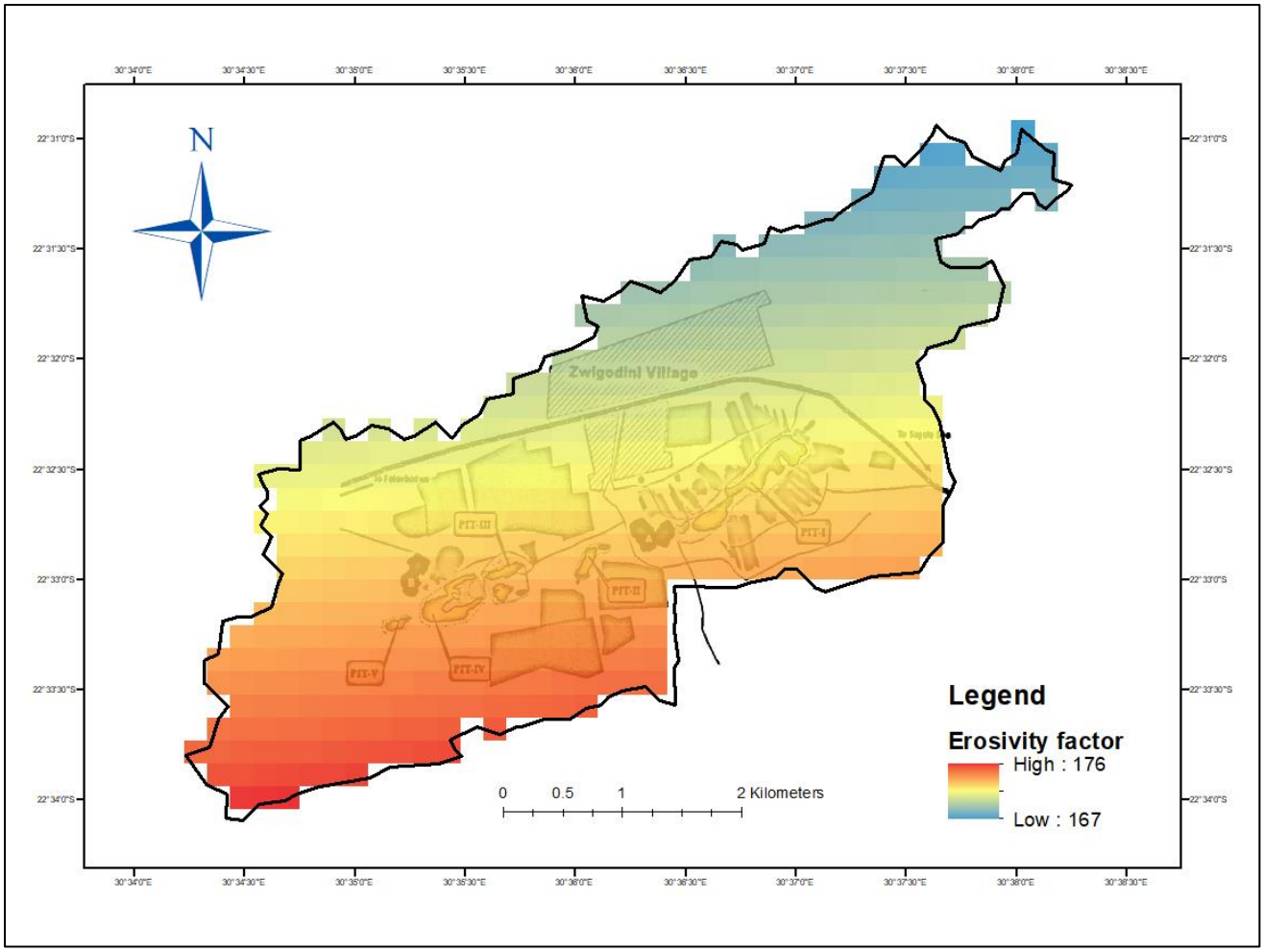

Figure 4.6: Erosivity factor map for the study area

4.2.3 Determination of the erosion hazard index

After obtaining the rainfall erosivity (R-value) and the soil erodibility (Fb-value), the exponential equation adopted from Morgan (1995) was used within ArcGIS raster calculator to generate the Erosion Hazard Index (Ib) in Figure 4.7. The erosion hazard index is a function of soil erodibility and rainfall erosivity. According to Mhangara *et al.* (2012), R factor which is a quantitative expression of the erosivity of local mean annual rainfall is largely influenced by the intensity, volume, duration, and pattern of rainfall and the resultant runoff rate. As such, findings from this study indicate that rainfall erosivity has a minimum bearing on the erosion hazard. However, soil losses are clearly correlated to soil type. The grain size distribution curves indicate that the area has high modified silt content and fine sandy soils which are more erodible thus indicating that soil texture is a more prominent soil erosion factor.

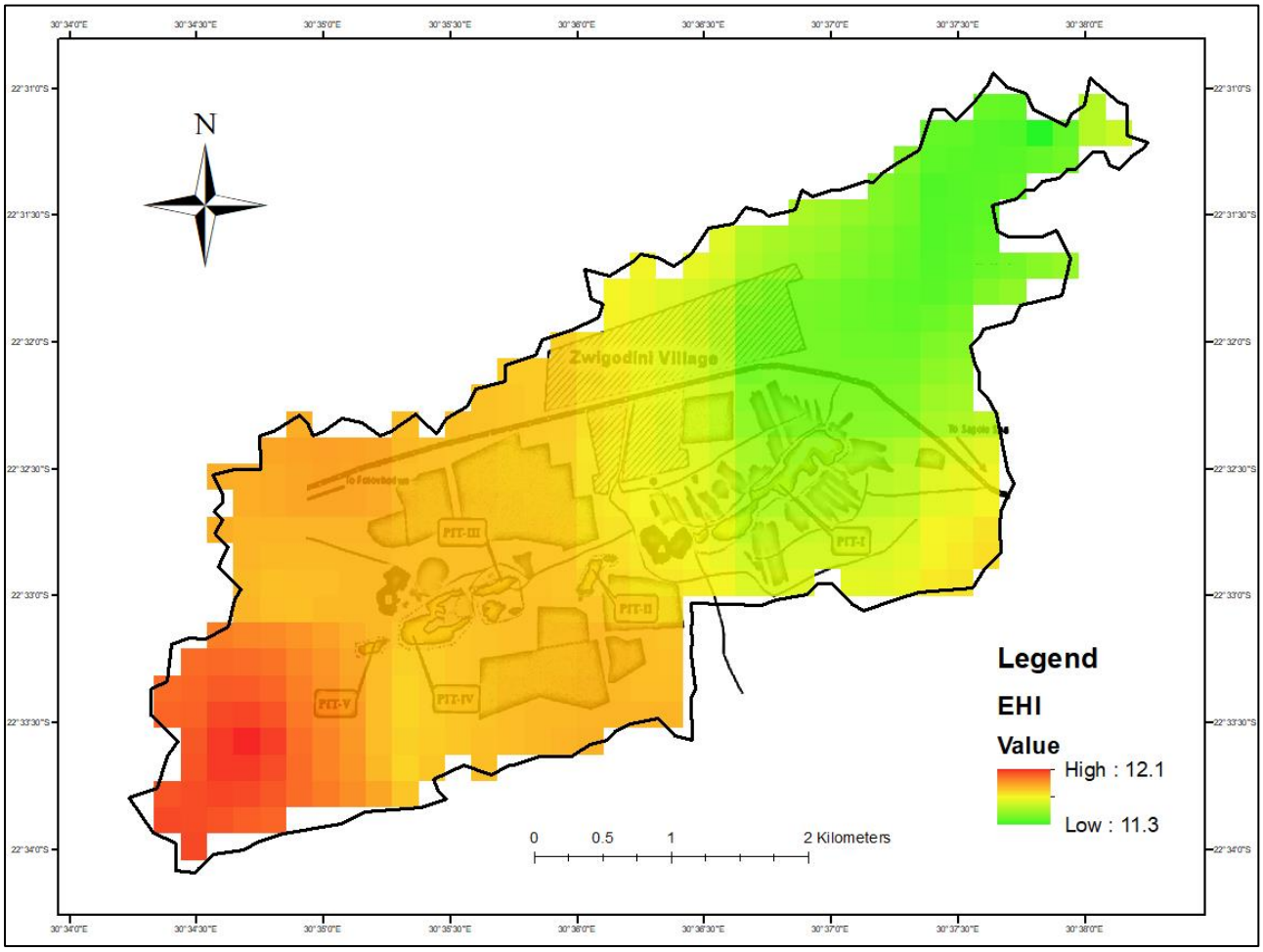

Figure 4.7: Erosion Hazard Index (EHI) map

These findings concur with several previous studies which indicate that soil erodibility resulting from rainfall and surface runoff will increase proportionally with an increase in the amount of fine sand and silt content (Lal, 1994; Hoyos, 2005; Yang *et al,* 2005; Rao *et al,* 2014). Furthermore, results from a study by Diodato *et al.* (2011) showed the highest erosion risks in areas with low annual mean rainfall are associated with high erodibility. Corroborating this, Mhangara *et al.* (2012) deducted from their findings that the finer and richer the soil texture in a clay ratio, the more resistant is soil to particle detachment and lower the erodibility factor is and vice versa. It can, therefore, be noted that in relation to this, the soil erodibility has a significant role in erosion hazard within the study area than rainfall erosivity.

4.3 LAND USE/COVER (C-VALUE) FACTOR

The Landsat ETM+ imagery retrieved on 16 October 2016 (path: 169; row: 76) from United States Geological Survey (USGS) was used to prepare a land use and land cover map of the study area. The image was first processed using the ENVI v5.1 software and the ArcGIS 10.3 software was used to carry out a supervised digital image classification of the study area shown in Figure 4.8. With the aid of field surveys to provide information about the types of land use and land cover; three land use/ cover classes were recognized. These include agricultural, built-up and natural, mainly composed of bare land and shrubs.

The land use/land cover map of the study area in Figure 4.8 was used to determine the C-values. Table 4.4 shows the C-value corresponding to each land cover estimated from the SLEMSA guide used in this study. The land use/land cover factor map of the study was generated by applying each corresponding C-value to each land use class in GIS using the reclass tool method with C Factor value ranging from 0.57 to 0.17 (Figure 4.9).

Table 4.4: Land use/cover C factor values

land-cover/land-use type	**C factor value**	**References**
Forest	0.02	Hurni (1998)
Grassland	0.01	Eweg & van Lammeren (1996)
Agricultural land	0.17	Hurni (1998)
Bare land	0.6	BCEOM (1998)
Shrub	0.014	Wischmeier and Smith (1978)

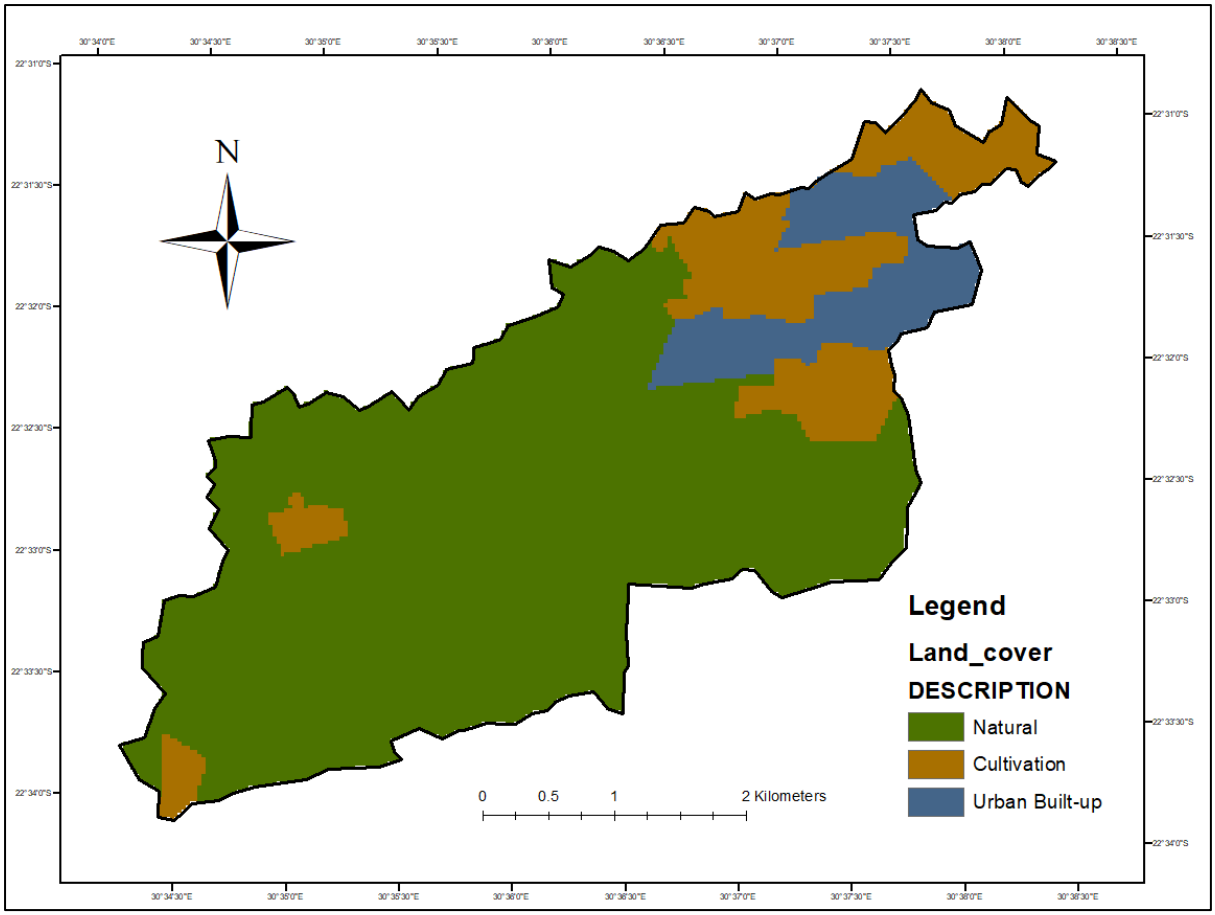

Figure 4.8: Land-use/land-cover types of the study area

The northeastern part of the study area is characterized by human activities. The observed expansion of settlements and rainfed agriculture have accentuated the mining impacts that include widespread removal of vegetation cover. In a study by Mhlongo *et al.* (2012), there have been prominent changes in land cover/use that has taken place in and around the abandoned mine. Various scholars have also indicated that vulnerability to higher surface water erosion related to adverse impacts of land use and land cover changes (Mashesha *et al,* 2014; Samuel, 2014; Daba, 2003). Accordingly, this has increased the susceptibility of soils to erosion as the findings indicate a strong relationship between high erosion hazard (Figure 5.8) and the intensification of cultivation and expansion of settlements.

As such, continued expansion in settlements and cultivation could have had an impact on the increased high erosion hazard observed in the study. Flügel *et al.* (2003) confirm this trend in the Mkomazi catchment in KwaZulu-Natal where they noted that sprouting informal

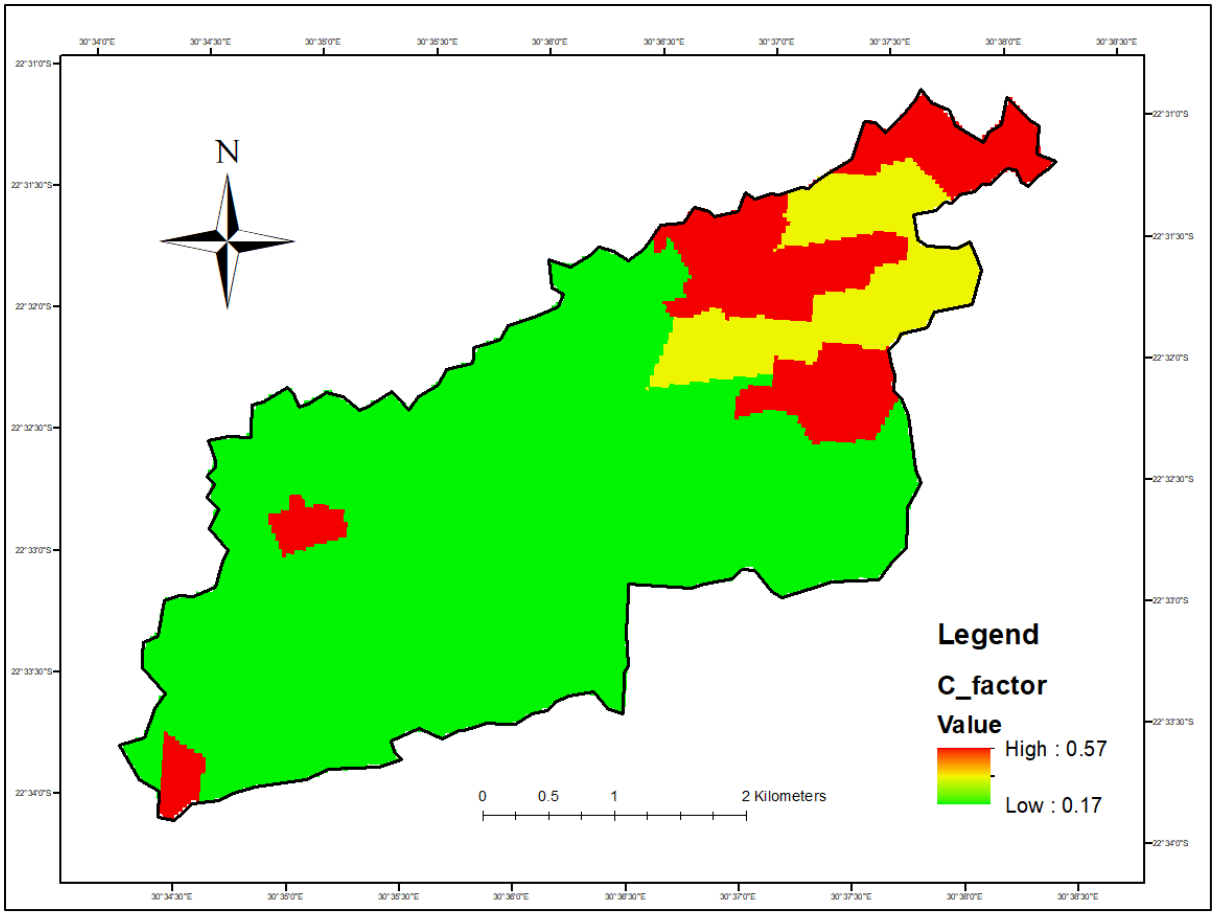

Figure 4.9: Land use/cover factor C-values in the study area.

settlements were associated with an increase in high erodibility values. Furthermore, the results of this research corroborate findings from a study by Dube (2011) and Antwi *et al.* (2008) that intensification in agriculture was the main factor contributing towards an increase in soil erosion hazard. Agriculture usually increases erosion significantly by loosening and dislodging soil particles through the tilling of the soil (Antwi *et al,* 2008). Furthermore, results confirm the findings by Sharma *et al.* (2010) that disappearance of forest patches and intensification of cultivation practice in relatively more erosion-prone soil were the main factors contributing toward the increase in soil erosion.

4.4 SOIL LOSS RATIO

According to Bizuwerk *et al.* (2008) the slope length (L) and slope steepness (S) can be applied in a single index within ArcGIS, which expresses soil loss ration according to the definition provided by Wischmeier and Smith (1978). Equation 4.1 and 4.2 (Bizuwerk *et al,*

2008) were suggested for calculating the LS as a single index in ArcGIS. The values of L and S parameters were derived from Aster Digital Elevation Model (DEM) with a resolution of 30 m. To calculate the L value, the derivation of Flow Accumulation was based on the DEM after conducting the Fill and Flow Direction processes respectively in ArcGIS.

$$L = (flow\ accumulation \times cell\ value) \quad (4.1)$$

By substituting L, the topographic ratio equation becomes;

$$X = \frac{(flw\_accum \times cell\_val)^m \times (0.76 + 0.53S + 0.076S^2)}{25.65} \quad (4.2)$$

Where: X = Topographic Ratio

L = Slope Length (m)

S = Slope Steepness (%)

The ArcGIS Software Slope (%) was used to derive the DEM. The value of *m* (which is an exponent that relies on slope steepness) varies from 0.2 - 0.5 depending on the slope as shown in Table 4.5.

Table 4.5: m values for LS factor

***m*_Value**	**Slope (%)**
0.5	> 5
0.4	3 – 5
0.3	1 – 3
0.2	< 1

The first step comprised the modification of the elevation value by filling the sinks in the grid. This is necessary for avoiding the challenge of discontinuous flow that emanates due to

entrapment of water in a cell surrounded by cells with higher elevation. This was achieved by utilizing the Fill tool under Hydrology section falling under Spatial Analyst Tool Function in ArcGIS.

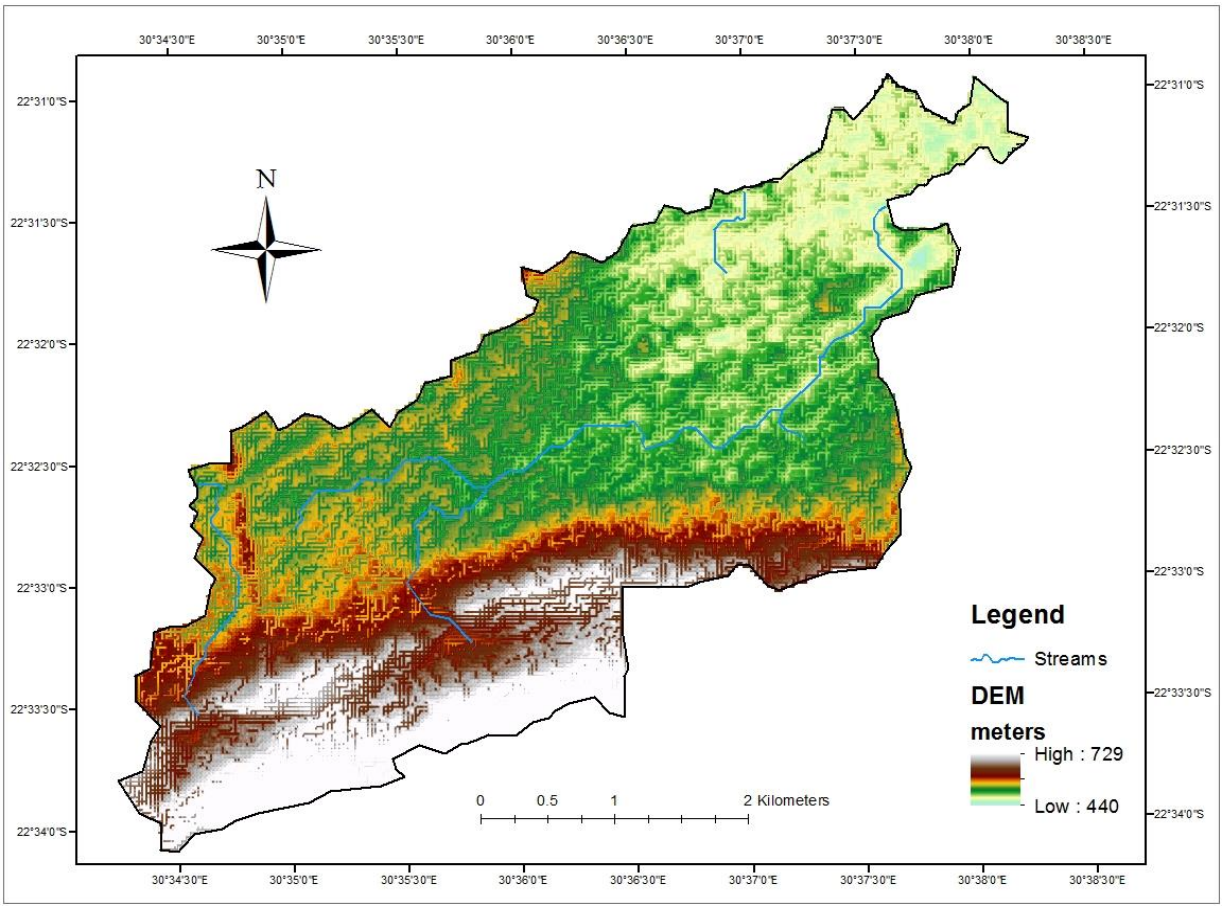

Figure 4.10: DEM showing the elevation of the study area

Subsequently, the Fill grid was used to generate the Flow direction. Identification of the down-slope direction for each cell is achieved by the Flow direction tool which considers a terrain surface. In this grid is the presentation of the on-surface water flow direction from one cell to any one of the eight neighbouring cells. The Flow direction tool under Hydrology section of the Spatial Analyst Tool Function in ArcGIS was used for this identification.

The Flow accumulation was then calculated using the Flow direction. The main function of the Flow accumulation tool is to identify the amount of surface flow that accumulates in each cell, and cells with high accumulation values are usually streams or river channels. It also used to identify local topographic highs (areas of zero flow accumulation) such as mountain peaks and

ridgelines. This was done by using the Flow accumulation tool under Hydrology section which falls under Spatial Analyst Tool Function in ArcGIS.

Finally, computing of the LS factor was done using the modified equation 3.2 which was input with the aid of the Spatial Analyst feature, the Raster calculator function, while the selection of the *m* value of 0.4 (Table 4.5) was based on the slope calculations gathered from the field survey. The resulting topographic ratio map is shown in Figure 4.11. After extracting the DEM within the study area, the minimum and maximum altitude of the area were 440 and 729 m, respectively (Figure 4.10), which is comparable to the observed minimum and maximum altitudes. The mean elevation is 585 m with standard deviation of 45.

Results indicate that the study area has a predominant LS factor value less than 25 with maximum values of greater than 100 being observed in areas that are characterized by relatively high slope percentage (67.85 %). A study by Abate explains this phenomenon as it reported that high soil loss rate and heightened soil erosion hazard is closely associated with steep slopes. The findings of this study which show increase soil erosion in the very steep slope areas that contribute to approximately 73.5% of the total soil loss are consistent with findings of a study by Karamage *et al.* (2016) for the Nyabarongo River Catchment in Rwanda.

Haarhof *et al.* (1994) highlighted that the effect of slope steepness in South Africa is significant on steep slopes of 20 % or more. A report by Gelagay & Minale (2016) showed a positive correlation between soil erosion and topography while Meshesha *et al.* (2014) observed an increased severity of soil erosion in Ethiopia's eastern highlands as the slope changed from 10 to 20 %. On a slope of 20 %, they recorded a total soil loss of 215 t/ha/yr. from bare lands in contrast to soil loss of 12.6 t/ha/yr. on a 1 % slope. It is vital, however, to point out that the amount of soil loss cannot only be accounted for by slope angle and slope length parameters. Various intricate interrelationships exist between the microtopography, rainfall energy, plant cover, and soil properties at these localities that contribute to soil loss.

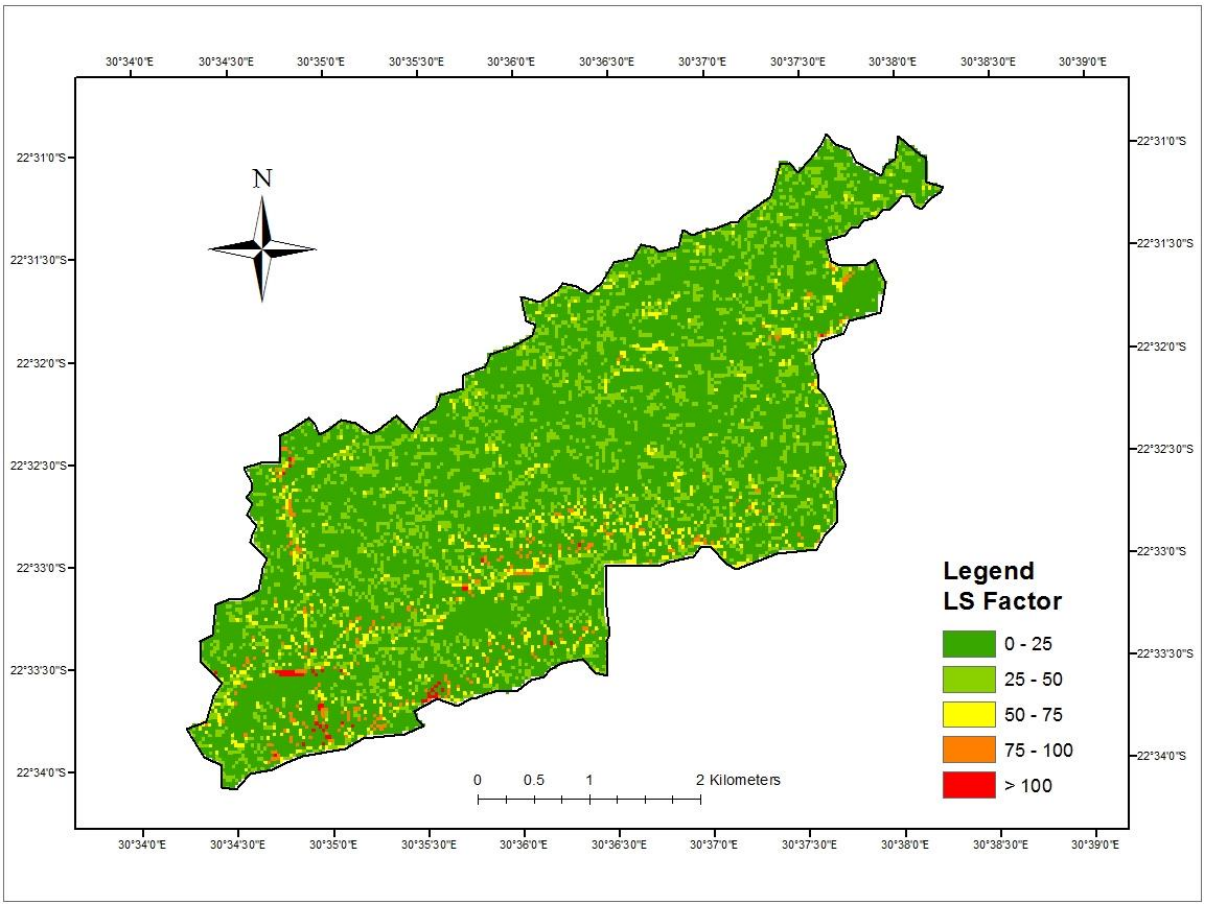

Figure 4.11: Map showing the LS factor (topographic ratio)

However, despite the prevalence in areas of high slope percentage, the findings indicate that 79.1 % of the study area still has a low LS value (< 25). This clearly points out to a strong inverse relationship between soil erosion hazard and vegetation cover. Though the effect of other soil erosion factors such as raindrop impact is accentuated by slope steepness or runoff increase with slope length, the influence of slope on soil erosion, however, remains inferior to that of vegetation cover. Confirming this, Li *et al.* (2011) and Efe *et al.* (2008) pointed out that the existence of vegetation cover diminishes the severe impact of slope gradients on soil erosion intensity.

4.5 SOIL EROSION MODELING

Soil erosion models integrated in GIS may be essential in the assessment of the spatial distribution of soil loss, the identification of areas of concern and the simulation of probable

management scenarios (Flacke *et al,* 1990; Busacca *et al,* 1993; Desmet & Govers, 1996; Mitasova *et al,* 1996; Pretorius and Smith, 1998; Breetzke, 2004).

4.5.1 Application of SLEMSA in ARCGIS MODEL_BUILDER

An ArcGIS toolbox was developed using Model_builder, for the automated estimation of soil erosion based on the SLEMSA equation, named ArcSLEMSA. The flowchart of the implementation of the SLEMSA model within ArcGIS Model_builder environment is shown in Figure 4.12.

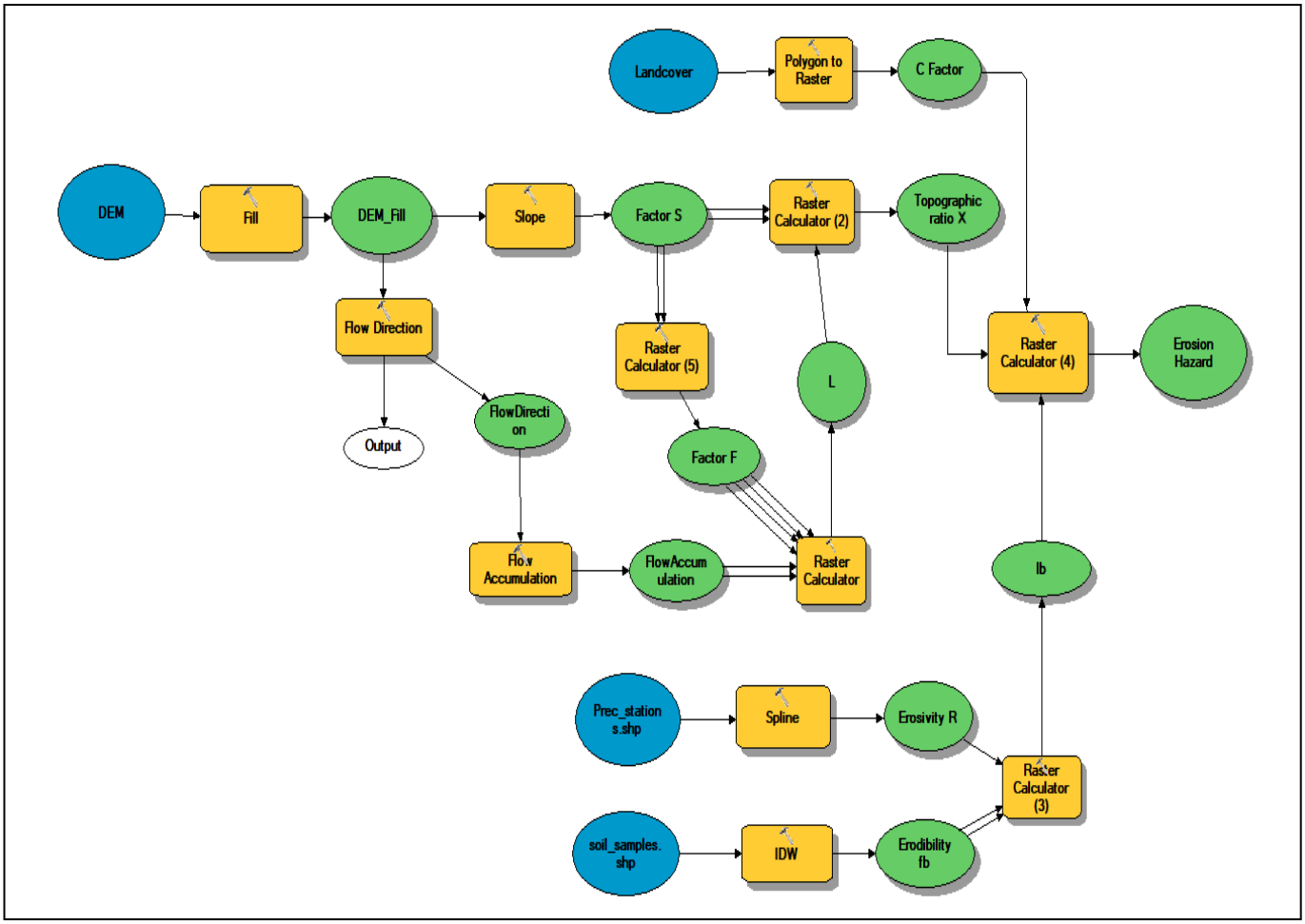

Figure 4.12: Development of SLEMSA soil erosion model in ArcGIS Model builder.

4.5.2 Erosion hazard

The resulting soil loss map of the study area was obtained by multiplying the derived parameters of the SLEMSA model using the raster calculator function tool in the ArcGIS

environment by a cell by cell analysis. Figure 4.13 represents the average annual soil loss rate map of the Nyala mine watershed. The maximum soil loss rate observed is 4.48 tons/ha/yr. and the minimum soil loss rate is 0.39 tons/ha/yr. Much of the watershed (approx. 75%) annual soil loss ranges from 0 in the central parts of the study area to over 4.4 tons/ha/yr. in the northeastern areas of the watershed. High soil loss rates are also noted along the southeastern boundary largely to the steep slopes present. The total average annual soil loss for the entire Nyala mine watershed was estimated at 2.76 tons per year from 1 725 ha.

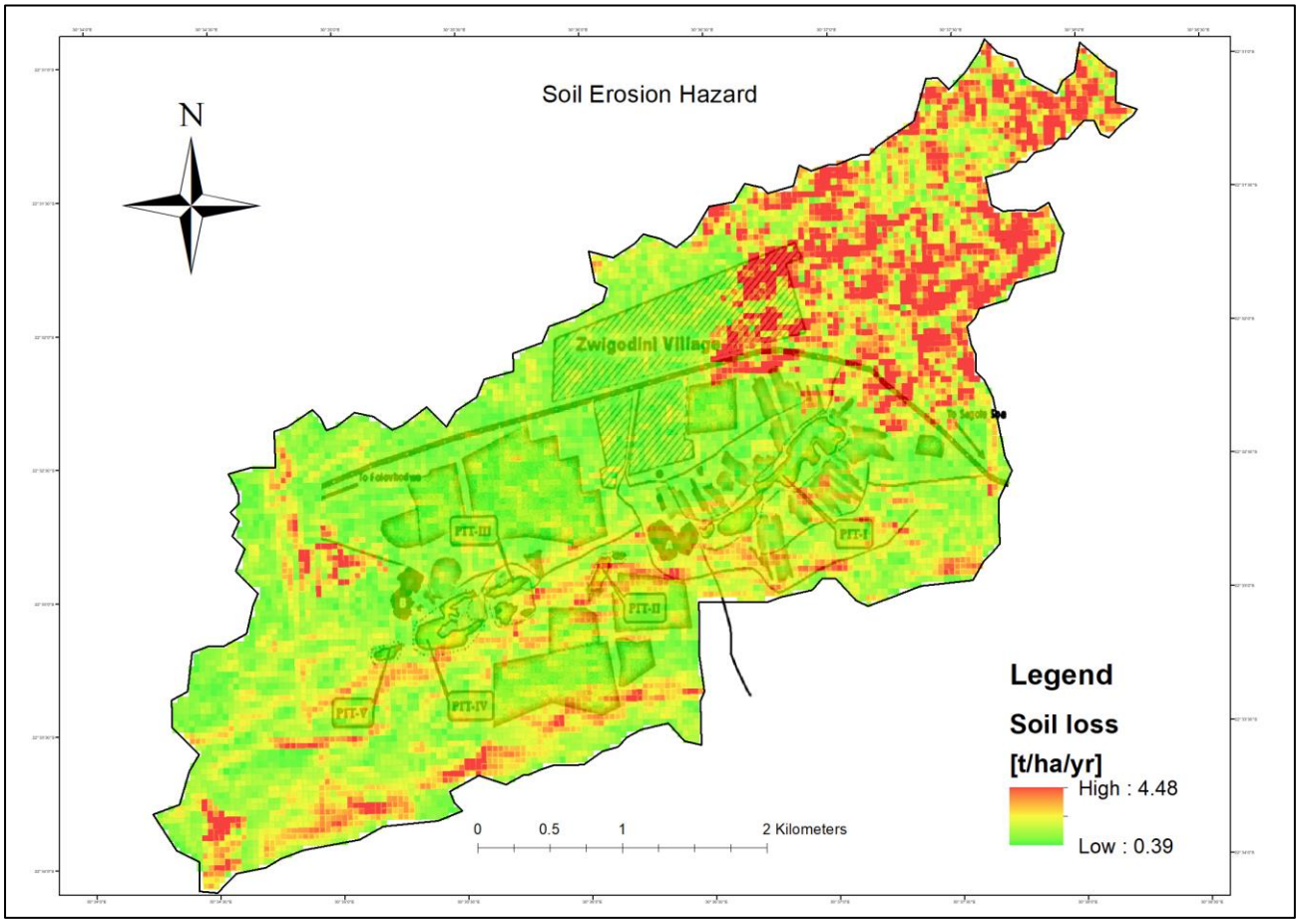

Figure 4.13: Annual soil loss map for the study area

4.6 SPATIAL VARIATION OF EROSION HAZARD

According to Stocking *et al.* (1988), soil erosion is a complex process which should be expressed as a dimensionless number in Erosion Hazard Units (EHU). Dube (2011) argues that it is the relative variation in the rate than the actual values that are significant in carrying

erosion hazard assessment over a given area. Based on their work, Figure 4.14 represents a soil hazard map showing the spatial variation classified into five erosion hazard classes.

It can be observed that much of the area is under class 1 of low erosion hazard (EHU ≤ 10). This is greatly attributed to the general low slope of the study area (see map in Appendix). Despite the high erodibility of abandoned mining areas particularly characterized by disturbed soils, the area has a low erosion hazard, and this is mainly due to the gentleness of the slopes, which according to Stocking *et al.* (1988), counteracts the high erodibility of the soil. This indicates that the topographic effects on erosion within the study area are minimal.

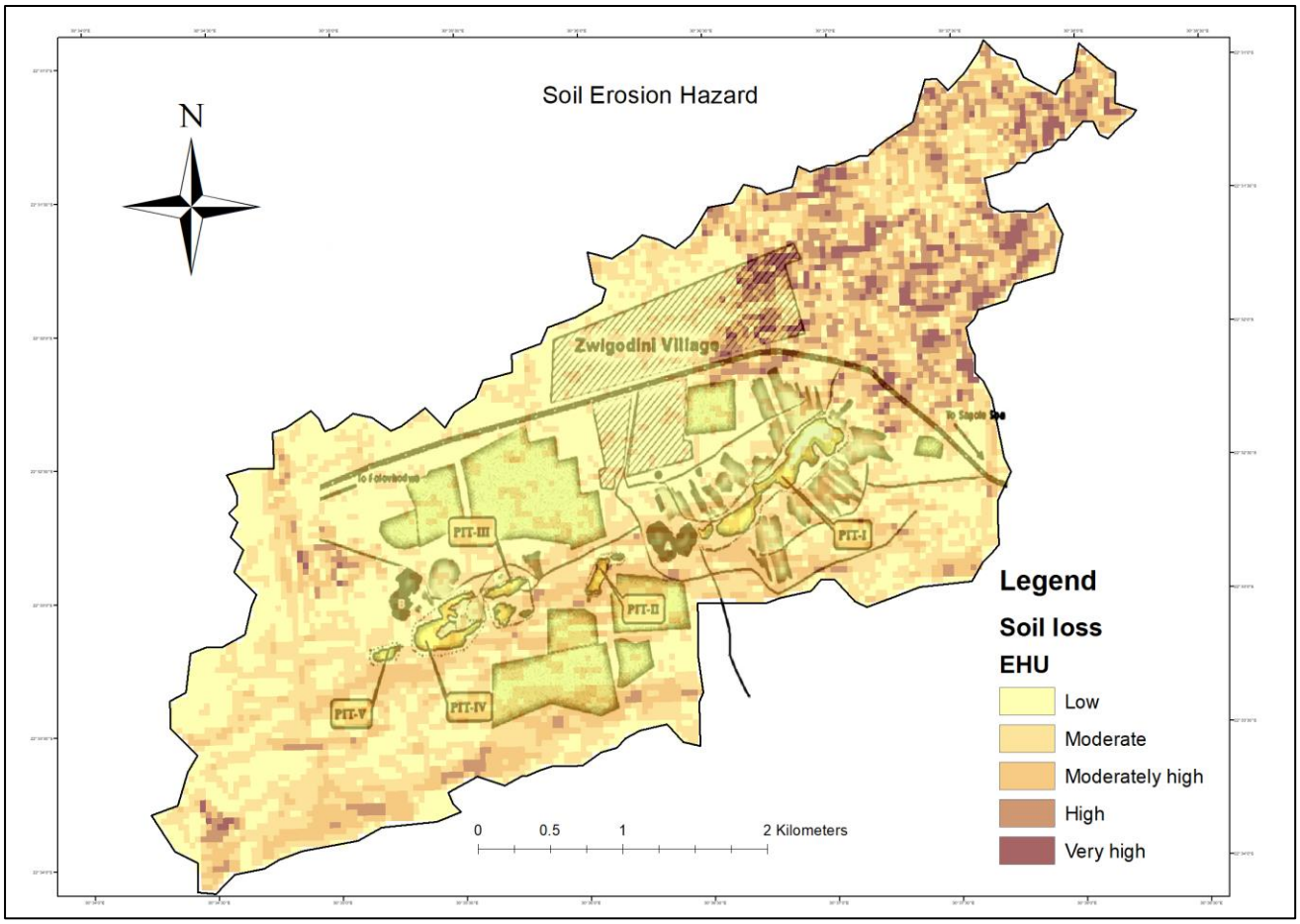

Figure 4.14: Soil erosion hazard map for the study area

Figure 4.15 illustrates the area covered by each erosion hazard class within the study area. The greater part of the area is in the low erosion hazard class (≤ 10 EHU) constituting 41.6 % of the watershed followed by the moderate class (10 < EHU ≤ 25) which covers 32.7 %. The

moderately high class (25 < EHU ≤ 50) covers 16.3 % of the total area while the high erosion hazard class (50 < EHU ≤ 100) and the very high erosion hazard class (EHU > 100) covers 7.2 % and 2.6 % respectively.

Findings indicate that 74.3 % of the whole watershed falls within the low and moderate erosion hazard classes. This can be attributed to the combination of a low topographic ratio and low erosivity factor. The study ascertained that 63.1 % of the abandoned mining area has a percentage slope of 5 % or less, which accordingly compensate the effects of easily erodible soils. The results prove that classes with extreme soil loss constitute 26.1 % of the total study area yet accounting for approximately 54 % of the total soil loss. This agrees with various research results that only a small proportion of a watershed accounts for much of the total soil loss (Mati *et al,* 2000; Tripathi *et al,* 2003).

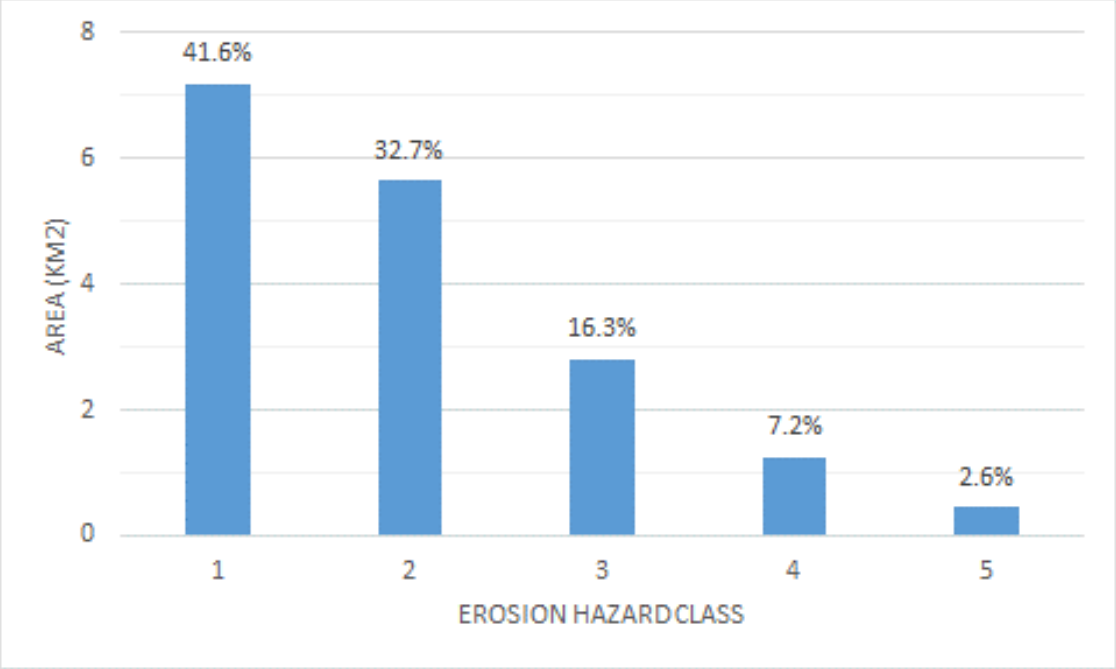

Figure 4.15: Percentage area for each erosion hazard class

The north-east part of the study area is characterized by high to very high erosion classes. This soils in the area are significantly disturbed by mining activities (Eweg and van Lammeren, 1996), hence they have a high erodibility factor and as such highly prone to erosion.

Topography and soil cover have been altered owing to the digging of open cast mine and discarding of overburden rock mass in the form of large heaps. The mining area soils that have been exposed to further erosion are a result of mass deforestation.

The south-eastern boundary is characterized by moderate high erosion hazard with various pockets of high erosion hazard. This is largely attributed to the steep slopes as this part of the area forms part of the Soutpansberg mountain range. These results are in line with various studies (Borselli *et al,* 2012; Wordofa, 2011; Marker *et al,* 2001) that there is a strong correlation between slope steepness and erosion hazard. Wordofa (2011) concluded that annual soil loss and total runoff in relation to slope gradient increase exponentially with degree in slope and distance from runoff onset. Gete and Hurni (2000) made similar conclusions that the erosive force of runoff increases with both slope steepness and distance downslope.

4.7 MODEL VALIDATION

From the sensitivity analysis, the most sensitive parameter in SLEMSA is the lb factor and mainly the soil erodibility value (fb value). A 15% increase in the fb value caused a 21.34 % decrease in soil loss. This implies that as the value of fb increases, it reduces the lb value, which in return reduced the amount of soil loss calculated. Therefore, the higher the fb value the less erodible the soil is and the vice versa.

Table 4.6: Factor-value calculations applied for the sensitivity analysis of the model.

Factor varied	*Lb*	*C*	*X*	Varied Z	Calculated Z	% change in soil loss
fb	9.37	0.57	0.65	3.52	4.48	21.34
i	12.1	0.55	0.65	4.39	4.48	2.01
S	12.1	0.57	0.57	3.96	4.48	11.4

The second sensitive parameter was found to be the topographic ratio especially the slope steepness where a 15 % increase in the slope steepness caused 11.4 % increase change in

the soil loss. This implies that as the slope steepness increases, the amount of soil eroded from the land also increases and this might be due to increased runoff velocity.

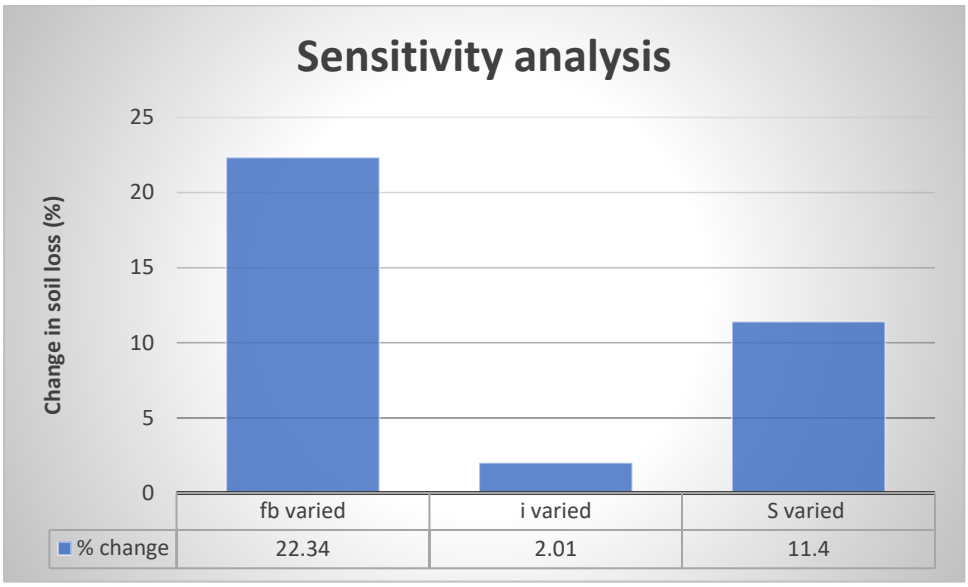

Figure 5.16: Sensitivity analysis of the SLEMSA model.

4.8 IMPLICATION OF FINDINGS

An accurate validation of the soil loss rates obtained is challenging, as there is a dearth of empirical investigations covering soil loss in Limpopo and absence of calculated soil loss data from run-off plots in the watershed. It was beyond the scope of the study to develop a set of field data to assess the accuracy of the SLEMSA model but rather to give a general quantitative assessment of soil erosion around the abandoned Nyala mine in order to support mine reclamation and rehabilitation. However, the SLEMSA model as used by many scientists in Africa and South Africa alike has been applied at such scales and these studies have demonstrated that the model is capable of adequately predicting soil loss under different land use, despite being applied to conditions beyond the original database.

The spatial scale with which the SLEMSA model was applied in the study is not the spatial scale for which it was conceived. The mismatch between the small spatial and temporal scales of data collection and model conceptualisation, and the large spatial and temporal scales of most intended uses of the model is a major challenge in soil erosion modelling.

However, the study has shown that the use of GIS and remote sensing can be significant in determining the spatial distribution of soil erosion hazard using the SLEMSA model. Costly and tedious field methods of obtaining land cover (Bartsch *et al,* 2002) have been replaced by remote sensing derived land cover from satellite imagery. The study demonstrates that geospatial technologies integrated with SLEMSA provide a useful tool to estimate erosion hazard over abandoned mines and facilitate reclamation and rehabilitation efforts, through the delineation of erosion-prone areas (Stillhardt, Herweg, and Hurni, 2002; Nyssen *et al,* 2004; Kaltenrieder, 2007; Bewket & Teferi, 2009).

It can be noted that there are numerous studies on erosion risk assessment, but none provided for an easier automated tool for easy estimation. The aim of this study was thus the development and implementation of an automatic procedure in ArcGIS Model Builder for soil erosion risk assessment for the study area using the SLEMSA Equation.

The major benefit to the use of the ArcGIS Model Builder for the application of SLEMSA and the assessment of soil erosion risk for the study area was the automation of a spatial analytical procedure. There are dynamic processes in the model and their relations which enable the dynamic automatic update of the model, making the modification, sharing and reuse of the model by several users for future applications in abandoned mines a simple task.

An assessment of erosion hazard around the abandoned Nyala mine has produced the spatial variability of soil erosion hazard with low hazard areas covering a total area of 41.6 %, while the moderate hazard areas cover 32.7 %. The areas covered by moderate high, high hazard and very high erosion hazard are 16.3 %, 7.2 %, and 2.6 % respectively. These indicate areas that need immediate attention in abandoned mine reclamation and rehabilitation efforts.

4.9 CHAPTER SUMMARY

This chapter has presented results from this research and how they were obtained using the methodology outlined in chapter three. The GIS software was used to derive the SLEMSA model parameters, the EHI derived from erodibility and erosivity, cover factor and the

topographic ratio (LS factor). The respective results were also discussed and compared with literature from other studies. In this study, spatial distribution patterns of soil loss and the critical sites of erosion in a catchment were highlighted. There is more evidence of alarming soil erosion rates with catchment areas resulting from anthropogenic activities that had been brought to light by this study. The effect of the role of human activities in vegetation cover monitoring and other conservation management activities on soil erosion have been identified.

CHAPTER FIVE

SUMMARY, CONCLUSIONS, AND RECOMMENDATIONS

5.1 INTRODUCTION

The summary, conclusions, and recommendations of the study on assessment of soil erosion hazard around an abandoned Nyala mine in Mutale Municipality are presented in this chapter. The conclusions and recommendations emanate from the findings of the study. The purpose of recommendations is provision of guidelines and information for miners and geotechnical engineers on the evaluation, analysis and control of surficial erosion and long-term geomorphic-induced regional erosion that may affect the environment of reclaimed and closed mine sites.

5.2 SUMMARY

Soil erosion processes are natural geological phenomena that have operated on the environment throughout the course of time. However, the process, has in recent years, accelerated largely owing to the ever-increasing human intervention on the environment. Such activities including mining have accelerated the rate of soil erosion thus endangering clean water supplies/reservoirs, posing a serious threat to agricultural production and causing ecosystem degradation.

The study was intended to assess the soil erosion hazard associated with the abandoned Nyala mine. The SLEMSA model framework developed by Elwell (1978) was adopted to estimate the spatial variation in soil loss since it is easy to understand and apply, have simple parameters and have been used throughout Africa and Southern Africa. This was coupled with geospatial technologies particularly Geographic Information Systems and remote sensing to provide viable results that could support abandoned mine reclamation and rehabilitation planning. However, in this study, the modified version of the SLEMSA model (Stocking *et al,* 1998) was integrated with the ArcGIS software where the model parameters, Erosion Hazard

Index (lb), the topographic ratio (x) and land cover factor (c) were derived. The soil erosion hazard was determined by a cell by cell analysis by multiplying the respective SLEMSA factor values interactively in ArcGIS 10.3 using the raster calculator.

The results of the study indicate that much of the watershed (74.3 %) is experiencing low to moderate erosion hazard. This is because of the combination of the minimum effects of topography in the area (with slopes ≤ 8% constituting 63.1 % of the entire area); and the low rainfall erosivity. The results from the soil loss map indicate that a maximum rate of 4.8 tons/ha/yr. is lost within the watershed while the minimum soil loss rate is estimated at 0.39 tons/ha/yr. The total average annual soil loss for the watershed area is estimated at 2.76 tons/ha/yr.

5.3 CONCLUSIONS

Various studies on soil erosion and their subsequent impacts have been conducted and findings have shown that soil erosion assessment is a tedious and capital intensive and time-consuming process (Bewket & Teferi, 2009; Dabral *et al,* 2008; Flugel *et al,* 2003). This research demonstrates how GIS and remote sensing enhances our capacity to assess and model soil erosion hazard in an affordable and time effective way. The study also demonstrates that the SLEMSA model can be used to estimate erosion hazard in abandoned mines to aid reclamation and rehabilitation planning. Proper mitigation actions for the affected area may thus be devised for areas of high soil erosion potential. The main benefit of using this approach is the rapid assessment of soil erosion potential on a watershed scale.

The potential use of GIS and remote sensing to carry out SLEMSA estimations can be valuable in the reclamation and rehabilitation of the prevalent abandoned mine lands in South Africa. Regarding the new procedure on African conditions, characterized by minimal data availability and coverage at a sub-continental scale; the SLEMSA framework has proved to be an important tool in designing a suitable methodology. Variables for the measurement of

influence of relief, rainfall, vegetation, and soil on erosion were derived via the major factors in erosion.

Results from the study clearly demonstrates the effectiveness of implementation of the SLEMSA model as means of modeling soil erosion hazard in abandoned mining lands. The implementation of SLEMSA in the research has clearly shown the applicability of coupling an empirical soil loss model and geomatics techniques (GIS and remote sensing) to assess the spatial variation of soil erosion and the relative erosion hazard over a given geographical area. Incorporating the use of geomatics allows the drawing of conclusions from multiple databases and adds the capability of updating and improving the information as new data are acquired.

Findings from the study indicate that erosion hazard is most severe at the abandoned mine sites in relation to the surrounding areas, where the soil has been greatly disturbed and vegetation cover is minimum. High erosion is also noted at relatively high elevations where slopes are steep. In contrast, low elevation areas with gentle slopes exhibit a relatively low erosion hazard, despite minimum vegetation cover and this is greatly attributed to the low rainfall erosivity. The model provided a unique ability to discover the relevant parameters that control erosion potential in each part of the watershed without the need of conducting intensive fieldwork.

5.4 RECOMMENDATIONS

The SLEMSA model was originally developed for agricultural field soil assessment. Though it has been successfully implemented in various environments, there is further need for refining and calibrating the model specifically for mining lands, as well as extending the application to other abandoned mine lands in South Africa for universal applicability. This would enhance future environmental impact assessments and facilitate abandoned mine reclamation and rehabilitation planning.

There are no actual soil erosion measurements for the study area hence the validation of the SLEMSA results was not possible. As with all models, the parameters of the model should be

validated within the area in which they are being applied. It will be imperative to conduct a sensitivity analysis of the model after calibration. Model calibration and parameter estimation can add reliability of the model estimates.

The SLEMSA model does not estimate rill or gully erosion. The study does not account for areas having severe gully erosion, hence another model needs to be incorporated to consider gully erosion hazard for this area as well as other similar abandoned mines. In addition, although the use of GIS and remote sensing have proved to be valuable, further studies with limited spatial scale using high resolution and multi-temporal data is recommended to closely monitor and mitigate erosion hazard appropriately.

REFERENCES

Abate, S. 2011. Estimating soil loss rates for soil conservation planning in the Borena Woreda of South Wollo Highlands, Ethiopia. J. Sustain. Dev. Afr., 13, 87–106.

Alam, T. 2014. Precipitation Distribution and Erosivity in Bangladesh 1981-2010.

Alewell, Egli, & Meusburger. 2015. An attempt to estimate tolerable soil erosion rates by matching soil formation with denudation in Alpine grassland. *Journal of Soils and Sediments*.

Ali, S. A. and Hagos, H. 2016. Estimation of soil erosion using USLE and GIS in Awassa Catchment, Rift Valley, Central Ethiopia. Geoderma Regional.

Allen, C., Maurer, A. and Fainstein, M. 2001. Mine Site Rehabilitation: An Economic Review of Current Policy Issues, ABARE Report presented to the Department of Industry, Science, and Resources, Canberra.

Alphan, H., Doygun, H. and Unlukaplan, Y. 2009. Post classification of land cover using multitemporal Landsat and ASTER imagery: the case of Kahramanmaras, Turkey. *Environmental Monitoring and Assessment, 151(1-4), 327-336.*

Amir Gandomkar. 2009. Using GIS in Soil Erosion Control (Case study: Mousa Abad Basin, Isfahan, Iran). GIS Ostrava. 25. - 28. 1.

Amsalu, T. and Mengaw, A. 2014. GIS-Based Soil Loss Estimation Using RUSLE Model: The Case of Jabi Teheran Woreda, ANRS; Ethiopia. *Natural Resources*, 5, 616-626.

Anache, J.A.A.; Bacchi, C.G.V.; Panachuki, E.; Sobrinho, T.A. 2015. Assessment of Methods for Predicting Soil erodibility in Soil Loss Modeling. São Paulo, UNESP. *Geociências, 34, 32–40.*

Angima, S. D., Stott, D. E., O'Neill, M. K. and Weesies, G. A. 2003. Soil erosion prediction using RUSLE for central Kenyan highland conditions. Agriculture, Ecosystems, and Environment 97: 295–308.

Antwi, B.O., Ando, H.F., Wokatsuiki, T., and Atakora, E.T. 2012. Estimation of Soil Erodibility and Rainfall Erosivity Patterns in the Agroecological Zone of Ghana. *Journal of Soil Science and Environmental Management, 3(11): 275-279.*

Antwi, E. K., Krawczynski, R., & Wiegleb, G. 2008. Detecting the effect of disturbance on habitat diversity and land cover change in a post-mining area using GIS. *Landscape and Urban Planning, 87*, 22-32.

Aragon, F., and Rud, J. 2012. Mining, Pollution and Agricultural Productivity: Evidence from Ghana. Nova Africa Centre.

Auditor-General South Africa. *Report of the Auditor-General to Parliament on a Performance Audit of the Rehabilitation of Abandoned Mines at the Department of Minerals and Energy.* Auditing to Build Public Confidence (2009). Available at http://www.environmentalauditing.org/Portals/0/AuditFiles/SouthAfrica_f_eng_Rehabilitation-of-Abandoned-Mines.pdf.

Ayalew, G.; Selassie, Y.G. 2015. Soil Loss Estimation for Soil Conservation Planning using Geographic Information System in Guang Watershed, Blue Nile Basin. *J. Environ. Earth Sci. 5, 126–134.*

Bartsch, K. P., Van Migroet, H., Boettinger, J., and Dobrowolski, J. P. 2002. Using Empirical Erosion Models and GIS to determine Erosion Risk at Camp Williams, Utah. *Journal of Soil and Water Conservation.* Vol. 57(1): 29-36.

Beasley, D. B., and Huggins, L. F. 1982. ANSWERS (Areal Nonpoint Source Watershed Environmental Response Simulation) User's Manual. Chicago: U.S. Environmental Protection Agency Report No. 905/9-82-001.

Beck, M. B. 1987. Water quality modeling: A review of uncertainty. *Water Resources Research 23, 1393-1442.*

Bergsma, E., Charman, P., Gibbons, F., Hurni, H., Moldenhauer, W. C., Panichapong, S. 1996. Terminology for Soil Erosion and Conservation. ISSS, ITC, ISRIC.

Bewket, W. and Teferi, E. 2009. Assessment of soil erosion hazard and prioritization for treatment at the watershed level: case study in the Chemoga watershed, Blue Nile basin, Ethiopia. Land degradation & development. Published online in Wiley InterScience (www.interscience.wiley.com) DOI: 10.1002/ldr.944

Birte, J. 2010. GIS Use of remote sensing, New approach for assessing environmental degradation in the zone of West Africa option in Badume, Kano state Nigeria. *R4D review IITA researches to nourish Africa.*

Bizuwerk, A., Taddese, G. and Getahun, Y. 2008. Application of GIS for Modeling Soil Loss Rate in Awash Basin, Ethiopia. International Livestock Research Institute, Addis Ababa, Ethiopia.

Boardman, J. 2006. Soil Erosion Science: Reflections on the Limitations of Current Approaches, *Catena*, Vol. 68, p73 – 86.

Bobe, B. 2004. *Evaluation of Erosion in Harare Region of Ethiopia using soil loss models, Rainfall Simulation and Field Trials*, Ph.D. Dissertation, Department of Plant Production and Soil Science. University of Pretoria South Africa.

Bonilla, C. A., Reyes, J. L. and Magri, A. 2010. Water Erosion Prediction Using the Revised Universal Soil Loss Equation (RUSLE) in a GIS Framework, Central Chile. *Chilean Journal of Agricultural Research 70(1):159-169.*

Borselli, L., Torri, D., Poesen, J., and Iaquinta, P. 2012. A robust algorithm for estimating soil erodibility in different climates. Catena*, 97*, 85-94.

Borselli, L.; Vigiak, O.; Cavalli, M.; Azalea J. And Rodríguez, O. 2014. Using connectivity to assess soil erosion and mass movement processes in the landscape: applications and discussion of a new paradigm –keynote lecture – CONNECTEUR –COST Action ES1306

Brady, L. M. 2000. GIS analysis of the spatial variability of contaminated watershed components in a historically mined region, basin and range province, Southeast Arizona. Master thesis, University of Arizona, 127 p. Tucson, Arizona.

Brady, L. M., Gray, F., Wissler, C. A., & Guertin, D. P. 2001. Spatial variability of sediment erosion processes using GIS analysis within watersheds in a historically mined region, Patagonia Mountains, Arizona. U.S. Geological Survey Open-File Report: OF 01-267.

Breetzke, G. D. 2004. A critique of soil erosion modeling at a catchment scale using GIS. Unpublished MSc Thesis, Vrije Universiteit Amsterdam, The Netherlands

Brito, P. L., and Quintanilla, J. A. 2012. A literature review, 2001-2008, of classification methods and inner urban characteristics identified in multispectral remote sensing images. Paper presented at the Proceedings of the 4th GOEBIA; Rio de Janeiro, Brazil.

Burley, J. B. 2001. Environmental design for reclaiming surface mines. The Edwin Mellen Press, New York.

Busacca, A. J., Cook, C. A. & Mulla, D. J. 1993: Comparing landscape-scale estimation of soil erosion in the Palouse using Cs-137 and RUSLE, *Journal of Soil and Water Conservation*, 48: 361-367.

Chakela, Q. and Stocking, M. 1988. An Improved Methodology for Erosion Hazard Mapping Part II: Application to Lesotho, *Physical Geography*, Vol. 70, (3), p181-189.

Chamber of Mines 2011: *Facts & Figures 2010-2011* Chamber of Mines of South Africa. URL:http://www.bullion.org.za/Publications/Facts&Figures2010/F%20&%20F%202011_Final.pdf. [Accessed 29.06.2015]

Choi, Y., 2012. A new algorithm to calculate weighted flow-accumulation from a DEM by considering surface and underground stormwater infrastructure. *Environmental Modeling and Software 30, 81–91.*

Choi, Y., Park, H. D., Kwon, H. H., Yoon, S. H., Go, W. R. 2009. Development of a GIS-based decision support system for planning the reforestation at abandoned coal mines. *Journal of the Korean Society for Geosystem Engineering 46 (6), 691–702.*

Choi, Y., Park, H. D., Sunwoo, C. 2008. Flood and gully erosion problems at the Pasir open pit coal mine, Indonesia: a case study of the hydrology using GIS. *Bulletin of Engineering Geology and the Environment 67 (2), 251–258.*

Clarke, K. C. 2001. Getting started with geographic information systems. 3rd ed. Prentice Hall Series in Geographic Information Science, Prentice-Hall Inc., Upper Saddle River, New Jersey.

Coetzee, H., Winde, F. & Wade, P.W. 2006. An assessment of sources, pathways, mechanisms, and risks of current and potential future pollution of water and sediments in gold-mining areas of the Wonderfonteinspruit Catchment. WRC Report No. 1214/1/06. Pretoria: Water Research Commission.

Crosby, C. T., Smithen, A. A. and McPhee, P. J. 1983. Introduction of the Universal Soil Loss Equation in the Republic of South Africa, Paper No. 83.2072. *Proc. of the 1983 Summer Meeting of the ASAE*. 26-29 June, Bozeman, Montana, USA.

Daba, S. 2003. An investigation of the physical and socioeconomic determinants of soil erosion in the Hararghe highlands, eastern Ethiopia. *Land Degrad. Dev. 14, 69–81.*

Dabral, P. P., Baithuri, N. and Pandey, A. 2008. Soil erosion assessment in a hilly catchment of North Eastern India using USLE, GIS, and remote sensing. *Water Resources Management 22 (12), 1783 - 1798.*

De Carvalho, D.F.; Durigon, V.L.; Antunes, M.A.H.; Almeida,W.S.; Oliveira, P.T.S. 2014. Predicting Soil Erosion Using RUSLE and NDVI Time series From TM Landsat 5. Pesq. Agropec. Bras. 49, 215–224.

Dee Roo, A. 1996. Soil Erosion Assessment using GIS. In V. Singh, & M. Florentino, *Geographical Information Systems in Hydrology* (pp. 339-356). The Netherlands: Kluwer Academic Publishers.

Desmet, P.; Govers, G. 1996. A GIS procedure for automatically calculating the USLE LS factor on topographically complex landscape units. *J. Soil Water Conserv. 51, 427–433.*

Diodato; Bellocchi; Romano; Chirico. 2011. *How the aggressiveness of rainfalls in the Mediterranean lands is enhanced by climate. Clim. Chang., 108* (3), pp. 591-599.

DWAF. 2014. Water, mining, and waste: A historical and economic perspective on conflict management in South Africa. *The economics of peace and security journal, 2(2): 33-41.*

Efe, R.; Ekinci, D.; Cürebal, I. 2008. Erosion Analysis of Fındıkli Creek catchment (Northwest of Turkey) using GIS based on RUSLE (3D) Method. *Fresenius Environ. Bull. 17, 576–586.*

Eltaif, N., Gharaibeh, M., Al-zaitawi, F., and Alhamad, M. N. 2010. Approximation of rainfall erosivity factors in north Jordan. *Pedosphere, 20,* 711-717.

Elwell, H. A. 1976. Natal Agricultural Research Bulletin No. 7: Soil Loss Estimator for Southern Africa. Department of Agricultural Technical Services, Natal, South Africa.

Elwell, H. A. 1978. Modeling soil losses in southern Africa. *Journal of Agricultural Engineering Research 23 117-127.*

Elwell, H. A. 1996. Environmental monitoring of land degradation and soil erosion methods and techniques. Guidelines for the SADC region. Compiled for SADC-ELMS, Maseru.

Elwell, H. A., 1990. The development, calibration and field testing of a soil loss and runoff model derived from a small-scale physical simulation of the erosion environment on arable land in Zimbabwe, *Journal of Soil Science 41: 239-253.*

Elwell, H. A., and Stocking, M. A. 1982. Developing a simple yet practical method of soil-loss estimation. Tropical Agriculture, 59:43-48.

Evans, R. 2000. Some soil factors influencing accelerated water erosion of arable land, *Progress in Physical Geography*, 20: 205-215.

Eweg, H. and Van Lammeren, R. 1996.The application of a geographical information system at the rehabilitation of degraded and degrading areas. A case study in the highlands of Tigray, Ethiopia Centre for Geographical Information Processing, Agricultural University Wageningen.

Fengxia, G. U. and Wenbao, L. I. U. 2010. Applications of Remote Sensing and GIS to the Assessment of Riparian Zones for Environmental Restoration in Agricultural Watersheds. *Geo-Spat. Inf. Sci. 13* (4), 263–268.

Flacke, W., Auerswald, *K.,* and Neufang, L. 1990. Combining a Modified Universal Soil Loss Equation with a Digital Terrain Model for Computing High-Resolution Maps of Soil Loss Resulting from Rain Wash. *Catena.* Vol. 17(4-5): 383-397.

Flugel, W. A., Marker, M., Moretti, S., Rodolfi, G., and Sidrochuk, A. 2003. Integrating Geographical Information Systems, Remote Sensing, and Ground truthing and Modeling Approaches for Regional Erosion Classification of Semi-arid Catchments in South Africa. *Hydrological Processes.* Vol. 17(5): 929-942.

Ganasri, B. P., and Ramesh, H. 2016. Assessment of soil erosion by RUSLE model using remote sensing and GIS - A case study of Nethravathi Basin. *Geoscience Frontiers 7 (2016) 953 – 961.*

Gandomkar A. 2011. estimating the real capacity of rain erosion using GIS (the Fournier case study for Isfahan). *International Journal of Agricultural Science, Research and Technology.* 1(1): 33-38.

Garland, G. G., Hoffman, M. T. and Todd, S. 2000. Soil degradation. In M. T. Hoffman, Todd, S., Ntshona, Z., Turner, S (Ed.), *A National Review of Land Degradation in South Africa* (pp. 69-107). Pretoria, South Africa: South African National Biodiversity Institute.

Gelagay, H. S. and Minale, A. S. 2016. Soil loss estimation using GIS and Remote sensing techniques: A case of Koga watershed, North-western Ethiopia. *Int. Soil Water Conserv. Res.* 4, 126–136.

Gete, Z. 2000a. Landscape Dynamics and Soil Erosion Process Modeling in the North Western Ethiopian High Lands. African Studies Series A16, Geographic Bernensia, Berne.

Gete, Z. and Hurni, H. 2000b. Land Use/Land Covers Dynamics and Implications on Mountain Resource Degradations in the North-Western Ethiopian Highlands. University of Bern, Bern.

Gobin, A., Govers, G., Jones, R., Kirkby, M. J., Kosmas, C. and Gentile, A. R. 2003. Assessment and Reporting on Soil Erosion; Background and Workshop Report. Technical Report. European Environment Agency, Copenhagen, Denmark. http://reports.eea.europa.eu/technical.

Gregory, D. B. 2004. A critique of soil erosion modeling at a catchment scale using GIS. A dissertation for the degree of Master of Science, Vrije Universiteit Amsterdam (The Netherlands):37-38.

Haarhoff, D., Smith, H. J., Beytell, J. F. and Schoeman, J. L. 1994. The testing of techniques for the determination of the erosion potential of areas in South Africa. ISCW report no. GW/A/94/6. National Department of Agriculture, Pretoria.

Hakkou, R., Khalil, A. and Lepage, M. 2014. GIS-based environmental database for assessing the mine pollution: A case study of an abandoned mine site in Morocco. *Journal of Geochemical Exploration*, Available at http://dx.doi.org/10.1016/j.gexplo.2014.03.023, [Accessed on 18/11/16].

Hoyos, N. 2005. Spatial Modeling of Soil Erosion Potential in a Tropical Watershed of the Colombian Andes. *Catena.* 63, 85–108.

Hudson, C. A. 1987. A Regional Application of the SLEMSA in the Cathedral Peak Area of the Drakensberg. M.Sc. Dissertation, University of Cape Town, Cape Town, South Africa.

Igwe C. A.; AKamigbo F.O.R, bagwu J.S.C.M. 1997. Application of SLEMSA and USLE erosion models for potential erosion hazard mapping in southeastern Nigeria, University of Nigeria.

Ishtiyaq, A. and Verma, M. K. 2013. Application of USLE Model & GIS in Estimation of Soil Erosion for Tandula Reservoir. *International Journal of Emerging Technology and Advanced Engineering.* Vol. 3 (4).

Issamaldin, M., Hatim, N. and Ahmed, A. 2017. Coupling Universal Soil Loss Equation and GIS Techniques for Estimation of Soil Loss and Sediment Yield in Algash Basin*. International Journal of Advanced Remote Sensing and GIS, Volume 6, Issue 3, pp. 2050 - 2067*.

Jain, S. K., Kumar, S., and Varghese, J. 2001. Estimation of soil erosion for a Himalayan watershed using GIS technique. *Water Resources Management* 15 (1), 41 - 54.

Johnston, D., Potter, H., Jones, C., Rolley, S., Watson, I. and Pritchard, J. 2008. Abandoned mines and the water environment: Science project, Environment Agency, Bristol.

Kakembo, V. and Rowntree, K. M. 2003. The relationship between land use and soil erosion in the communal lands near Peddie Town, Eastern Cape, South Africa. *Land Degradation & Development, 14*, 39-49.

Kakembo, V., Xanga, W. W. and Rowntree, K. 2009. Topographic thresholds in gully development on the hillslopes of communal areas in Ngqushwa Local Municipality, Eastern Cape, South Africa. *Geomorphology, 110*, 188-194.

Kaltenrieder, J. 2007. Adaptation and Validation of the Universal Soil Loss Equation (USLE) for the Ethiopian-Eritrean Highlands. MSc Thesis, University of Berne, Centre for Development and Environment. *Geographisches Institut.*

Karamage, F.; Zhang, C.; Kayiranga, A.; Shao, H.; Fang, X.; Ndayisaba, F.; Nahayo, L.; Mupenzi, C.; Tian, G. 2016. USLE-Based Assessment of Soil Erosion by Water in the Nyabarongo River Catchment, Rwanda. *Int. J. Environ. Res. Public Health*. 13, 835.

Kefi, M., Yoshino, K., Zayani, K. and Isoda, H. 2009. Estimation of soil loss by using a combination of erosion model and GIS: the case of study watersheds in Tunisia. *J Arid Land Stud, 19,* 287-290.

Khanna. S. K & Justo C. E. (2001). Highway Engineering, Nem Chand & Bros Publications, Roorkee (U.A), Eighth Edition.

Kim, H. S. 2006. Soil *erosion modeling using RUSLE and GIS on the Imha watershed, South Korea*. A thesis submitted in fulfilment of the requirements for the degree of Master of Science. Colorado State University.

Kowal, J. M., and Kassam, A. H. 1976. Energy load and instantaneous intensity of rainstorms at Samaru, northern Nigeria. *Tropical Agriculture 53*: 185-197.

Lal, R. 1982. The temperature profile of soil during infiltration. *Nigerian Journal of Soil Science 2:* 87-100.

Lal, R. 1994. Soil Erosion Research Method, 2nd ed.; Soil and Water Conservation Society: Ankeny, IA, USA.

Lal, R. 1998a. Agronomic Impact of Soil Degradation. In: Lal, R., Blum, W. H. Valentine, C., and Stewart, B. A. (Editors). *Methods for Assessment of Soil Degradation.* New York: CRC Press. pp. 459-473.

Lal, R. 1998b. Soil Quality and Sustainability. In: Lal, R., Blum, W. R, Valentine, C., and Stewart, B. A. (Editors). *Methods for Assessment of Soil Degradation.* New York: CRC Press. pp. 17-30.

Lal, R. 2004. Soil carbon sequestration impacts on global climate change and food security. Science, 304, 1623–1627.

Lal, R. and Elliot, W. 1994. Erodibility and Erosivity. In: Lal, R. (Editor). *Soil Erosion: Research Methods.* 2nd Edition. Florida: Soil and Water Conservation Society and St. Lucie Press. pp. 181-208.

Le Roux J. J., Morgenthal, T. L., Malherbe, J., Smith, H. J., Weepener, H. L. and Newby, T. S. 2006. Improving spatial soil erosion indicators in South Africa. ISCW report no. GW/A/2006/51. National Department of Agriculture, Directorate Land and Resources Management, Pretoria.

Le Roux, J. J. 2010. Soil erosion prediction in South Africa: Existing Knowledge and limitations. *Water Research Commission Report no. 1765/1/10 Appendix J, Pretoria, South Africa*.

Le Roux, J. J., and Germishuyse, T. 2007. Modeling sediment yield for an agricultural research catchment in KwaZulu-Natal. ISCW report no. GW/A/2007/40.Water Research Commission, Pretoria.

Le Roux, J. J., Morgenthal, T. L., Malherbe, J., Sumner, P. D., Pretorius, D. J. 2008. Water erosion prediction at a national scale for South Africa. *Water SA* 34(3): 305-314.

Le Roux, J.J., Newby, T.S, and Sumner, P.D. 2007. Monitoring soil erosion in South Africa at a regional scale; review and recommendation, *South African Journal of Science, Vol 103 Nos 7-8 pp 329-335.*

Li, X.S.; Wu, B.F.; Wang, H.; Zhang, J. 2011. Regional soil erosion risk assessment in Hai Basin. *J. Remote Sens. 5*, 372–387.

Lu H., Prosser, I. P., Moran, C. J., Gallant, J. C., Priestle, Y. G. and Stevenson, J. G. 2003. Predicting sheet wash and rill erosion over the Australian continent. *Aust. J. Soil Res. 41:* 1037-1062.

Makgae, M. 2012. The status and implication of the AMD legacy facing South Africa. Annual Conference, 2012, *International Mine Water Association (IMWA),* Bunbury, Australia, pp. 327–634.

Mallam, I. 2016. Soil Erosion Hazard Assessment Using SLEMSA Model in Out sketch Parts of Kano Metropolis. *Dutse Journal of Pure and Applied Sciences (DUJOPAS)* Vol. 2 No. 2.

Mallick, J., Alashker, Y., Mohammad, S. A., Ahmed, M., & Hasan, M. A. 2014. Risk assessment of soil erosion in semi-arid mountainous watershed in Saudi Arabia by RUSLE model coupled with remote sensing and GIS. *Geocarto International.* http://dx.doi.org/10.1080/10106049.2013.868044

Mantel, S.; Schulp, C.J.E., and M. van den Berg. 2014. Modeling of soil degradation and its impact on ecosystem services globally, Part 1: A study on the adequacy of models to quantify soil water erosion for use within the IMAGE modeling framework Report 2014/xx, ISRIC—World Soil Information, Wageningen.

Märker, M., Moretti, S. and Rodolfi, G. 2001. Assessment of water erosion processes and dynamics in semiarid regions of southern Africa (KwaZulu/Natal RSA; Swaziland) using the Erosions Response Units Concept. *Geografia Fisica Dinamica Quaternaria, 24*, 71-83.

Mati B. M, Morgan R. P. C, Gichuki F. N, Quinton J. N, Brewer T. R, Liniger H. P. 2000. Assessment of erosion hazard with the USLE and GIS: A case study of the Upper Ewaso Ng'iro North basin of Kenya. *International Journal of Applied Earth Observation and Geoinformation 2*: 1–9.

McCarthy, T. S. 2011. The impact of acid mine drainage in South Africa. *South African Journal of Science, Vol. 107,* pp. 107–712.

McPhee, P. J., and Smithen, A. A. 1984. Application of the USLE in the Republic of South Africa. *Agric. Eng. S. Afr*. 18 5-13.

Meadows, M. E. 2003. Soil erosion in the Swartland, Western Cape Province, South Africa: Implications of past and present policy and practice. *Environmental Science & Policy, 6,* 17-28.

Merritt, W. S., Letcher, R. A. and Jakeman, A. J. 2003. A review of erosion and sediment transport models. *Environ. Modell.Software* 18: 761-799.

Meshesha, D.T.; Tsunekawa, A.; Tsubo, M.; Ali, S.A.; Haregeweyn, N. 2014. Land-use change and its socio-environmental impact in Eastern Ethiopia's highland. Reg. *Environ. Chang. 14,* 757–768.

Mhangara, Paidamwoyo & Kakembo, Vincent & Jae Lim, Kyoung. 2012. Soil erosion risk assessment of the Keiskamma catchment, South Africa using GIS and remote sensing. *Environmental Earth Sciences. 65*. 2087 - 2102. 10.1007/s12665-011-1190-x

Mhlongo, S. E., Dacosta, F. A. and Mphephu, N. F. 2013. In search of appropriate rehabilitation strategies for abandoned Nyala Magnesite mine, Limpopo province of South Africa. *Int. J. Eng. Appl. Sci. 2*, Islamabad, Pakistan, pp. 58–70.

Mhlongo, S.E. 2012. *Development of a modeling framework for the design of low-cost and appropriate rehabilitation strategies for Nyala Abandoned Mine*. Unpublished MSc. Dissertation, Department of Mining and Environmental Geology, University of Venda, Thohoyandou, Republic of South Africa.

Milisav, T. 2014. The use of methods of remote sensing and GIS applications in monitoring water quality on the example of the mining basin Kolubara, *Lazarevac. Geonauka*. Vol. 2, No.1. Lazarevac, Serbia.

Miller, G. T. 1999. Environmental science: Working with the earth (7th edition), Belmont, Wadsworth.

Mills, A. J., and Fey, M. V. 2003. Declining soil quality in South Africa: effects of land use on soil organic matter and surface crusting. *South African Journal of Science 99*, 429- 436.

Mishra, S. K., Hitzhusen, F. J., Sohngen, B. L. and Guldmann, J. M., 2012. Costs of abandoned coal mine reclamation and associated recreation benefits in Ohio. *J. Environ. Manag. 100,* 52–58.

Mitasova, H., Hofierka, J., Zlocha, M., and Iverson, R. 1996. Modeling Topographic Potential for Erosion and Deposition using GIS. *Int. Journal of Geographical Information Science 10* (5), 629-641.

Mohammed, I. 2016. *Estimating soil erosion using universal soil loss equation and GIS in Algash Basin.* MSc Thesis. Department of GIS and Cartography, Faculty of Geographical and Environmental Sciences, University of Khartoum.

Morgan, R. P. C. 1995. Soil Erosion and Conservation (2nd edition.). Longman Group Limited, London, UK.

Morgan, R. P. C. 2005. Soil Erosion and Conservation (3rd edition). Blackwell Science: Oxford.

Morgan, R. P. C., Quinton, J. N., Smith, R. E., Govers, G., Poesen, J. W. A., Auerswald, K., Chisci, G., Torri, D. and Styczen, M. E. 1998. The European soil erosion model (EUROSEM): a process-based approach for predicting soil loss from fields and small catchments. *Earth Surf. Process. Landf.* 23, 527–544.

Mughogho, M. T. 1998. Evaluation of the Revised Universal Soil Loss Equation (RUSLE) and the Soil Loss Estimation Model for Southern Africa (SLEMSA) under Malawi conditions: A case study of Kamundi catchment near Mangochi. Project Report, University of Malawi.

Mulooka, C. 2008. *Relationship Between Stream Bank Cultivation and Soil Erosion in Dedza Malawi*, MSc. Thesis, Civil Engineering Department, University of Zimbabwe, Harare.

Mutowo, G. and Chikodzi, D. 2013. Erosion Hazard Mapping in the Runde Catchment: Implications for Water Resources Management. *Journal of Geosciences and Geomatics, 2013, Vol. 1, No. 1, 22-28.*

Nearing, M. A. 1998. A single continuous function for slope steepness influence on soil loss. *Soil Sci. Soc. Am. J*. 61, 917-919.

Nearing, M. A., Pruski, F. F., and O'Neal, M. R. 1994. Expected climate change impacts on soil erosion rates, a review. *Journal of Soil Water Conservation, 59*(1), 43-50.

Nigel, R. and Rughooputh, S. D. 2010. Soil erosion risk mapping with new datasets: An improved identification and prioritization of high erosion risk areas. *Catena, 82,* 191–205.

Nordstrom, D. K., and Alpers, C. N. 1999. Geochemistry of acid mine waters. *Rev. Econ. Geol.* 6A, 133–160.

NRI. 2001. National Resources Inventory, 2001 Annual NRI, Soil Erosion. United States Department of Agriculture: National Resources Conservation Service, USA. http://www.nrcs.usda.gov.

Nyssen, J., M. Veyret-Picot, J. Poesen, J. Moeyersons, M. Haile, J. Deckers, and G. Govers. 2004. The effectiveness of loose rock check dams for gully control in Tigray, northern Ethiopia.

Panagos, P.; Borrelli, P.; Meusburger, K. 2015. A New European Slope Length and Steepness Factor (LS-Factor) for Modeling Soil Erosion by Water. *Geosciences. 5,* 117–126.

Paris, S. 1990. Erosion hazard model (modified SLEMSA). Field document no 13, second version, land resource evaluation project, Malawi, 17 pp.

Pretorius D. J. 1998. *The development of land degradation monitoring and auditing techniques with the aid of remote sensing and GIS technology. ISCW report no. GW/A/98/27.* National Department of Agriculture, Directorate Land and Resources Management, Pretoria.

Pretorius, D. J., and Smith, H. J. 1998. The development of a GIS-based land information system for developing areas. *Proc. of the 21st SSSSA Conf*. 21-23 January, Drakensberg, South Africa.

Prosser, I. P., Rutherford, I. D., Olley, J. M., Young, W. J., Wallbrink, P. J., Moran, C. J. 2001. Large-scale patterns of erosion and sediment transport in river networks, with examples from Australia. *Marine and Freshwater Research* 52: 81-99.

Pyatt, F.B., Grattan, P.J., 2001. Some consequences of ancient mining activities on the health of ancient and modern human populations. J. *Public Health Med. 23*, 235–236.

Rao, C.V.; Ashenafi, T.; Aminnedu, E. 2014. Erosion risk identification study using RUSLE model in G. Madugula Mandal, Visakhapatnam District, A.P., India. *Eur. Acad. Res. 2,* 12246–12260.

Rees, W. G., 2004. Least-cost paths in mountainous terrain. *Computers and Geosciences 30* (3), 203–209.

Reichardt, M. 2012. A history of mine wastes rehabilitation techniques in South Africa: a multidisciplinary overview of mine waste rehabilitation and the non-scientific drivers for its implementation, University of the Witwatersrand, Republic of South Africa.

Renard, K. G., Foster, G. R., Weesies, G. A., McCool, D. K. and Yoder, D. C. 1994. RUSLE Users Guide. Predicting Soil Erosion by Water: A Guide to Conservation Planning with the Revised Universal Soil Loss Equation. USDA, Agriculture Handbook No. 703, Washington DC, USA.

Röder, A., & Hill, J. 2009. *Recent Advances in Remote Sensing and Geoinformation Processing for Land Degradation Assessment.* Aiken, The Netherlands: CRC Press.

Rydgren, B. 1996. Soil erosion; its measurement, effects, and prediction. A case study from the southern Lesotho lowlands, *Zeitschrift für Geomorphology.* 40: 429-445.

Saaty, T. L., 1977. A scaling method for priorities in hierarchical structures. *Journal of Mathematical Psychology 15* (3), 234–281.

Saavedra, C. 2005. Estimating spatial patterns of soil erosion and deposition in the Andean region using geo-information techniques: a case study in Cochabamba, Bolivia Ph.D. dissertation, Wageningen University, The Netherlands.

Samuel, L.M. 2014. Prediction of Runoff and Sediment Yield Using AnnAGNPS Model: Case of Erer-Guda Catchment, East Hararghe, Ethiopia. *ARPN J. Sci. Technol. 4*, 575–595.

Schulze, R. E. 1979. Soil loss in the key area of the Drakensberg – A regional application of the Soil Loss Estimation Model for Southern Africa (SLEMSA). In: *Hydrology and Water Resources of the Drakensberg.* Natal and Regional Planning Commission, Pietermaritzburg, South Africa. pp. 149-167.

Smith, H. J. 1999. Application of empirical soil loss models in southern Africa: A review. *S. Afr. J. Plant & Soil* 16 (3) 158-163.

Smith, H. J., Vanzyl, A. J., Claassens, A. S., Schoeman, J. L., Smith, H. J. C. and Laker, M.C. 2000. Soil Loss Modeling in the Lesotho Highlands Water Project (LHWP) Catchments Areas. Lesotho Highlands water project. Erosion and sedimentation: Soil loss and sedimentation yield modeling.

Somayeh S. S.; Mojgan E.; Majid G. and Zahra D. 2012. Assessment Rate of Soil Erosion by GIS (Case Study Varmishgan, Iran). *J. Basic. Appl. Sci. Res.*, 2(12)13115-13121, 2012

Stillhardt B. 1999. The Variability of Soil Erosion in the Highlands of Ethiopia and Eritrea. Average and Extreme Erosion Patterns. Soil Conservation Research Report 33. Berne, Switzerland: University of Berne *Landscape Dynamics and Soil Erosion... (PDF Download Available)*. Available from: https://www.researchgate.net/publication/33804549_Landscape_Dynamics_and_Soil_Erosion_Process_Modeling_in_the_North-Western_Ethiopian_Highlands, [accessed March 18 2017].

Stocking, M. A. 1982. Modeling soil losses. Suggestions for a Brazilian approach. UNDP BRA/82/001, Report of the Overseas Development Group, University of East Anglia.

Stocking, M. A. 1987. A methodology for erosion hazard mapping of the SADCC Region. Paper prepared for the Workshop on Erosion Hazard. Nilapping, Lusaka, Zambia April 1987.

Stocking, M. A. 1994. Assessing Vegetative Cover and Management Effects. In: *Soil Erosion Research Methods*. R. Lal (Editor). *Soil and Water Conservation Society*, St. Lucie Press, Pp. 211-232.

Stocking, M. A., Chakela, Q. and Elwell, H. A. 1988. An improved method for erosion hazard mapping. Part I: The technique. *Geografiska Annaler 70* (A.3): 169-180

Strager, M. P., Fletcher, J. J., Strager, J. M., Yuill, C. B., Eli, R. N., Petty, J. T., Lamont, S. J. 2010. Watershed analysis with GIS: the watershed characterization and modeling system software application. *Computers & Geosciences 36* (7), 970–976.

Swart, E. 2003. The South African legislative framework for mine closure, proceedings of the colloquium on mine closure for sustainable development, *J. South Afr. Inst. Min. Metall.* Vol. 103, pp. 489–492.

Symeonakis, E., Bonifaçio, R. and Drake, N. 2009. A Comparison of Rainfall Estimation Techniques for Sub-Saharan Africa, International *Journal of Applied Earth Observation and Geoinformation*, Vol. 11, p15-26.

Tripathi, M.P.; Panda, R.K.; Raghuwanshi, N.S. 2003. Identification and prioritization of critical sub-watersheds for soil conservation management using the SWAT model. *Biosyst. Eng.,* 85, 365–379.

Trustrum, N.A., Gomez, B., Page, M.J., Reid, L.M. & Hicks, D.M. 1999. Sediment production, storage, and output: The relative role of large magnitude events in steep land catchments, *Zeitschrift für Geomorphology*, 115: 71-86.

Wang, X. D., Zhong, X. H., Liu, S. Z., Liu, J. G., Wang, Z. Y. and Li, M. H., 2008. Regional assessment of environmental vulnerability in the Tibetan Plateau: Development and application of a new method. *J. Arid Environ.* 72, 1929–1939.

Williams J. R. and Ham, R. W. 1978. Optimal operation of large agricultural watersheds with water quality constraints. Texas Water Resources Institute, Texas A&M Univ, Tech. report No. 96.

Wischmeier, W. H., and Smith, D. D. 1978. Predicting Rainfall Erosion Losses, a Guide to Conservation Planning. U.S. Department of Agriculture, Agricultural Handbook No. 537, Washington DC, USA.

Wordofa, G. 2011. Soil Erosion Modeling using GIS and RUSLE on Eurajoki Watershed, Finland.

Yahya, F.; Zregat, D.; Farhan, I. 2013. Spatial Estimation of Soil Erosion Risk Using RUSLE Approach, RS, and GIS Techniques: A Case Study of Kufranja Watershed, Northern Jordan. *J. Water Resour. Prot. 5*, 1247–1261.

Yang, C. L., Guo, R. P., Yue, Q. L., Zhou, K. and Wu, Z. F. 2013. Environmental quality assessment and spatial pattern of potentially toxic elements in soils of Guangdong Province, China. *Environ. Earth Science. 70*, 1903–1910.

Yang, S.; Lianyou, L.; Ping, Y.; Tong, C. 2005. A review of soil erodibility in water and wind erosion research*. J. Geogr. Sci. 15*, 167–176.

Yenilmez, F., Kuter, N., Emil, M. & Aksoy, A. 2011. Evaluation of pollution levels at an abandoned coal mine site in Turkey with the aid of GIS. *International Journal of Coal Geology*, 12-19.

Young, R. A., Onstad, C. A., Bosch, D. D. and Anderson, W. P. 1989. AGNPS: A nonpoint-source pollution model for evaluating agricultural watersheds. *J. Soil Water Conserv.* 44, 4522–4561.

Zhang, Z., Sheng, L., Yang, J., Chen, X. A., Kong, L., and Wagan, B. 2015. Effects of land use and slope gradient on soil erosion in a red soil hilly watershed of southern China. *Sustainability, 7,* 14309-14325.

APPENDICES

APPENDIX A: HYDROMETER TABLES

The following tables contain constant values used in hydrometer analysis. The hydrometer analysis procedure is explained in Chapter 4 of this thesis.

Table A1.1: Values of Effective Depth Based on Hydrometer and Sedimentation Cylinder of Specific Sizes

Hydrometer 151H		Hydrometer 152H			
Actual Hydrometer Reading	Effective Depth, L (cm)	Actual Hydrometer Reading	Effective Depth, L (cm)	Actual Hydrometer Reading	Effective Depth, L (cm)
1.000	16.3	0	16.3	31	11.2
1.001	16.0	1	16.1	32	11.1
1.002	15.8	2	16.0	33	10.9
1.003	15.5	3	15.8	34	10.7
1.004	15.2	4	15.6	35	10.6
1.005	15.0	5	15.5	36	10.4
1.006	14.7	6	15.3	37	10.2
1.007	14.4	7	15.2	38	10.1
1.008	14.2	8	15.0	39	9.9
1.009	13.9	9	14.8	40	9.7
1.010	13.7	10	14.7	41	9.6
1.011	13.4	11	14.5	42	9.4
1.012	13.1	12	14.3	43	9.2
1.013	12.9	13	14.2	44	9.1
1.014	12.6	14	14.0	45	8.9
1.015	12.3	15	13.8	46	8.8
1.016	12.1	16	13.7	47	8.6
1.017	11.8	17	13.5	48	8.4
1.018	11.5	18	13.3	49	8.3
1.019	11.3	19	13.2	50	8.1
1.020	11.0	20	13.0	51	7.9
1.021	10.7	21	12.9	52	7.8
1.022	10.5	22	12.7	53	7.6
1.023	10.2	23	12.5	54	7.4
1.024	10.0	24	12.4	55	7.3
1.025	9.7	25	12.2	56	7.1
1.026	9.4	26	12.0	57	7.0
1.027	9.2	27	11.9	58	6.8
1.028	8.9	28	11.7	59	6.6
1.029	8.6	29	11.5	60	6.5
1.030	8.4	30	11.4		
1.031	8.1				
1.032	7.8				
1.033	7.6				
1.034	7.3				
1.035	7.0				
1.036	6.8				
1.037	6.5				
1.038	6.2				
1.039	5.9				

Table A1.2: Values of k for Use in Equation for Computing Diameter of Particle in Hydrometer Analysis

Temperature °C	Specific Gravity of Soil Particles								
	2.45	2.50	2.55	2.60	2.65	2.70	2.75	2.80	2.85
16	0.01510	0.01505	0.01481	0.01457	0.01435	0.01414	0.0394	0.01374	0.01356
17	0.01511	0.01486	0.01462	0.01439	0.01417	0.01396	0.01376	0.01356	0.01338
18	0.01492	0.01467	0.01443	0.01421	0.01399	0.01378	0.01359	0.01339	0.01321
19	0.01474	0.01449	0.01425	0.01403	0.01382	0.01361	0.01342	0.01323	0.01305
20	0.01456	0.01431	0.01408	0.01386	0.01365	0.01344	0.01325	0.01307	0.01289
21	0.01438	0.01414	0.01391	0.01369	0.01348	0.01328	0.01309	0.01291	0.01273
22	0.01421	0.01397	0.01374	0.01353	0.01332	0.01312	0.01294	0.01276	0.01258
23	0.01404	0.01381	0.01358	0.01337	0.01317	0.01297	0.01279	0.01261	0.01243
24	0.01388	0.01365	0.01342	0.01321	0.01301	0.01282	0.01264	0.01246	0.01229
25	0.01372	0.01349	0.01327	0.01306	0.01286	0.01267	0.01249	0.01232	0.01215
26	0.01357	0.01334	0.01312	0.01291	0.01272	0.01253	0.01235	0.01218	0.01201
27	0.01342	0.01319	0.01297	0.01277	0.01258	0.01239	0.01221	0.01204	0.01188
28	0.01327	0.01304	0.01283	0.01264	0.01244	0.01255	0.01208	0.01191	0.01175
29	0.01312	0.01290	0.01269	0.01269	0.01230	0.01212	0.01195	0.01178	0.01162
30	0.01298	0.01276	0.01256	0.01236	0.01217	0.01199	0.01182	0.01165	0.01149

Table A1.3: Temperature Correction Factors CT

Temperature °C	factor C_T
15	1.10
16	-0.90
17	-0.70
18	-0.50
19	-0.30
20	0.00
21	+0.20
22	+0.40
23	+0.70
24	+1.00
25	+1.30
26	+1.65
27	+2.00
28	+2.50
29	+3.05
30	+3.80

Table A1.4: Correction Factors a for Unit Weight of Solids

Unit Weight of Soil Solids, g/cm³	Correction factor a
2.85	0.96
2.80	0.97
2.75	0.98
2.70	0.99
2.65	1.00
2.60	1.01
2.55	1.02
2.50	1.04

APPENDIX B: PARAMETERS DERIVED FOR THE SLEMSA MODEL

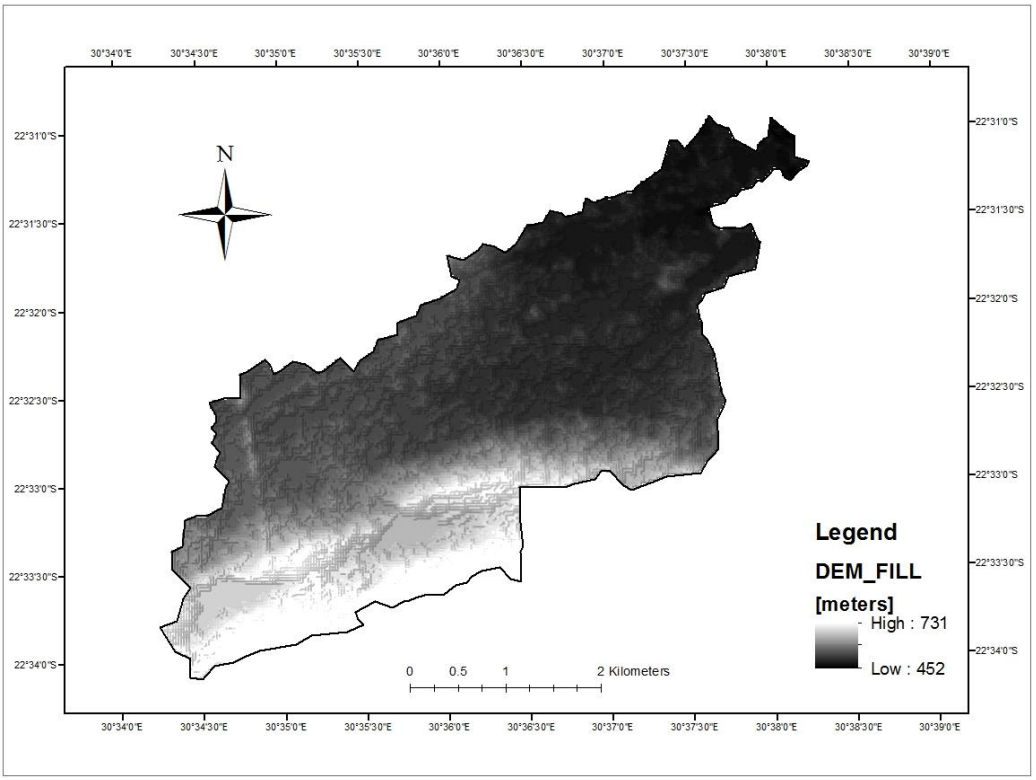

Appendix B1.1: Digital Elevation Model Fill for Nyala mine

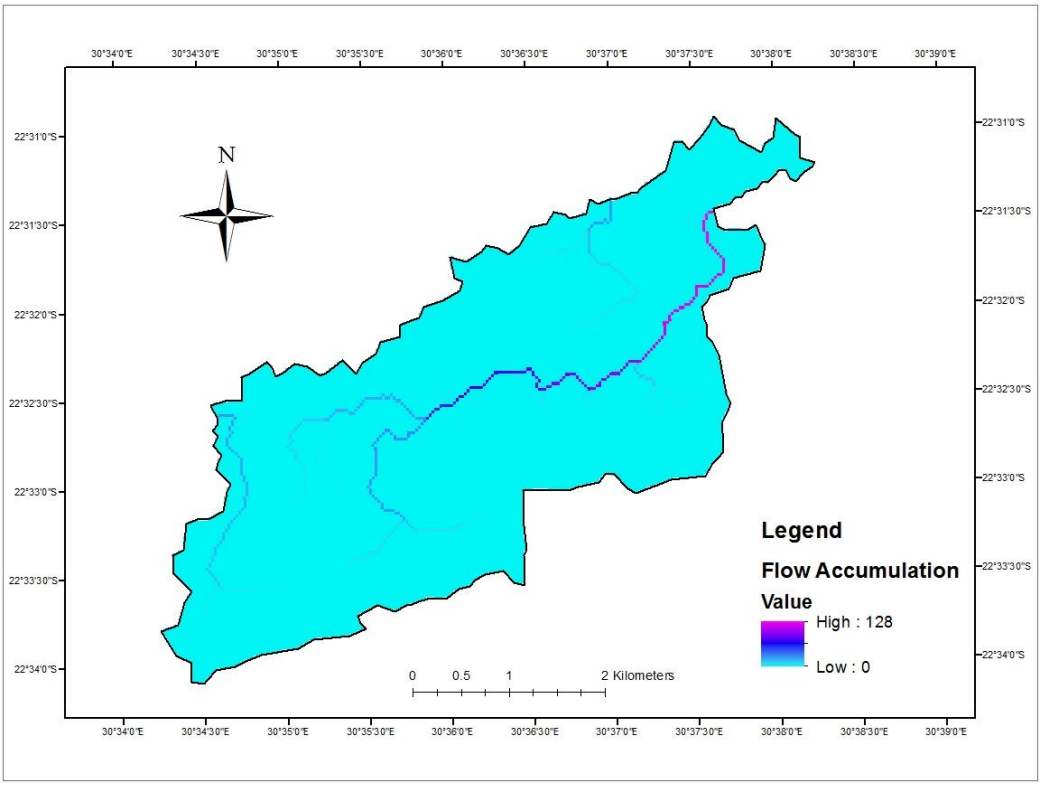

Appendix B1.2: Flow Accumulation map for Nyala mine

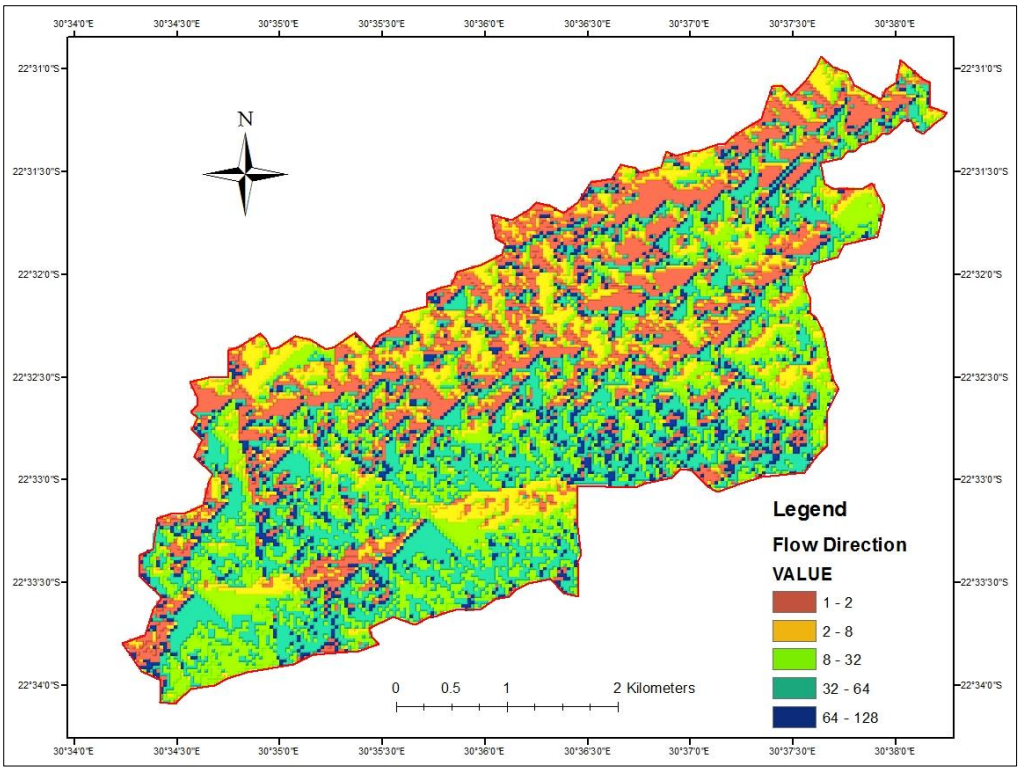

Appendix B1.3: Flow Direction map for Nyala mine

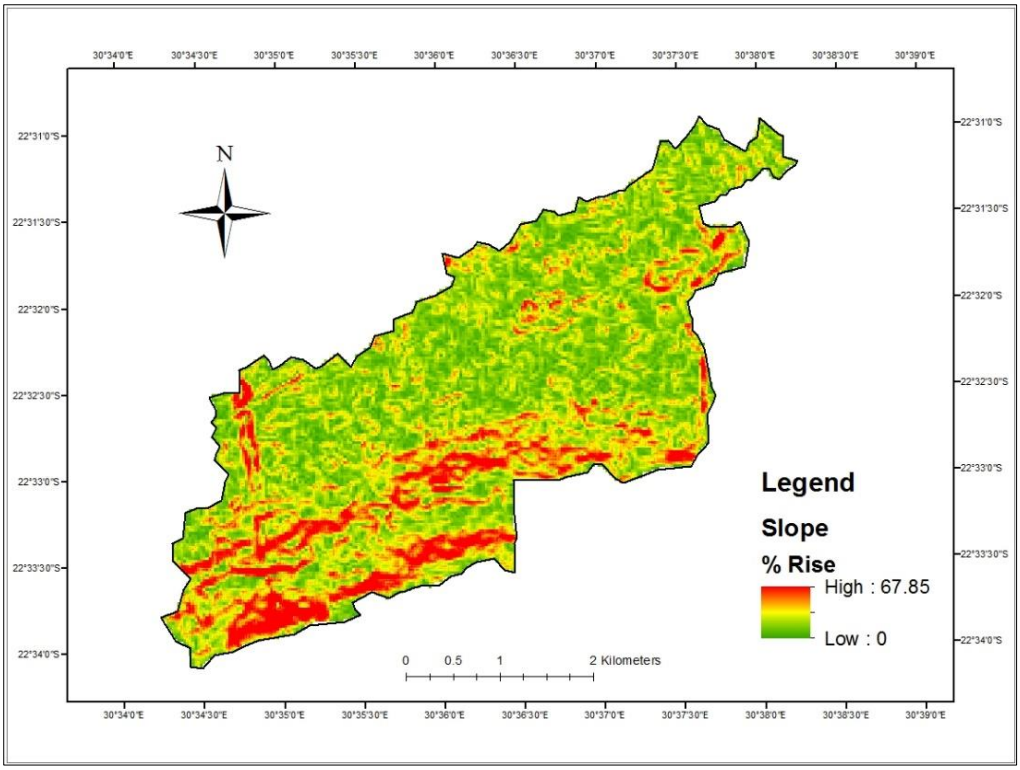

Appendix B1.4: Slope map for Nyala mine (%)